Author:
Roberts, Timothy D

Title:
The pharmacodynamics of the antiplatelet drug ticagrelor
mode of action, onset and reversibility.

School of Physiology, Pharmacology and Neuroscience

The pharmacodynamics of the antiplatelet drug ticagrelor: mode of action, onset and reversibility.

Timothy Daniel Roberts

A dissertation submitted to the University of Bristol in accordance with the requirements for award of the degree of Master of Research in the Faculty of Life Sciences.

Supervisors: Prof. Stuart Mundell & Dr. Thomas Johnson.

Start date: September 2018.

Submission date: September 2020.

Word count: 29,597.

Abstract

Platelets are the smallest, yet arguably the most pivotal blood constituent in the context of haemostasis and wound healing. However, vascular perturbations that result in ischaemic tissue injury has implicated platelets as a major player in the disease progression caused by arterial thrombosis. Platelets responses are influenced by the auto- and paracrine release of prothrombotic ligands acting upon platelet-expressed G-protein coupled receptors (GPCRs). These receptors initiate distinct intracellular signal pathways responsible for the interrelated processes of platelet adhesion, activation, secretion and aggregation. Of the many platelet expressed GPCRs, the activation of the $P2Y_{12}$ receptor ($P2Y_{12}R$) is well known to be responsible for sustained aggregation and thus thrombus formation. Consequently, the $P2Y_{12}R$ is an attractive and efficacious target for drug development, birthing the modern standard of care of dual antiplatelet therapy (DAPT) in patients with acute coronary syndromes (ACS). Of the currently available antiplatelet agents, ticagrelor has been shown to be superior both in clinical trials and laboratory studies. However, much debate exists around the pharmacodynamics attributed to ticagrelor and how this may influence its perceived clinical superiority. Additionally, amid concerns of the increased bleeding risk associated with ticagrelor as with all antiplatelet agents, recent international expert consensus guidelines have emerged to provide clarity on how and when to switch pharmacotherapies. Therefore, the aim of this thesis was to further define the pharmacodynamics of ticagrelor antiplatelet therapy, characterising the drugs mode of action, onset and reversibility. Assessment of the inhibitory effect of ticagrelor on $P2Y_{12}R$ activation was facilitated by bioluminescence resonance energy transfer ($BRET^2$) technology in $P2Y_{12}R$-transfected cells and complemented by observations seen with light transmission aggregometry in isolated human platelets. Our results demonstrate that ticagrelor acts as an inverse agonist in a concentration-dependent manner. Further, the proposed reversibility of this drug is questioned with data suggesting that versus ADP, this drug acts in an irreversible manner. This may impact upon clinical practice regarding antiplatelet therapy administration, especially in consideration of the currently available switching guidelines.

Acknowledgement

I would firstly like to express my unending gratitude to my project supervisor, Professor Stuart Mundell of the School of Physiology, Pharmacology and Neuroscience at the University of Bristol. Professor Mundell's door was always open, offering invaluable guidance towards reaching my research aims and additionally helping me with my own personal struggles. I am truly grateful for the unwavering support and incredible patience exhibited by yourself and the Faculty.

I would also like to thank Dr Jawad Khalil of the Mundell Laboratory. Your infectiously positive attitude, effortless approachability, incredible work ethic and constant guidance had an invaluable and lasting influence on my personal development. Most importantly, you gave me confidence in my capabilities. Thank you, my friend.

Additionally, I would like to acknowledge and thank all members of the Bristol Platelet Group and the Henderson & Kelly Laboratory. From the technical staff to the Principle Investigators, thank you for the opportunity to integrate so seamlessly and for being so welcoming.

Finally, I must express my profound gratitude towards my parents and siblings. Those close to me understand the various personal challenges we have faced as a family, and how that has directly influenced and precipitated my interest and motivation for a career in biomedical research. Without your continuous support, encouragement and words of wisdom, this journey would not have been possible.

Author's Declaration

I declare that the work in this dissertation was carried out in accordance with the requirements of the University's *Regulations and Code of Practice for Research Degree Programmes* and that it has not been submitted for any other academic award. Except where indicated by specific reference in the text, the work is the candidate's own. Work done in collaboration with, or with the assistance of others, is indicated as such. Any views expressed in the dissertation are those of the author.

SIGNED: ……. DATE: ……..

Table of Contents

List of Figures

List of Tables

Chapter 1: Introduction

1.1. Acute coronary syndromes

Cardiovascular disease (CVD) is an umbrella term used to describe a group of disorders related to the heart and blood vessels. Encompassed within this anatomical classification are the following: coronary heart disease (CHD), coronary artery disease (CAD) and acute coronary syndromes (ACS). Coronary heart disease results from the pathogenesis of coronary artery disease, characterised by the accumulation of unstable atherosclerotic plaque (atheroma) within the vasculature (Sanchis-Gomar, Perez-Quilis et al. 2016).

The development of an atheroma within the coronary vasculature may be asymptotic, and therefore CAD may be unrecognised until a time at which symptoms arise. At advanced stages in the disease progression, whereby the accumulated atheroma is liable to rupture, the plaque and constituents may travel antegrade to occlude narrowing coronary vessels. The clinical manifestations attributed to this occlusion of coronary vessels include angina, shortness of breath, nausea and sweating (Lippi, Sanchis-Gomar et al. 2016). At this time, a patient presenting with these symptoms is likely to be suffering from an acute coronary syndrome (ACS) (Lippi and Cervellin 2016).

ACS is further sub-categorised into unstable angina (UA) or myocardial infarction (MI). The former refers to a partial occlusion that may dissolve to re-occlude the vessel further antegrade, nevertheless producing discomfort and perceived chest pain. MI refers to the total occlusion of a coronary vessel, whereby the heart tissue that is being served by the occluded vessel begins to die, a cellular process of necrosis resulting from ischaemic hypoxia (Konstantinidis, Whelan et al. 2012). Regardless of the relative severity of each acute coronary syndrome, these advanced stages of CVD progression are well known as the major player in the alarmingly high mortality rate attributable to these group of disorders.

1.2. Prevalence/incidence/mortality rates: A global perspective

Recent breakthroughs in medical technology have enabled clinicians to utilise novel, highly sensitive cardiac troponin immunoassays to more successfully and accurately diagnose MI (Carlsson, Bandstein et al. 2017). Consequently, the treatment and therapy of patients presenting with acute coronary syndromes in the developed world has improved drastically, and is reflected by the estimated 24-50% fall in overall mortality rate for CVD and CHD since 1975 (Sanchis-Gomar, Perez-

Quilis et al. 2016). However, CVD still remains the number one cause of death globally (World Health Organisation 2017) (Figure 1.1.).

In a 2019 update of heart disease and stroke statistics, the American Heart Association (AHA) reported that 18.2 million people residing in the United States over 20 years of age had CHD. Moreover, estimating that every 40 seconds an American will suffer an MI (Benjamin, Muntner et al. 2019). Similarly harrowing reports have existed for over a decade, long attributing CHD as a major cause of premature death and disability (Roger 2007). In addition, CHD is responsible for a third of all deaths in people older than 35 years of age (Nichols, Townsend et al. 2014). This prevalence and trend in mortality has long been reflected among similarly developed countries around the world (Levi, Lucchini et al. 2002).

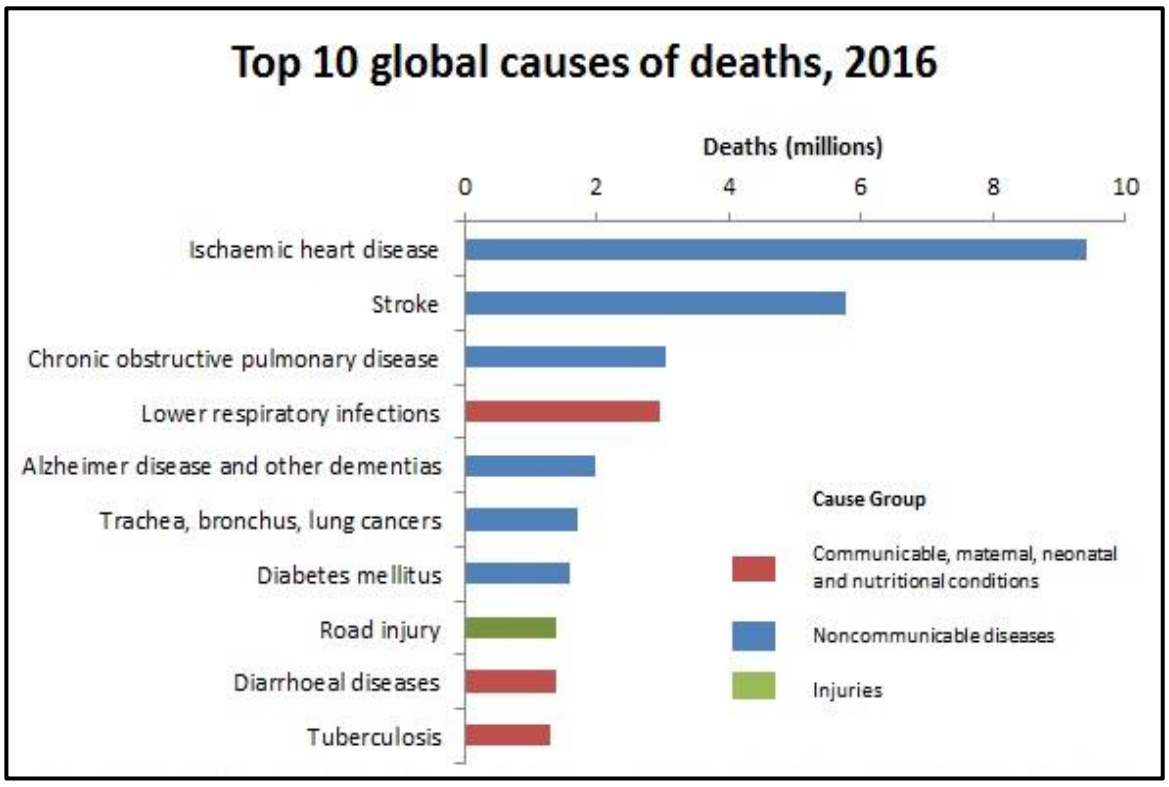

Figure 1.1. Top 10 global causes of death, 2016. Ischaemic heart disease and stroke are the top 2 causes of death, respectively (World Health Organisation 2017).

It is estimated that each year, 3.9 million Europeans are killed by CVD, accounting for 45% of the total mortality rate within the continent (Wilkins, Wilson et al. 2017). Further, the European Heart Network (EHN) estimates that more than 85 million Europeans were living with CVD in 2015. Additionally, the British Heart Foundation reports that acute coronary syndromes remain one of the

leading causes of death in the United Kingdom, aligning with similar trends in mortality rates within the developing world (Timmis 2015).

CVD is largely well-known as a preventable, non-communicable disease. Exposure to various risk factors that influence the progression of CAD; bad nutrition practices, physical inactivity and smoking are highly attributed to the development and progression of the disease (Danaei, Ding et al. 2009) (Figure 1.2.). Aligning with this, the EHN attribute dietary factors to provide the largest contribution to the risk of CVD mortality above all other behavioural factors (Wilkins, Wilson et al. 2017). Raised systolic blood pressure is one of the largest contributors in respect to risk of CVD and CHD (Yano, Stamler et al. 2015). As such, increased sedentary and obesogenic lifestyles within developed western countries may provide at least a partial explanation to the problem.

For example, the global fast-food industry has been projected to be valued at a staggering USD $843.4 billion by 2026 (ResearchStraits. 2019). Thus, highlighting the extent of the demand and abundance of relatively cheap, easily accessible, and unhealthy nutrition alternatives in an ever-expanding market of consumers. This draws insight into the correlation between comorbidities associated with obesity and resulting CVD (see Fig 1.2).

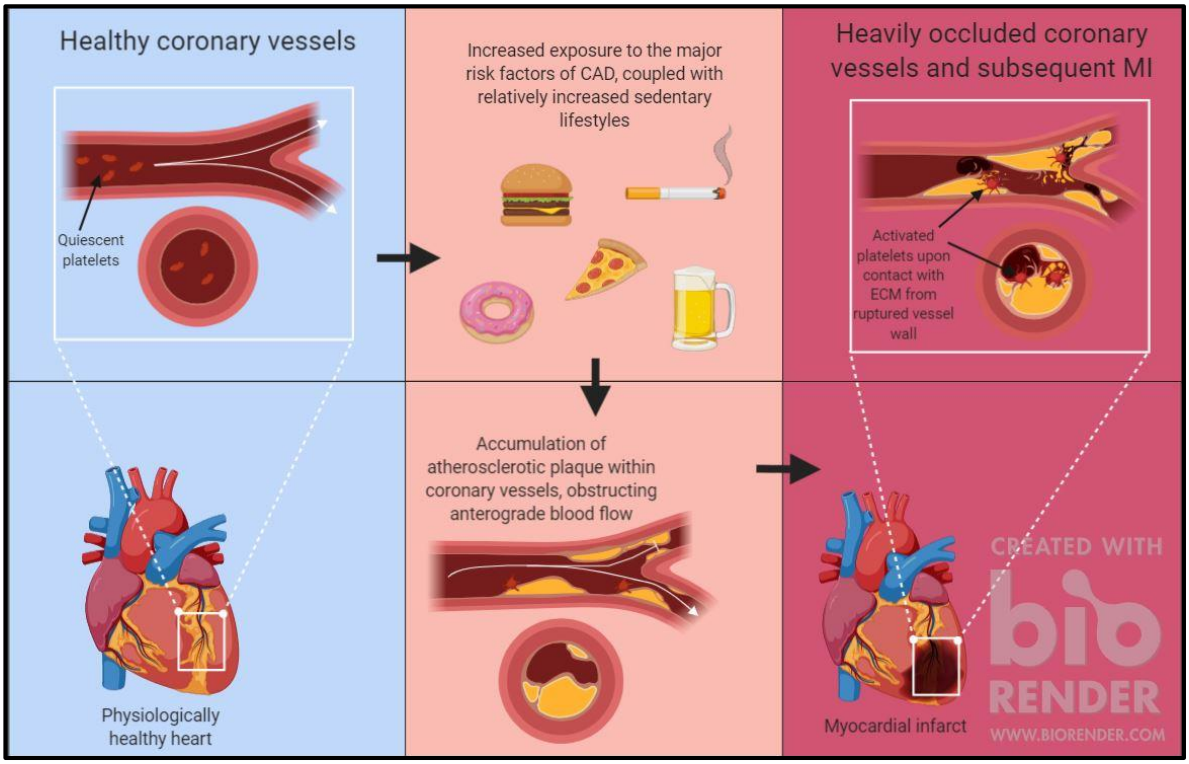

Figure 1.2. Pathogenesis of CVD and ACS. Healthy coronary vessels become occluded with the accumulation of atherosclerotic plaque, influenced by the contribution of various risk factors of CAD, eventually resulting in a myocardial infarct. Illustration created with BioRender.com

As developing countries begin to emerge on the world stage, and their growing populations become subject to increased post-modern industrialisation, it has been projected that CHD mortality will double from 1990 to 2020 (Okrainec, Banerjee et al. 2004). Okrainec and colleagues further suggest that rapid socioeconomic growth coupled with greater exposure to the risk factors for CAD, will compound with the relative lack of preventative measures available, to demonstrate similar trends in mortality and economic burden that exists within developed, western countries.

1.3. Economic implications

It is estimated that CVD generates a loss of €210 billion to the EU economy every year. Of that total loss; ~53% due to health care costs, ~26% to productivity losses and ~21% to the informal care of CVD patients (Wilkins, Wilson et al. 2017). Similar reports exist in respect to the cost of CVD to the economy of the U.S., a figure estimated to be approximately USD $213 billion (DeVol, Bedroussian et al. 2007). Collectively, these estimations reveal the gravity of the socioeconomic burden of CVD and consequently highlights the importance of mitigating the prevalence of the disease, additionally in the context of healthcare resource conservation.

Knowledge of the contributing behavioural and dietary factors implicated in the disease progression is understood by the general public with government-led public health intervention strategies to mitigate the rise of obesity-related CVD (Pell, Penney et al. 2019). For example, the introduction in the UK of the soft drinks industry levy (SDIL) in April 2018. The British government introduced additional taxation on high sugar-containing drinks to provide a tangible and concerted deterrence to the projected increased prevalence of obesity, targeting the beverage industry in the United Kingdom (Lifestyles Team 2019). Consequently, industry was incentivised to reformulate their respective beverages to align with government policy, where the increased revenue generated would be used as public health investiture for preventative initiatives and education regarding childhood obesity. The public health initiative sought to change individuals' unhealthy behaviour with the aims of improving their health and to conserve healthcare resources (Veliz, Maslen et al. 2019). Ultimately, the SDIL incentivises consumers to purchase less of the beverage whilst simultaneously igniting industry-wide reformulation, reducing sugar content. Proving to be a powerful and successful example of government-led deterrence, Public Health England (PHE) report that between 2015 and

2018, sugar content within drinks subjected to the SDIL decreased by 28.8% (Niblett, Coyle et al. 2019).

Public health initiatives in the form of taxation have long existed, similarly showing efficacy in decreasing consumption with regards to tobacco (Chaloupka FJ, Yurekli A et al. 2012) and alcohol (Elder, Lawrence et al. 2010). Although showing promise in the deterrence of the development of obesity with the example of the SDIL, it constitutes a relatively small concession in the array of contributing factors of CVD. Further, the beverage industry is merely a constituent of the problem where arguably, the fast food industry precedes (Bahadoran, Mirmiran et al. 2015). Thus, albeit a step in the right direction, the ability to tangibly decrease CVD prevalence rests with the consumer.

As developing countries emerge on the world stage, rapid socioeconomic growth and cultural shifts predicated towards more sedentary lifestyles, coupled with the projected growth of the global fast-food industry, the overall global prevalence of CVD and ACS appears unlikely to decrease with respect to time. Thus, the consideration that the disease is mutually exclusive to industrialised countries appears short-sighted. Therefore, the focus shifts towards the improvement of current interventional therapies available to patients that develop ACS, and by enhancing the collective understanding of the available pharmacotherapies to optimise their use within clinical practice, thus generating more positive patient outcomes that can be reflected globally.

Coronary vessel occlusion, underpinning the clinical manifestations of ACS, begins with the generation and propagation of an atheroma at the luminal wall of a coronary artery. The atheroma is comprised of accumulated fatty deposits and scar tissue that eventually grows large enough to either occlude the vessel itself, or rupture to occlude narrowing vessels further antegrade (Figure 1.2.). With the rupture of an atheroma, the extracellular matrix (ECM) of the vessel is exposed to circulating quiescent platelets within the blood. This leaves platelets liable to adhere to these thrombogenic extravascular sites, ultimately propagating the generation of arterial thrombosis (Jackson 2011).

Through a complex interplay of tightly regulated intracellular signalling pathways, mediated by several surface-expressed proteins and their respective ligands, the pathophysiology of platelet responses has been well-studied in the context of wound healing and primary homeostasis (Golebiewska and Poole 2015). However, due to the role platelets play in the context of vascular disease, they are implicated as being significant contributors to end-stage CVD.

1.4. Platelets and Megakaryocytes

Platelets (thrombocytes) are bioactive cellular fragments that enter the circulatory system after maturation steps of their progenitor, the megakaryocyte (MK). MKs are located within the bone marrow. The generation of MKs begins with a series of mechanistic steps of differentiation in haematopoietic stem cells (HSC). Consequently, the ability of HSC to commit their lineage to the maturation, and production of megakaryocytes relies on the presence of chemokines and other factors within their microenvironment. A process largely well known as megakaryopoiesis.

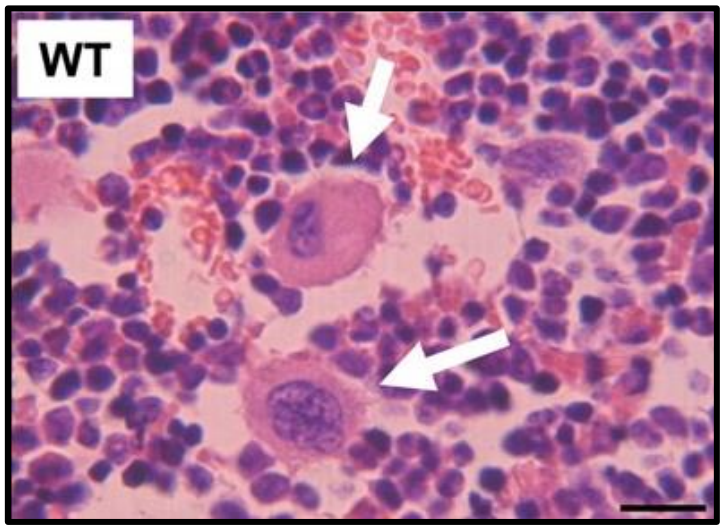

Figure 1.3. Megakaryocyte morphology. Confocal image of bone marrow sample. Megakaryocytes are indicated by the white arrows. Scale bar = 30µm. Authors grant permission for the re-use of this image in this thesis (Eckly, Strassel et al. 2009).

As a result of this tightly regulated differentiation, megakaryocytes perform their unique cellular process of maturation, endomitosis. A process extensively studied; the mechanism elucidated as an abortion of mitosis in late anaphase of the cell cycle, driven by thrombopoietin (TPO) ligand binding at MK-specific receptor, c-Mpl (Machlus, Thon et al. 2014) (Patel, Hartwig et al. 2005). The endomitotic nature of the MK cell cycle enables MKs to generate progressive polyploidy, accumulating large nuclear mass and additionally increasing cytoplasmic volume, without division (Geddis and Kaushansky 2006). Thus, mature MKs appear large morphologically at 30-100um in diameter, and can be characterised by their unique polylobate nucleus (Figure 1.3.), in addition to their invaginated membrane system (IMS) (Thon and Italiano 2012).

Derived from the plasma membrane, the IMS functions primarily as a membrane reservoir for the MK, permeating the cytoplasm and facilitating subsequent proplatelet evagination events. It is only after the maturation of the MK, that they begin to migrate from the osteoblastic niche within the

bone marrow, to subendothelial regions near venous sinusoids (Guo, Wang et al. 2015). Here, the MK elongates its proplatelet pseudopodia via the polymerisation of the microtubule cytoskeleton, initiated within the cell body, towards the periphery (Machlus, Thon et al. 2014). Consequently, the elongation of these cytoplasmic extensions penetrates the luminal wall of the endothelium, whereby the proplatelet extensions fragment, releasing thousands of nascent platelets into the bloodstream (Patel, Hartwig et al. 2005). This process continues with the successive budding of the MK cytoplasm, until eventually depleted and the entirety of the remaining cell body is transformed into proplatelets. Subsequently shed as platelets into the circulation, facilitated by shear from the luminal flow of blood (Guo, Wang et al. 2015). Thus, platelets can be thought of as fragmented, bioactive blood constituents of their precursor MK.

1.5. Platelet structure/ultrastructure

Platelet structure has been studied extensively, and is widely accepted as having a biconvex, discoid shape when quiescent. Typically measuring 2-3um in diameter, they are widely known to be the smallest constituent of whole blood and interestingly, one of the most numerous; 150,00-400,000/uL.

Although described as bioactive cytoplasmic fractions of the MK, they inherit organelles and specialised structures of traditionally described cells. Platelets have extensive plasma membrane expression of glycoproteins and contain inherited cytoplasmic structures from the MK; dense granules, alpha granules and lysosomes (Figure 1.4.). However, unlike traditionally characterised cells, platelets lack a nucleus. Additionally, they possess two distinct internal membrane systems. The dense tubular system (DTS) and the open canalicular system (OCS) (Rumbaut and Thiagarajan 2010).

The absence of a nucleus underscores the relatively expendable nature of platelets, unneeded after performing their functional responses in the context of vascular homeostasis. As such, the lifespan of the platelet is relatively short at just 10 days. Thus, the TPO-mediated proliferation and maturation of the MK is paramount in the biogenesis of new platelets.

The DTS exists as an internal membrane system for the platelet and is thought to be derived from the MK endoplasmic reticulum (Gerrard, White et al. 1978). Structurally, it can be thought of as thin and elongated membrane extensions within the platelet. It functions primarily as an intracellular sink for calcium that can be mobilised or sequestered and is implicated in various cellular processes (Fitch-

Tewfik and Flaumenhaft 2013). Membrane-expressed calcium channels mediate ionic flux from the DTS. Analogous to the ion channels in the sarcoplasmic reticulum of skeletal muscle cells. Importantly, the DTS lacks continuity with the outer surface of the plasma membrane and is only interconnected with the OCS at one or two sites, forming uncommon membrane complexes.

The OCS of the platelet is an additional internal membrane system, playing a critical role in the facilitation of various functional responses upon platelet activation. Continuous with the plasma membrane surface, the OCS permeates the cytoplasm of the platelet in the form of a network of interconnected tubular canaliculi (White and Clawson 1980).

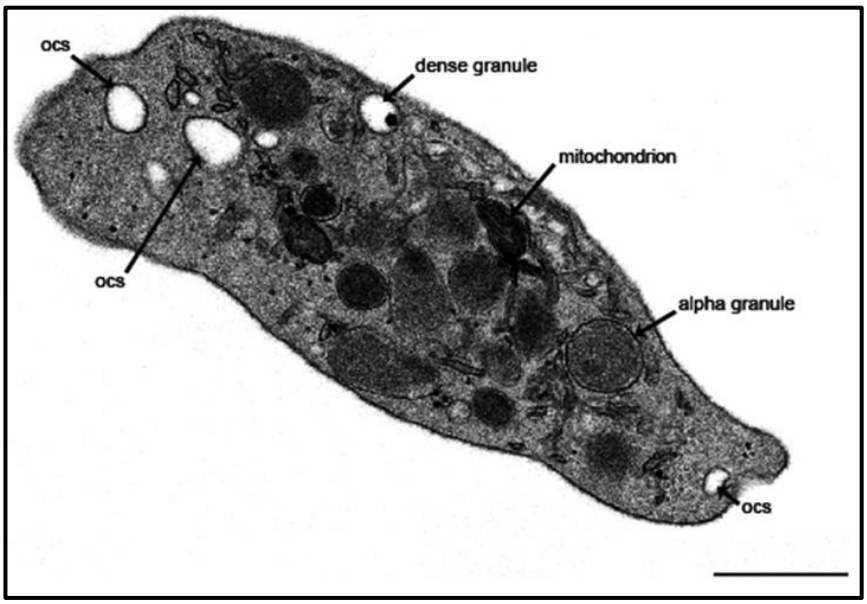

Figure 1.4. Platelet ultrastructure. TEM image of a human platelet, highlighting their unique intracellular features. Scale bar = 0.5um. Authors grant permission for the re-use of this image in this thesis (Selvadurai and Hamilton 2018).

The OCS lipid composition is identical to that of the plasma membrane of the platelet, invaginating to provide a source of membrane reserve. Additionally it contains numerous surface expressed glycoproteins (Selvadurai and Hamilton 2018). Further, the ability of the platelet to become activated and subsequently perform its functional responses relies heavily on the interactions of these glycoproteins with a wide range of substrates within their vascular niche.

Once released into the bloodstream, nascent platelets are inhibited from activation with the release of soluble nitric oxide (NO) and prostaglandin I_2 (PGI_2) from healthy endothelial cells (Jurk and Kehrel 2005). Thus, they are kept in a quiescent state until a time whereby the integrity of the vasculature

becomes compromised, facilitating initial adhesion events via one of their many types of surface expressed glycoproteins (GP), termed integrins.

Ultimately, the platelets' role as orchestrators of primary homeostasis pivots on the ability of the platelet to sense vascular damage within the microenvironment and to respond accordingly with the transduction of complex intracellular signalling cascades. Platelets initiate and propagating a series of functional responses: adhesion, activation, granule secretion and finally, aggregation.

1.6. Adhesion

Integrins constitute a superfamily of cell-surface GP receptors that are widely expressed in mammalian tissues. They exist as heterodimeric transmembrane GP complexes, consisting of 2 non-covalently bound alpha and beta subunits. Each respective subunit has a large N-terminal extracellular ectodomain and additionally contains a relatively short (20-60 amino acids) intracellular C-terminal tail that provides a docking site for various cytoplasmic proteins. Integrins allow platelets to initiate signalling cascades in response to the ligand in a bidirectional manner. Bidirectional transfer of information across the plasma membrane that facilitates inside-out and downstream outside-in signalling events, ultimately propagating platelet activation. Thus, although previously simply thought of as adhesion proteins, integrins serve as highly dynamic regulators of platelet cell function (Durrant, van den Bosch et al. 2017).

At the site of injury within the luminal wall of the vasculature, the ECM of the underlying sub-endothelium becomes exposed to the circulating constituents of the blood. Freely circulating von Willebrand factor (VWF) binds to the exposed collagen, effectively immobilising the soluble protein (Reininger, Heijnen et al. 2006). Consequently, platelets initially adhere to these thrombogenic pro-inflammatory sites, which serve as ECM ligands with affinity for the platelet-expressed GPIb-IX-V complex and GPVI. The (GP) Ib-IX-V exists as four subunits with the interaction of this complex with immobilised VWF facilitating the slowing of the platelets to the site of vessel injury (Li and Emsley 2013). Additionally, the interaction of GPVI and collagen initiates clustering of the integrins whilst concurrently increasing the affinity of integrins; α2β1 and αIIbβ3 (Nieswandt, Pleines et al. 2011). Therefore, once captured, the constituents of the glycoprotein coat play a major role as drivers of platelet activation.

1.7. Activation

During activation, the platelet undergoes drastic morphological changes resulting in the manipulation of its OCS. The invaginating membrane system functions as a reservoir for the platelet, facilitating a store of membrane that can be rapidly mobilised, crucial in the context of shape change. Thus, upon activation, the platelet rapidly undergoes cytoskeletal polymerisation events resulting in a change of shape from discoid to spherical, beginning with the disassembly of the circumferential microtubule ring, eventually generating outward projections of filopodia and lamellipodia (Paul, Daniel et al. 1999).

An additional consequence of platelet activation results in the priming of GP IIb/IIIa. The integrin exists as a heterodimer, consisting of an alpha (αIIb) and beta (β3) subunit (Rumbaut and Thiagarajan 2010). When resting, platelets express around 80,000 copies of the integrin on their surface, in an inactive 'closed' conformation. The integrins' nodular head of the ectodomain is kept in a bent over, 'V' shape, whereby the ligand binding site is inaccessible and kept in a low-affinity state (Durrant, van den Bosch et al. 2017). Once the platelet becomes activated, the integrin undergoes a conformational change in the headpiece whereby each subunit separates, exposing the ligand binding site and thus increasing affinity. Consequently, the integrin is liable to bind to a range of ligands such as vitronectin, fibronectin, VWF and notably fibrinogen.

These morphological changes of the OCS, in addition to the dynamic regulation of surface expressed integrins, enables the platelet to spread at the site of the injured vessel to increase its respective surface area, whilst generating an adhesive monolayer for the recruitment of additional platelets. Shape change is known to be reliant on the ability of the DTS to flux calcium, acting as an important substrate for the cytoskeletal and contractile machinery within the cytosol. Further calcium flux is implicated as a modulator of prostaglandin synthesis (Gerrard, White et al. 1978) and further facilitates the translocation of cytoplasmic alpha and dense granules and lysosomes to fuse with the plasma membrane, resulting in platelet secretion.

1.8. Secretion

The secretion of the cytoplasmic contents of the platelet is facilitated via a mechanism termed exocytosis. Upon platelet activation, granules become localised centrally whereby they may fuse with each other, a process termed homotypic fusion (Chen, Lemons et al. 2000).

Rapid cytoskeletal polymerisation of F-actin facilitates transport of the granules to the periphery of the platelet, interacting directly with soluble NEM-sensitive attachment protein receptors (SNAREs) (Woronowicz, Dilks et al. 2010). SNAREs are a significant element of the secretory machinery at the OCS/plasma membrane. However, not all SNAREs are the same. Classified according to their respective localisation to the outer membrane of vesicles (vSNAREs) or the cytosolic face of the target membrane (tSNAREs). Vesicle-associated membrane protein 8 (VAMP8) is known to be the most dominant in platelets. Platelet tSNAREs; SNAP-23, syntaxin 2 and syntaxin 4 regulating platelet granule secretion. Additionally, the involvement of SNARE-associated protein, Munc18 and the GTPase, RAB27b are implicated (Golebiewska and Poole 2015).

Alpha granules are the largest and most prevalent granules. Alpha granules primarily contain; larger polypeptides including chemokines, growth factors, adhesion molecules as well as factors involved in coagulation and aggregation (vWF and fibrinogen) (Rumbaut and Thiagarajan 2010). The smallest granules, termed dense granules, contain small molecules; serotonin (5HTP), calcium (Ca^{2+}) and additionally nucleotides; adenosine diphosphate (Figure 1.11.)(ADP) and adenosine triphosphate (ATP) (Rendu and Brohard-Bohn 2001). Once translocated to the plasma membrane, the contents are released into the OCS, eventually diffusing into the extracellular space.

Irrespective of the type of granule secreted, the purpose of their release is to ultimately enable the recruitment (chemotaxis) and further activation (amplification) of platelet responses. This is mediated by subsequent outside-in signalling via surface expressed G-protein coupled receptors (GPCRs). This, a well-described mechanism of positive feedback is a fundamental contributor to the platelets' final functional response after activation, aggregation.

1.9. Aggregation

Aggregation refers to the physical interaction between adjacent activated platelets via the molecular cross-linking of their respective 'primed' GP IIb/IIIa, bound by extracellular fibrinogen, forming a bivalent bridge (Figure 1.6). The released constituents of granule secretion act as endogenous ligands at a wide range of surface expressed GPCRs, with receptor activation initiating distinct intracellular signalling events that essentially converge, increasing the robustness of platelet responses. The positive feedback loop generated following secretion is critical for the facilitation of inside-out

signalling; ultimately resulting in dynamic changes within the platelet, bolstering their physiologically indicated effectiveness.

In the context of wound healing and primary haemostasis, this final functional response of aggregation is widely beneficial, resulting in the consolidation of the platelet plug, attenuating blood loss. However, in the context of metabolic disease that results in the generation of an atherosclerotic plaque liable to rupture (CAD), the platelet's aggregatory response directly implicates them as significant players in arterial thrombosis (Jackson 2011), which underpin the platelet contribution to the pathogenesis and clinical manifestations attributed to ACS. The complexity of the mechanisms underlying their functional responses is bolstered by the remarkable variety of membrane bound GPCRs, and their distinct signal transduction pathways.

1.10. The GPCR-G-protein complex

GPCRs constitute the largest class of membrane proteins existing in the human genome (Alexander, Christopoulos et al. 2019). They share a similar structure across all receptor types, consisting of a single polypeptide with an extracellular N-terminus, 7 membrane spanning hydrophobic helices and an intracellular C-terminus. Additionally, as alluded to within the name, these receptors signal through preferential coupling to distinct intracellular heterotrimeric G-proteins (Purves, Augustine et al. 2001).

G-proteins are heterotrimers, comprised of 3 subunits: alpha (α), beta (β) and gamma (γ). The α subunit containing a nucleotide binding pocket with GTPase activity. Whilst the β and γ subunits exist as a heterodimer (Gβγ). In unstimulated receptors, GDP is bound within the α subunit with Gβγ-association inhibiting GDPs release. This stabilises the heterotrimeric protein in an inactive conformation. Following GPCR activation, the G-protein complex binds to the stimulated GPCR; rapidly exchanging GDP for GTP. This results in the dissociation of the respective α and βγ subunits. Thus, the GPCR-G-protein complex becomes disassembled, and each subunit is free to activate various downstream effectors (Jastrzebska 2013).

G-proteins are classified into four subfamilies according to the structural similarity of their alpha subunits and the type of modulatory response that they are responsible for. The subfamilies are classified as the following: Gα*s*, Gα*i/o*, Gα*q/11* and Gα*12/13* (Jastrzebska 2013). Platelet receptor subtypes associate with specific monomeric G-proteins according to their respective function.

Hence, allowing tightly controlled modulation of various cytosolic target proteins. The differential coupling of the monomeric G-protein alpha subunits to the various receptor subtypes of; protease-activated receptors (PAR), Thromboxane receptors (TP), prostanoid receptors (IP) and crucially the purinergic receptors ($P2Y_1$ & $P2Y_{12}$) of platelets drives distinct intracellular signal transduction pathways stimulating platelet activation.

1.11. Endogenous inhibitory signalling

In an unperturbed vascular environment, endothelial cells (ECs) synthesise and constitutively release the endogenous prostaglandin, prostacyclin (PGI_2) as well as nitric oxide (NO) and other anti-inflammatory mediators (Kanthi, Sutton et al. 2014). The platelet utilises the former, an eicosanoid, as an agonist at the prostacyclin receptor (IP), resulting in Gαs-mediated signal transduction (Alexander, Christopoulos et al. 2019). Dissociation of Gαs directly stimulates the activation of adenylate cyclase (AC); a membrane bound enzyme responsible for the catalysis of ATP to cyclic adenosine monophosphate (cAMP). Receptor activation leads to an approximate 10-fold increase in cytosolic [cAMP]. This cAMP in turn robustly dampens pro-thrombotic signal transduction (Midgett, Stitham et al. 2011). This is further evidenced by studies demonstrating the powerful ability of prostacyclin to rapidly reverse platelet aggregation (Best, Martin et al. 1977).

Additionally, ECs generate and secrete NO facilitating vasodilation and additionally inhibiting the breakdown of cAMP via the inhibition of phosphodiesterases (PDEs) (Stalker, Newman et al. 2012). Moreover, EC's express an additional membrane protein responsible for modulating platelet responsiveness, CD39. This evolutionarily conserved ectonucleotidase catalyses extracellular ATP and ADP into AMP; concurrently degrading the pro-thrombotic ligand for the purinergic platelet receptors (ATP/ADP) whilst providing the cell an excess of substrate for inhibitory signal transduction (cAMP) (Kanthi, Sutton et al. 2014). Further, the generated adenosine resulting from nucleotide degradation; via CD39, acts as endogenous ligands for the Gαs-coupled adenosine receptor (A_{2A}). Activation of this receptor whereby activation similarly enhances generation of cAMP (Fuentes, Fuentes et al. 2018).

Ultimately, the ability of ECs to constitutively release endogenous ligands serves as a brake to the positive feedback signal amplification that results from the auto- and paracrine secretion of platelet granules following their activation.

1.12. Stimulatory platelet receptors

1.12.1. Protease activated receptors (PARs)

Protease-activated receptors (PARs) are unique GPCRs. They are activated following a proteolytic cleavage within their first extracellular loop, generating a new N-terminus that functions as a tethered ligand (Rivera, Lozano et al. 2009). The receptor relies on proteolytic cleavage to become activated. Endogenous serine proteases localised at sites of vessel injury, including thrombin, are responsible. In human platelets, stimulating PAR-1 and PAR-4 via thrombin generates a comprehensive range of responses that directly trigger platelet activation and subsequent aggregation. PAR-1 and PAR-4 are known to couple to both Gαq and G$\alpha_{12/13}$ (Rumbaut and Thiagarajan 2010). Thus, stimulating these receptors with the agonist thrombin, initiates 2 distinct signalling pathways attributed to each Gα subunit.

Gαq stimulates phospholipase C (PLC), catalysing the liberation of diacyl glycerol (DAG) and inositol triphosphate (IP_3) from membrane-bound phosphatidylinositol-(4,5)-bisphosphate (PIP_2). The products; DAG and IP_3, are second messengers, facilitating the downstream activation of protein kinase C (PKC) which in turn stimulates the release of Ca^{2+} from the DTS (Woulfe 2005). Conversely, G$\alpha_{12/13}$ dissociation results in the activation of the small GTPase, RhoA and Rho kinase (RhoK). Both are implicated in the phosphorylation of myosin light chain kinase (MLCK); crucial in the modulation and reorganisation of the actin cytoskeleton (Rivera, Lozano et al. 2009). Signalling mediated through both PAR receptors generates an increase of cytosolic, free Ca^{2+} that in turn is used by the platelet to increase the robustness of the functional responses enhancing platelet activation, shape change, secretion and aggregation. Interestingly, PAR-1 stimulation has additionally been suggested to activate Gαi (Kahner, Shankar et al. 2006). Thus, thrombin's ability to initiate such a wide array of platelet responses via the preferential coupling of the PARs, warrants its accurate description as a potent platelet agonist.

Importantly, platelets require mechanisms to control unrestrained stimulation of surface expressed GPCR's that results in aggregation. Thus, their reactivity can be mediated in several ways, initiating endogenous paracrine signalling mechanisms and additionally the modulation of critical second messengers, ultimately bolstering inhibitory signal transduction through GPCRs coupled to Gαs.

1.12.2. Thromboxane receptor (TP)

Adding to the complexity of platelet-endothelial signalling, EC's have the capacity to synthesise not only anti-thrombotic prostaglandins such as prostacyclin (PGI_2), but additionally the pro-thrombotic prostanoid, thromboxane A_2 (TXA_2) (Feletou, Cohen et al. 2010). The mechanism by which EC's generate these biologically active lipids is conserved among platelets, starting with the liberation of arachidonic acid (A.A.) from the plasma membrane via the activation of phospholipase A2. The generated A.A. can then be further metabolised with the initiation of the cyclooxygenase enzymes; COX-1 and COX-2, resulting in the production of biologically active PGH_2 (Rao and White 1985). Platelets and EC's are understood to express both COX-1 and COX-2, thus they can generate PGH_2, respectively. However, the eventual determination of prostaglandin type is mediated by the activity of various tissue- and cell-specific synthases. For instance, PGI_2 is synthesised as the predominate metabolite of EC A.A. degradation, facilitated by endogenous PGI_2-synthase (PGI_2S) (Feletou, Cohen et al. 2010). Conversely, in platelets, following their activation at sites of vascular injury, A.A. is rapidly metabolised into TXA_2 via thromboxane synthase.

Interestingly, the generated prostaglandin is stored in platelet dense granules and thus can participate in the autocrine-mediated stimulation of the platelet expressed Gαq-coupled thromboxane receptor (TP). Similarly, in respect to PAR signal transduction, TP activation enhances the stimulatory pathways implicated in platelet shape change and subsequent aggregation (Sangkuhl, Shuldiner et al. 2011). The concomitant release of ADP and ATP from dense granules enhances TP stimulation. However, unlike the TP-TXA_2 axis, secreted ADP acts as a potent platelet agonist at the platelet purinergic GPCRs, $P2Y_1$ and $P2Y_{12}$.

1.12.3. $P2Y_1$ receptor

ADP's contribution to platelet shape change and aggregation was first described in 1961 (Gaarder, Jonsen et al. 1961). Understanding of the molecular mechanisms resulting from subtype-specific receptor activation, remained elusive until the late 1990's. The first purinergic receptors to be cloned, the $P2Y_1$ receptor ($P2Y_1R$) activation was shown to participate in ADP-mediated calcium mobilisation and subsequent platelet shape change (Jin, Daniel et al. 1998). The $P2Y_1$ receptor has a similar intrinsic G-protein coupling to that of the TP receptor, Gαq. Animal studies have demonstrated that mouse platelets deficient in Gαq have a greatly impaired ability to cause shape change, Ca^{2+}

mobilisation and aggregation, resulting in increased bleeding times (Offermanns, Toombs et al. 1997). Additionally, $P2Y_1^{-/-}$ KO mice demonstrate similar phenotypic characteristics, however they interestingly retain the ability to aggregate upon ADP-induced platelet activation (Stalker, Newman et al. 2012).

These findings led to suggestions of an additional P2Y receptor, responsible for mediating platelet aggregation with mechanisms distinct to that of the coupling of $P2Y_1$. Pharmacological studies followed, demonstrating concomitant activation of another receptor was required to achieve maximal ADP-induced aggregation. Crucially, the thienopyridine compound; clopidogrel, was shown to not antagonise $P2Y_1R$ (Hechler, Eckly et al. 1998). A further study demonstrating patients presenting with a genetic deficiency of ADP-induced platelet aggregation, revealed that their $P2Y_1$ gene and associated DNA and mRNA were normal, further suggesting evidence of an additional P2 receptor with coupling to A.C (Leon, Vial et al. 1999). Previous studies had also described a patient with an inherited bleeding disorder with a limited and rapidly reversible platelet aggregation following ADP-stimulation (Nurden, Savi et al. 1995). Shortly thereafter, the molecular identity of the $P2Y_{12}$ receptor was similarly characterised by expression cloning and ligand screening (Hollopeter, Jantzen et al. 2001).

1.12.4. $P2Y_{12}$ receptor

The $P2Y_1$ and $P2Y_{12}$ receptors share phylogenetic and structural similarities, however they differ via their intrinsic G-protein coupling. The human $P2Y_{12}$ GPCR consists of 342 amino acid residues and is assembled at the plasma membrane as 7 transmembrane-spanning alpha helices with an intracellular C-terminal tail parallel to that of the lipid bilayer (Figure 1.5). The extracellular N-terminus contains glycosylation sites that have been suggested to participate in the modulation of receptor activity (Cattaneo 2015). The receptor additionally contains an H-X-X-R/K motif within transmembrane domain (TM) 6 and extracellular loop (EL) 3, important for receptor function (Scavone, Femia et al. 2017). This motif is highly conserved among the P2Y receptor subtypes, and believed to be a crucial in the extracellular recognition of nucleotides (Parravicini, Abbracchio et al. 2010). Naturally occurring mutations in $P2Y_{12}R$ structure were first described in 1992 with the observation of a patient presenting with life-long, excessive and prolonged bleeding times (Cattaneo, Lecchi et al. 1992). The receptor variant responsible for this phenotype seen in this patient was attributed to a homozygous,

2 base-pair (bp) deletion in the reading frame at position 294 of the receptor, causing a shift in the introduction of a stop codon, resulting in premature truncation of the protein.

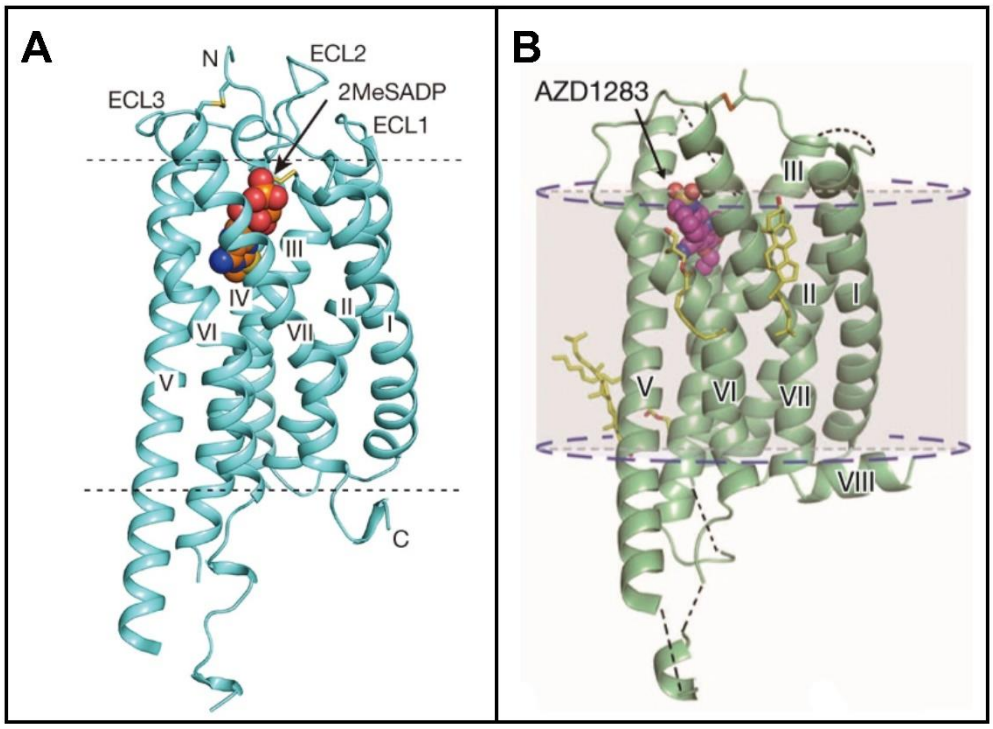

Figure 1.5. Crystal structures of the $P2Y_{12}R$ with agonist and antagonist binding. A) The crystal structure of $P2Y_{12}R$ showing agonist, 2MeSADP, ligand binding (3.5 Å) (Zhang, Zhang et al. 2014). B) The crystal structure of $P2Y_{12}R$, demonstrating binding of the non-nucleotide reversible antagonist, AZD1283, to the receptor protein (2.6 Å) (Zhang, Zhang et al. 2014).

More recently, studies have emerged demonstrating the importance of the cysteine residue at position 194 of the receptor (located within TM5) to be crucial in the binding of antagonists such as ticagrelor (Figure 1.5.B) (von Kügelgen, Lutz et al. 2014).

Additional naturally occurring mutations in $P2Y_{12}R$ structure have been described in patients presenting with similar lifelong history of excessive bleeding, attributed to single nucleotide polymorphisms of the receptor protein, R122C. The substitution of cysteine in place of arginine at position 122 of the receptor has been shown to be associated with impairment of $P2Y_{12}R$ function. This substitution occurs at a site at the boundary between TM 2 and ICL 2, termed the E/DRY motif and is suggested to be involved in GPCR activation and G-protein coupling (Rovati and Capra 2014). Interestingly, the R122C mutation has additionally been shown to impair the basal constitutive activity of $P2Y_{12}$. (Garcia, Maurel-Ribes et al. 2018). The $P2Y_{12}R$ has been shown to display a high degree of constitutive activity when overexpressed within cell based, *in vitro*, systems. Constitutive activity refers to the agonist independent GPCR isomerisation from an inactive conformation (R) into

an active, signalling conformation (R*). As such, constitutively active GPCRs have increased intrinsic G-protein activity (Seifert and Wenzel-Seifert 2002). It has been suggested that the constitutive activity observed with $P2Y_{12}$ may further sensitise the platelets of patients with type II diabetes mellitus, thus heightening their reactivity and limiting antiplatelet drug efficacy (Hu, Chang et al. 2017).

The $P2Y_{12}$ receptor ($P2Y_{12}R$) is G*αi/o*-coupled, activated upon ADP ligand binding. The resultant signal transduction is distinctive to that of the $P2Y_1$-ADP axis. Receptor activation via $P2Y_{12}$ initiates the dissociation of the G*αi/o* subunit from the βγ-dimer, whereby each subunit can elicit distinct intracellular cascades, ultimately facilitating aggregation.

The first arm of $P2Y_{12}$ signalling begins with the G*αi/o* subunit, directly inhibiting A.C. activity (Figure 1.6.). Consequently, intracellular cAMP synthesis is suppressed (Kahner, Shankar et al. 2006). The signal transduction initiated serves as a brake on the PGI_2-mediated cAMP synthesis, afforded by IP stimulation. Studies in mice lacking G*αi/o* had a significantly reduced ADP-induced platelet aggregation (Jantzen, Milstone et al. 2001). Additionally, patients with dysfunctional $P2Y_{12}$ expression suffer from a severe defect in A.C. inhibition and platelet aggregation. Moreover, the decrease in cAMP synthesis results in decreased activity of protein kinase A (PKA). PKA is responsible for a wide range of phosphorylation events of downstream effectors to provide an inhibitory effect on platelet adhesion, intracellular Ca^{2+} elevation, regulation of the cytoskeleton and platelet shape change (Wardell, Reynolds et al. 1989, Nakamura, Amieva et al. 1995, Yan, Li et al. 2009).

The second arm of $P2Y_{12}R$ signalling is governed by the Gβγ heterodimer and results in the modulation of an array of downstream effector proteins including phosphoinositide 3-kinases (PI3K), protein kinase B (Akt), Rap1b, Src-family tyrosine kinases (SFKs) and inwardly rectifying G-protein gated potassium channels (GIRKs) (Kahner, Shankar et al. 2006). The activation of these downstream effectors is vital in their contribution to platelet aggregation and culminates in co-operative reinforcement of the robust 'priming'; affinity modulation, and activation of the fibrinogen receptor: integrin $\alpha_{IIb}\beta_3$.

Phosphoinositide 3-kinases (PI3K) are a group of ubiquitously expressed signal transducer enzymes, whereby the prominent isoforms in platelets are PI3K-γ and PI3K-β (Kahner, Shankar et al. 2006). Transgenic mouse platelets deficient in PI3K-γ demonstrate significantly reduced fatal thromboembolism in response to ADP stimulation. Additionally, they exhibit a partial platelet

aggregation defect resulting from impaired fibrinogen receptor activation (Jackson, Yap et al. 2004, Guidetti, Canobbio et al. 2015). Pharmacological inhibitor studies targeting PI3K-β revealed it necessary in sustaining platelet aggregation, facilitating potentiation of agonist-induced granule release (Jackson, Schoenwaelder et al. 2005). Interestingly, PI3K has been found to additionally regulate integrin $\alpha_{IIb}\beta_3$ adhesive bond stability, directly potentiating aggregation under high shear. Irrespective of the PI3K isoform activated upon $P2Y_{12}R$ stimulation, they subsequently activate additional downstream effectors; crucially the Akt isoforms, that nevertheless converge into the concerted activation of the small GTPase; Rap1b (Figure 1.6.).

Protein kinase B (Akt) is a serine/threonine kinase with molecular weight of 57-kDa that becomes phosphorylated following ADP-induced $P2Y_{12}R$ stimulation, independent from $P2Y_1R$ signalling (Kim, Jin et al. 2004). Of the 3 isoforms known to exist in humans; Akt 1, Akt2 and Akt3, only the former; Akt1 and Akt2 are expressed in platelets. Their importance in platelet aggregation is suggested to directly modulate the function of integrin $\alpha_{IIb}\beta_3$ (Woulfe 2010). Both Akt isoforms utilise PIP_3; the lipid product generated from PI3K activity, to recruit crucial adaptor proteins to the plasma membrane, via a conserved pleckstrin homology (PH) domain (Guidetti, Canobbio et al. 2015). The most abundant, and arguably the most important, being that of Rap1b.

Subsequent downstream activation of the small GTPase from the Ras family; Rap1b, can be regulated directly by both PI3K isoforms. Moreover, the activation of Rab1b is understood to be further facilitated by guanine exchange factors (GEFs); primarily CalDAGGEFI, and GAP factor; Rasa-3. Rasa-3 exerts an inhibitory effect on Rab1b activation, restraining CalDAGGEFI signalling and thus keeping the platelet in a nascent state. Moreover, it has been suggested that the signalling afforded by $P2Y_{12}R$ activation is required for the inhibition of Rasa-3, therefore enabling sustained Rap1b activation and consequently facilitating thrombus formation (Stefanini, Paul et al. 2015). Regardless of the source of activation, Rap1b is responsible for modulating the interaction between the cytosolic domain of integrin $\alpha_{IIb}\beta_3$, with the subsequent recruitment of structural proteins; talin and kindlin (Durrant, van den Bosch et al. 2017). Ultimately, this promotes a conformational change within the integrin, separating the transmembrane domains to facilitate binding of various ligands with high affinity to the now revealed ectodomain (Guidetti, Canobbio et al. 2015).

Therefore, the now 'primed' $\alpha_{IIb}\beta_3$ can interact with a variety of ligands, fibrinogen, fibrin, vWF and fibronectin, enabling pro-thrombotic cross-linking between adjacent activated platelets via bivalent,

soluble fibrinogen, facilitating platelet aggregation. Thus, the importance of Rap1b to this end stage platelet functional response is critical and reflected as such in studies of Rap1b-deficient mice exhibiting impaired platelet aggregation in response to ADP and additionally, Rap1b-null mice showing an incapability to generate occlusive thrombi utilising an in-vivo model of carotid artery thrombosis (Chrzanowska-Wodnicka, Smyth et al. 2005, Kahner, Shankar et al. 2006).

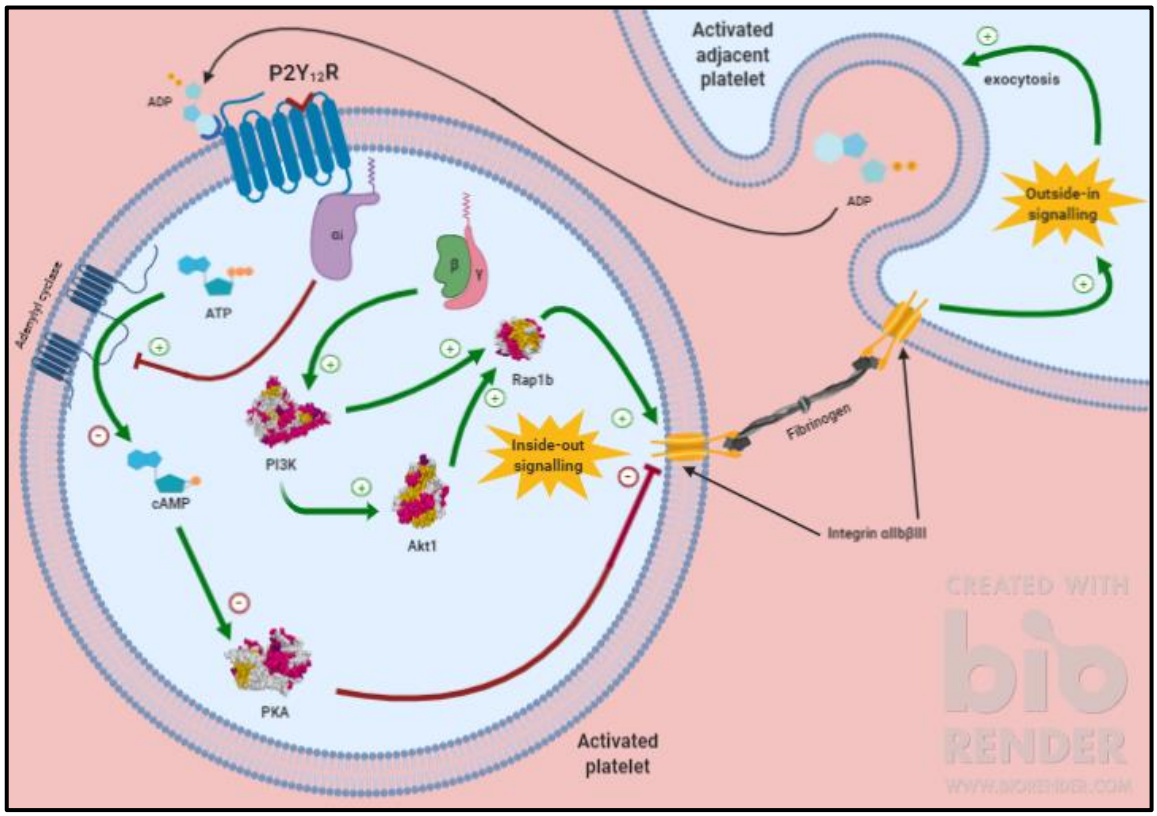

Figure 1.6. $P2Y_{12}$-mediated pro-thrombotic signalling elicited by endogenous agonist, ADP. Receptor activation with ADP causes a conformational change at the receptor level that initiates pro-thrombotic intracellular signalling, ultimately resulting in the activation of integrin $\alpha_{IIb}\beta_3$, facilitating platelet aggregation. Illustration created with BioRender.com.

Additionally, $P2Y_{12}$-Gβγ heterodimer dissociation is understood to be implicated in the direct activation of membrane bound G-protein-gated inwardly rectifying potassium channels (GIRKs). The Gβγ-activated channels have a crucial functional role as downstream effectors following $P2Y_{12}$ signal transduction. Their subsequent activation has been shown to contribute to the potentiation of Akt phosphorylation, dense granule secretion, irreversible platelet aggregation and ADP-induced TXA2 generation (Kahner, Shankar et al. 2006, Shankar, Kahner et al. 2006).

Due to the comprehensive array of pro-thrombotic platelet responses that can be directly elicited by ADP through the $P2Y_1$ and $P2Y_{12}$ signalling arms, P2Y-receptor activation is understood to be a fundamental contributor to ACS resulting from CVD pathogenesis. Unsurprising, considering $P2Y_{12}$'s

role in the formation of platelet aggregates. The ability to attenuate receptor activation and hence platelet reactivity, has made it an attractive target for antiplatelet pharmacotherapies.

1.13. Platelets and ACS pathology

The overall contribution of platelet functional responses in ACS pathology is complex and crucial. Responses are influenced by the localised concentration of auto- and paracrine secreted mediators from their environment, both pro- and anti-thrombotic. Platelet reactivity is modulated with this dynamic interplay of stimulatory and inhibitory signal amplification pathways. Moreover, the source of the stimuli that initiate the pro-thrombotic responses of platelets, is not present in healthy vessel walls. Thus, the inhibitory arm of signalling afforded by the surrounding EC's crucially keeps the platelets in an inactivated, quiescent state, until a time whereby their functional responses are needed and beneficial, i.e. - wound healing.

However, in the context of metabolic disease that results in the formation of unstable atherosclerotic plaque and consequential vascular occlusion, i.e. - ACS, the need for an antiplatelet agent to attenuate unwanted platelet activation and crucially $P2Y_{12}$-mediated aggregation, becomes paramount.

1.14. Percutaneous coronary intervention for acute coronary syndromes

When a patient is admitted to hospital and deemed to be suffering from an acute coronary syndrome; resulting from obstruction of normal coronary blood flow, percutaneous coronary intervention (PCI) may be performed, and is the current evidence-based standard of care within 12 hours of onset (Huynh, Perron et al. 2009, McCartney and Berry 2019). The procedure is carried out with the aim being to restore epicardial blood flow to oxygen-deprived cardiac tissue, termed reperfusion. The successful reperfusion of cardiac tissue is facilitated by the insertion of a stent within the artery that mechanically forces the occluded vessel lumen open (Dawkins, Gershlick et al. 2005). In any case, it is critical for the functional responses of platelets to remain inhibited for the duration of the procedure.

1.15. Antiplatelet agents

The current gold standard of care for patients with ACS, post-MI, is the use of dual antiplatelet therapy (DAPT), usually preceding percutaneous coronary intervention (PCI) and continued for up to 12 months after the intervention. This form of treatment consists of the combinatory therapy of aspirin and an oral $P2Y_{12}R$ inhibitor. As such, the benefit of DAPT versus the sole administration of aspirin has been reported in numerous large scale clinical trials and laboratory studies (2001, Cattaneo 2004, Mauri, Kereiakes et al. 2014). This has been suggested to be due to the different signalling pathways that each drug targets to elicit antithrombotic efficacy. For instance, aspirin targets the cyclooxygenase (COX) enzymes of platelets, a known generator of inflammatory intermediaries (Moscardo, Santos et al. 2011). Whereas $P2Y_{12}R$ inhibitors selectively target the pro-thrombotic signalling pathway initiated by $P2Y_{12}R$ activation (Figure 1.6). Resulting in a higher degree of platelet inhibition, although with a higher incidence of unwanted side effects such as major bleeding.

1.15.1. Aspirin

Aspirin, also known as acetylsalicylic acid (Figure 1.7.), elicits antiplatelet activity by a dose-dependent, irreversible inhibition of COX-1. In platelets, this selective inhibition prevents the conversion of A.A. to PGH_2 and thus, the formation of downstream TXA_2 leading to reduced TP receptor activity (Cattaneo 2004). Aspirin functions as an antiplatelet via its ability to dampen platelet activation by inhibiting the amplification pathway afforded by the TP-TXA_2 axis. However, due to the tissue distribution of the COX enzymes not being exclusive to platelets, aspirin can also inhibit the downstream production of anti-thrombotic PGI_2 by endothelial cells (Paez Espinosa, Murad et al. 2012). The optimal dose of aspirin in the primary prevention and management of major vascular events appeared controversial, until the emergence of the CURRENT-OASIS 7 trial. This demonstrated no difference in the risk of major bleeding complications in a head-to-head comparison of high-dose (>300 mg/day) and low-dose ($\leq$75-100 mg/day) aspirin (Mehta, Bassand et al. 2010).

The ability of aspirin to effectively inhibit platelet activation has cemented itself an essential place in the repertoire of antiplatelet agents available to clinicians. However, the need for additional antiplatelet agents that have mechanisms distinct to aspirin became apparent. This is due, in part, to the understanding of the contribution of the autocrine secretion of ADP acting as an agonist at the

pro-thrombotic purinergic receptor, $P2Y_{12}$, ultimately propagating the formation of platelet aggregates. Essentially, aspirin inhibits only one pathway of platelet activation whilst arguably more prothrombotic pathways exist. An additional drawback of aspirin alone in the prophylactic management of ACS is the incidence of patients allergic to the drug and moreover, the ability for patients to acquire aspirin resistance (Cattaneo 2004). So, despite the widespread use of aspirin, there became very evident drawbacks from sole administration as an antiplatelet.

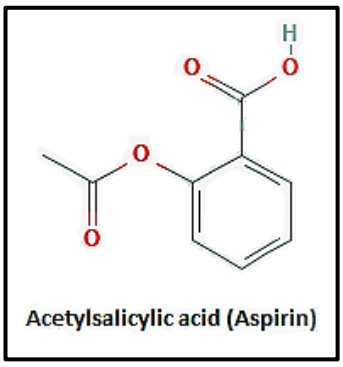

Figure 1.7. Chemical structure of acetylsalicylic acid (Aspirin). 2D-structure of aspirin, adapted to include compound name. PubChem identifier: CID 2244 (NCBI 2004).

1.15.2. Ticlopidine and clopidogrel

The documented antithrombotic success of ticlopidine, and later clopidogrel, heralded the potential of the $P2Y_{12}R$ pathway as a target for clinical drug development (Oestreich, Ferraris et al. 2013). Ticlopidine and clopidogrel belong to the thienopyridine class of antiplatelet agents, with a mechanism of action independent from aspirin. They both act as irreversible pharmacological antagonists with affinity to the $P2Y_{12}R$, and are similar in structure (Fig. 1.8 & 1.9) (Maffrand 2012). They both reduce the pro-thrombotic signalling that results from $P2Y_{12}R$ activation.

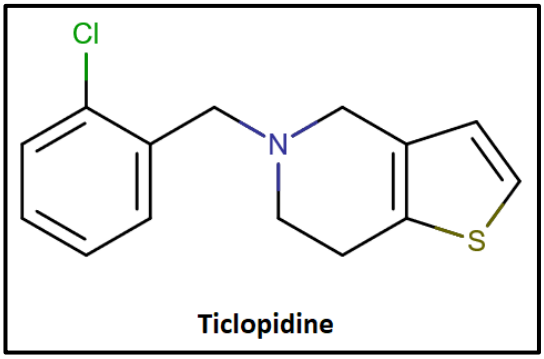

Figure 1.8. Chemical structure of ticlopidine. 2D-structure of the first generation thienopyridine, ticlopidine, adapted to include compound name. PubChem identifier: CID 5472 (NCBI 2005).

Indeed, clopidogrel's predecessor, ticlopidine, emerged as the first thienopyridine indicated for the reduction of thrombotic events in patients with ACS (MacKenzie 1977). However, several drawbacks were observed with its use. These included a high incidence of toxic effects, delayed onset of action and a remarkably high interindividual variability in response (Cattaneo 2006). Thus, clopidogrel superseded ticlopidine in the clinical setting, demonstrating a more favourable; less toxic, side effect profile. Clopidogrel does retain the delayed onset of action. Subsequently, a crucial study emerged assessing the effects of clopidogrel and aspirin coadministration. The PCI-CURE Study (Mehta, Yusuf et al. 2001). Interestingly, Mehta and colleagues conclude with compelling data; an overall reduction in cardiovascular death or myocardial infarction of 31% in clopidogrel-treated patients when compared to placebo-controlled.

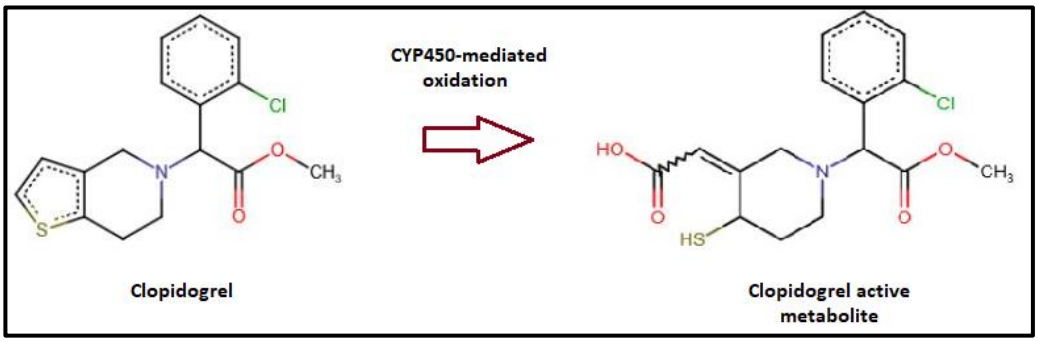

Figure 1.9. Chemical structure of clopidogrel and corresponding active metabolite. 2D-structures of clopidogrel before and following CYP450-mediated hepatic oxidation. PubChem identifier: CID 60606 and CID 10066813, respectively.

Despite showing promise as an effective adjunct to aspirin, and thus birthing the modern standard of care post-PCI; Dual antiplatelet therapy (DAPT), clopidogrel demonstrated some fundamental flaws that ultimately limited its therapeutic effectiveness. Like ticlopidine, clopidogrel is an oral pro-drug requiring hepatic metabolism to produce an active metabolite effective in the antagonism of $P2Y_{12}R$ (Maffrand 2012). The existence of clopidogrel non/low responders in ~ 50% of patients, demonstrated a significant interindividual variability in platelet inhibition. This was governed in part by the relative activity of the hepatic cytochrome P450 enzyme (Storey, Wilcox et al. 2002, Cattaneo 2004, Brandt, Close et al. 2007). Consequently, maximum inhibition of platelet reactivity is only reached 4-5 days after daily dosing of 75mg. Additionally, the ability for the active metabolite to irreversibly inhibit the $P2Y_{12}$ receptor raised concerns for patients requiring coronary bypass surgery due to the associated increase in blood loss, reoperation for bleeding and consequent prolonged intensive care unit stays (Cattaneo 2006, Cattaneo 2010). Despite generating $9.4 billion in global sales in 2010; the second best-selling drug for that year, these caveats in clopidogrel treatment

underscored not only the need for new antiplatelet agents to be developed, but highlighted the true market value and therapeutic benefit of these drugs in modern-day cardiovascular medicine (Maffrand 2012).

1.15.3. Prasugrel

Prasugrel is a newer generation of the thienopyridine class of oral drugs and similar in structure to that of ticlopidine and clopidogrel (Figure 1.10) (Cattaneo 2010). Prasugrel's conversion to the active metabolite, R-138727, has much less interindividual variances in hepatic metabolism when compared to clopidogrel (Farid, Payne et al. 2007). The reason for this variation in inhibition has been suggested to be due to the incidence of common loss of function polymorphisms in hepatic CYP-enzymes within 20-40% of the patient population. Specifically, the CYP2C19 and CYP2C9 variant genotypes fail to metabolise clopidogrel into the active metabolite. Conversely, prasugrel becomes rapidly hydrolysed within the blood stream via esterases. The product formed, thiolactone, requires a single further oxidation step that is facilitated by any of several different CYP-isoforms, bypassing the dependency of CYP2C19- and CYP2C9-mediated metabolisation. Therefore, the formation of the active metabolite of prasugrel is subject to less interindividual variation in $P2Y_{12}$R-inhibition (Brandt, Close et al. 2007). Consequently, the formation of the active metabolite is markedly increased in respect to that of clopidogrel (Payne, Li et al. 2007). Thus, prasugrel's onset of action is more rapid. $P2Y_{12}$R inhibition is seen within 15 minutes of dosing, producing greater mean inhibition of $P2Y_{12}$-mediated platelet responses, at much lower loading and subsequent maintenance doses than that of clopidogrel (Niitsu, Jakubowski et al. 2005).

In the randomised controlled trial, TRITON-TIMI-38; patients with ACS were treated with prasugrel or clopidogrel, in combination with aspirin. In summary, the study concludes a significant reduction in ischaemic events and stent thromboses of 27% and 57% respectively with prasugrel treatment versus clopidogrel (Wilcox, Iqbal et al. 2014). However, the incidence of bleeding complications in patients was higher in the prasugrel-treated group (13.4%) when compared to the clopidogrel-treated group (3.2%). Thus, although showing promise as a new, more potent thienopyridine being more efficacious than clopidogrel, prasugrel similarly failed to address the slow offset of action attributed to their use, due to the irreversible inhibition of the $P2Y_{12}$ receptor.

The most underscored and untenable side effect attributed to the thienopyridines collectively, is their irreversible inhibition of platelet function. Ultimately, this incapacitates platelets until they are

turned over and new platelets are synthesised. Thus, in a clinically relevant setting whereby a patient with ACS may need to undergo emergency coronary artery bypass grafting surgery (CABG), the need for fast-acting and crucially, reversible antagonists were suggested to be preferable in these acute situations (Nurden and Nurden 2003, Cattaneo 2006).

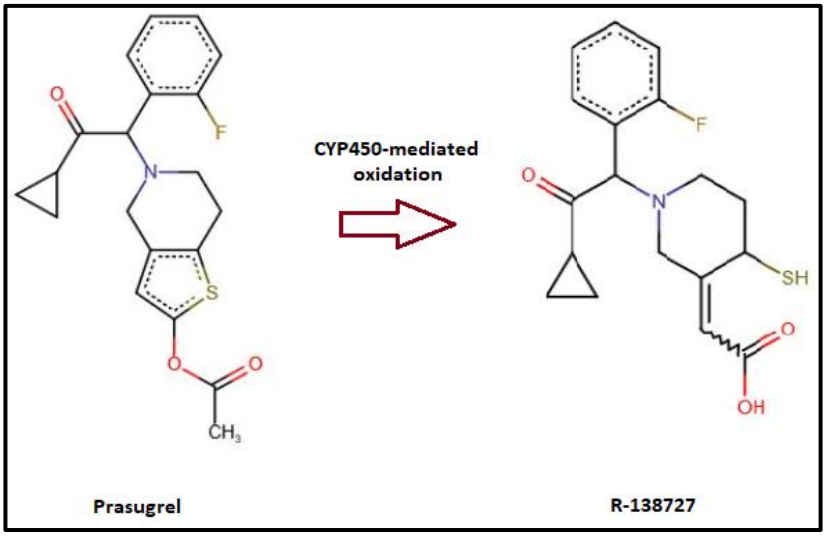

Figure 1.10. Chemical structure of prasugrel and active metabolite, R-138727. 2D-structures of prasugrel before and following CYP450-mediated hepatic oxidation. PubChem identifier: CID 6918456 and CID 10405534, respectively.

1.15.4. Cangrelor

Cangrelor is a potent and direct-acting $P2Y_{12}$ inhibitor, belonging to the novel nonthienopyridine ATP-analogous group of antiplatelet agents (Figure 1.11.) (Baker and Ingram 2015). The drug is different to the thienopyridines, not requiring hepatic metabolism to become activated. Crucially, the drug is reversible (Greenbaum, Grines et al. 2006). As such, the onset of action of cangrelor is rapid; peak plasma concentration reached within 2 minutes following intravenous (IV) bolus, achieving platelet inhibition greater than 90-95%. Additionally, it has a clinical half-life of less than 5 minutes; rapidly deactivated by plasma esterases (Cattaneo 2010, Angiolillo, Schneider et al. 2012, Baker and Ingram 2015).

In a pooled analysis of three pivotal comparative efficacy studies assessing the effectiveness of cangrelor against either clopidogrel or placebo in PCI (CHAMPION-PCI, CHAMPION-PLATFORM and CHAMPION-PHOENIX), the authors report cangrelor to reduce the odds of adverse outcomes by 19% and stent thrombosis by 41%. Ultimately, cangrelor reduced thrombotic complications in patients undergoing PCI, at the expense of increased bleeding (Bhatt, Stone et al. 2013, Steg, Bhatt et al.

2013). It must be noted, however, that although cangrelor clearly demonstrates superiority over the older thienopyridines, its use is limited largely due to its need for IV administration in peri-procedural situations: primarily as a bridge in treatment for patients undergoing surgery. Therefore, although addressing the fundamental caveats in thienopyridine treatment, cangrelor's efficacy is limited to a clinical setting. Thus, failing to fill the remaining gap in the need for an orally bioavailable, direct acting $P2Y_{12}$ inhibitor indicated for the long-term prophylactic treatment of ACS patients post-PCI.

1.15.5. Ticagrelor

Ticagrelor belongs to a new class of compounds, the cyclopentyl-triazolo-pyrimidines (Figure 1.11) made available to clinicians in the growing pharmacopeia of antiplatelet agents (van Giezen and Humphries 2005). The drug was ushered swiftly into the scientific literature, being described as a reversibly binding oral $P2Y_{12}R$ antagonist; the first of its kind (Husted and van Giezen 2009).

Synthesised by AstraZeneca; and previously known as AZD6140, the new class of drug was shown to have a unique binding site, non-competitive to that for ADP (Husted and van Giezen 2009, VAN Giezen, Nilsson et al. 2009). Unlike the thienopyridines, ticagrelor is reported to not irreversibly bind to $P2Y_{12}$. Therefore, there is no permanent conformational change at the receptor level that elicits zero intrinsic efficacy, as described by traditional drug-receptor theory of antagonism (Berg and Clarke 2018). Instead, ticagrelor's pharmacology is complex. As outlined above (1.12.4), the $P2Y_{12}R$ has a high degree of agonist-independent constitutive activity.

Elegant work from the Mundell laboratory and others indicated that ticagrelor was able to reduce agonist-independent receptor activity, indicating that it is an inverse agonist. In addition, ticagrelor demonstrates an off-target blockade of equilibrative nucleoside transporter 1 (ENT1); resulting in the accumulation of extracellular adenosine (Aungraheeta, Conibear et al. 2016).

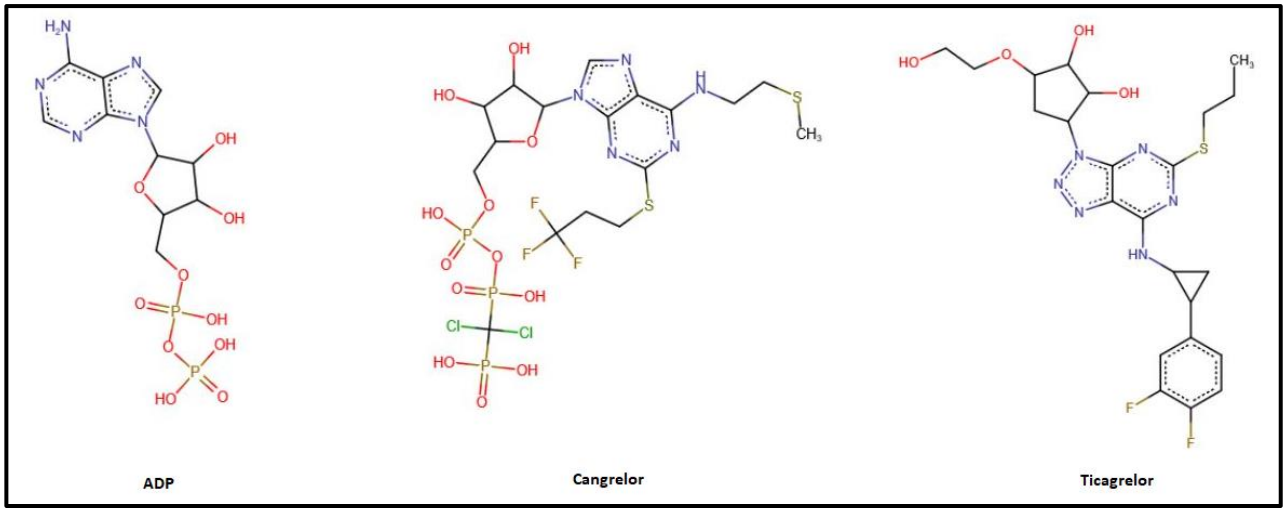

Figure 1.11. Chemical structures of ADP, cangrelor and ticagrelor. 2D-structures of ADP, cangrelor and ticagrelor. PubChem identifiers: CID 6022, CID 9854012 and CID 9871419, respectively.

The safety, efficacy and tolerability of ticagrelor was initially assessed by the DISPERSE trial (Cannon, Husted et al. 2007). The study involved patients with ACS, currently receiving aspirin; 75-100mg/day, and were switched to either ticagrelor (100mg/day) or clopidogrel (75mg/day) for 28 days. The authors established that ticagrelor inhibited platelet aggregation more rapidly and consistently than clopidogrel. However, ticagrelor did cause an increase in the incidence of moderate and minor bleeding that appeared dose related. Additionally, the drug was reported to cause dose-related adverse effects including headache, dizziness and interestingly, dyspnoea. In a sub-study of the DISPERSE trial (DISPERSE-2), ticagrelor use was associated with asymptomatic ventricular pauses (>2.5s) and additionally confirmed the increased incidence of dyspnoea (Storey, Husted et al. 2007).

The clinical superiority and effectiveness of ticagrelor over clopidogrel was further investigated. In the pivotal phase III PLATelet inhibition and patient Outcomes (PLATO) trial (James, Akerblom et al. 2009). In summary, the findings of the study were consistent with that of the TRITON-TIMI-38 study with ticagrelor showing greater antithrombotic efficacy over clopidogrel. However, following discontinuation of either ticagrelor (24-72 hours; last dose) and clopidogrel (5 days; last dose), both treatments exhibited similar incidences of bleeding during PCI or CABG.

Ultimately, the data from these studies indicate clopidogrel to be a superior adjunct to aspirin post-MI. This ushered in new guidance from the national institute of health and care excellence (NICE), recommending low dose ticagrelor as an adjunct with aspirin for as long as 3 years (Wise 2016). Ticagrelor is now described as the new gold standard of DAPT care. NICE have contraindicated the drugs' use in patients presenting with pathological bleeding, history of intracranial bleeding and

hepatic impairment. Thus, although addressing some of the existing limitations of the older thienopyridines, major bleeding and bleeding associated during emergency invasive procedures such as PCI, remain a pertinent clinical concern with ticagrelor, as all anti-platelet agents.

1.16. Drug switching

The rapid expansion of antiplatelet agents available to patients with ACS has enabled clinicians to have a greater degree of choice in tailoring treatment relevant to specific clinical scenarios. Therefore, it is not uncommon for switching to occur between the inhibitors and as such, concerns arise over the safety of the drug-drug interactions (DDIs) that may occur with their concomitant drug administration.

This culminated in an international expert consensus paper, with the goal to provide guidance on how and when to switch therapies (Angiolillo, Rollini et al. 2017). A comprehensive guideline of recommendations for switching therapies has been generated, underpinned by the crucial pharmacodynamic characteristics attributed to each $P2Y_{12}$ inhibitor. Ultimately, the modalities are defined broadly as:

i) Escalation; from a less intensive to a more intensive drug (clopidogrel to ticagrelor or prasugrel, respectively)
ii) De-escalation; vice versa (ticagrelor or prasugrel, to clopidogrel)
iii) Or change; switching between two similarly efficacious agents (ticagrelor to prasugrel) (see Figure 1.12).

Therefore, an accurate characterisation of the pharmacodynamics of each respective anti-platelet agent; mode of action, “onset” and reversibility, becomes paramount when considering their clinical expectations and reflected patient outcomes.

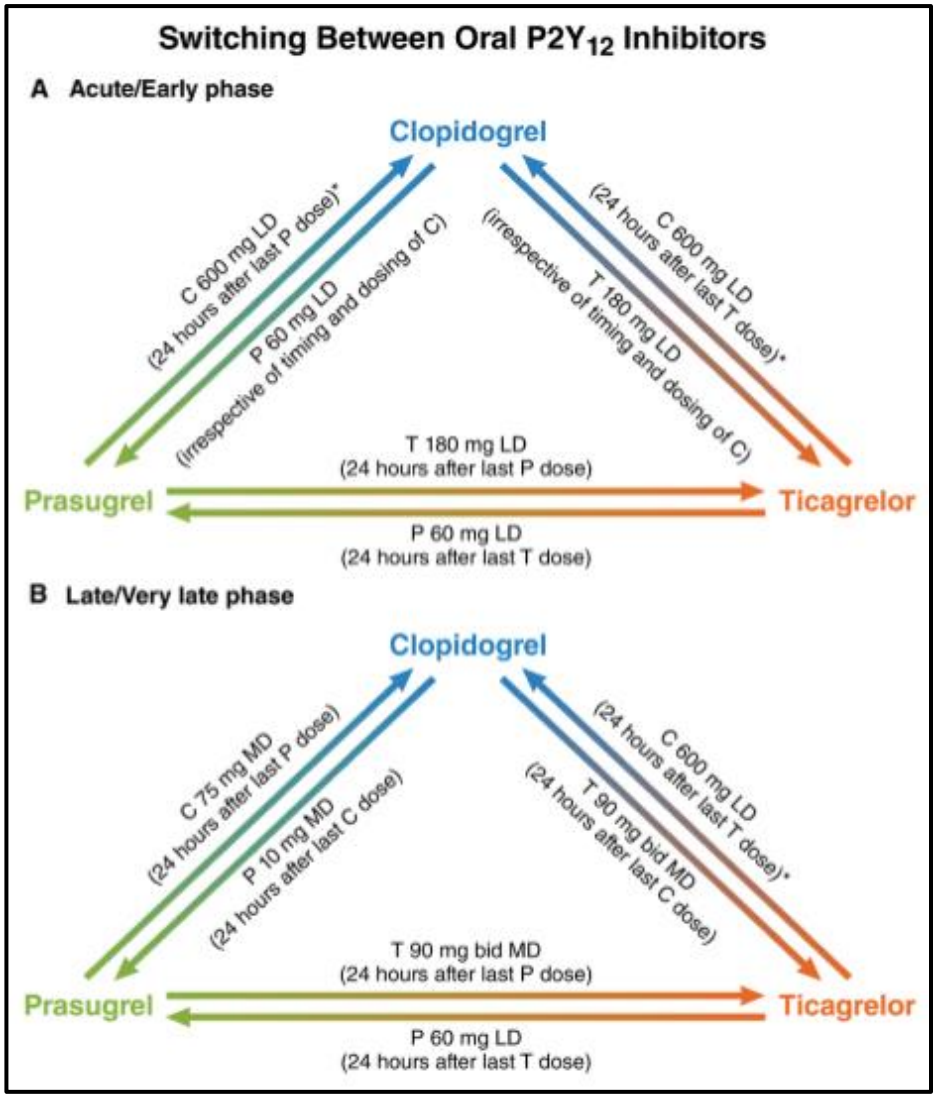

Figure 1.12. Recommendations for switching between oral antiplatelet agents. A) Recommendations for switching between oral $P2Y_{12}R$ inhibitors in the acute/early phase of treatment ($\leq$30 days post index event). B) Recommendations for switching between oral $P2Y_{12}R$ inhibitors in the late/very late phase of treatment (>30 days post index event) (Angiolillo, Rollini et al. 2017).

1.17. Research Aims

As outlined above, the pharmacodynamics of the currently available antiplatelet agents available to physicians must be clearly and accurately defined for their use to be safe, and beneficial in a clinical setting, whereby switching between therapies is common. Therefore, the potential for DDI's in respect to their concomitant administration must be considered, particularly with the newer and more efficacious, ticagrelor.

The pharmacodynamics of ticagrelor are still under investigation and debate, with questions raised regarding the inconsistencies in reversibility of drug administration within the clinical setting (Bhatt, Pollack et al. 2019, Zhang, Xu et al. 2019). Thus, the aim of this thesis was to investigate two interrelated hypotheses to help inform this discussion.

1) Ticagrelor, unlike other $P2Y_{12}R$ antagonists is an inverse agonist at the human purinoceptor, $P2Y_{12}$, attenuating basal signalling activity.
2) Ticagrelor is not reversible versus the endogenous $P2Y_{12}R$ agonist, ADP.

To examine these hypotheses, this study consequently aims to:

1) Further characterise ticagrelors pharmacodynamics at the receptor level, *in-vitro*, utilising cell lines and $BRET^2$ technology.
2) Examine the efficacy of ticagrelor administration in isolated human platelets, *ex-vivo*, utilising light transmission aggregometry.

Chapter 2: Materials & Methodology

2.1. Materials

Name	Species	Description
HEK293T	*Homo sapiens*	Transformed human embryonic kidney cells that express SV40 large T antigen.
Human platelets	*Homo sapiens*	Isolated from donated whole blood as described in 2.2.1.

Table 2.1. Mammalian cell line/cell types utilised in this study.

Plasmid construct	Species	Gene name	Concentration (µg/µl)	Volume (µl)
FLAG-$P2Y_{12}$	*Homo sapiens*	P2RY12	0.21	4.80
Gα	*Homo sapiens*	GNAi1	0.513	1.95
Gβ	*Homo sapiens*	GNB1	0.65	2.30
Gγ	*Homo sapiens*	GNG2	0.825	1.82

Table 2.2. Plasmid DNA constructs: species, gene name, respective concentrations and volumes utilised for transient cell transfection.

Vector	Description	Source
PcDNA^{TM}3.1	5.4 kb; Human cytomegalovirus immediate-early (CMV) promoter, neomycin resistance gene.	ThermoFischer Scientific

Table 2.3. Plasmid vector utilised in this study, its description and source.

Consumable	Supplier
Pipettes: 1-10 µL, 20-200 µL, 200-1000 µL	Gilson
Serological pipettes: 5 mL, 10 mL, 25 mL	ThermoFischer Scientific, USA
Cell culture dishes: 100 mm x 20 mm	Corning, Germany
Centrifugation vials: 10 mL	ThermoFischer Scientific, USA
96-well cell plates	Greiner bio-one, Austria
Falcon tubes: 15 mL, 50 mL	BD biosciences
Eppendorf tubes: 0.5 mL, 1.5 mL, 2 mL	Eppendorf
Pipette controller: Pipetboy 2	Integra
Syringes/Hypodermic needles	BD biosciences
Pipette tips: 10 µL, 200 µL, 1000 µL	Corning/Rainin/STARLAB

Table 2.4. Laboratory consumables and their supplier.

Compound	Description	Supplier
Ticagrelor	$P2Y_{12}R$ antagonist	AstraZeneca, Sweden
AR-C66096 tetrasodium salt (clopidogrel active metabolite)	$P2Y_{12}R$ antagonist	Tocris, UK
Cangrelor	$P2Y_{12}R$ antagonist	Tocris, UK
R-138727 (prasugrel active metabolite)	$P2Y_{12}R$ antagonist	Sigma-Aldrich, UK
Xanthine amine congener (XAC)	Non-selective adenosine receptor antagonist	Tocris, UK
Adenosine 5'- diphosphate (ADP)	$P2Y_{1/12}R$ agonist	Sigma-Aldrich, UK
U46619	TP receptor agonist	Tocris, UK
Dimethyl Sulfoxide (DMSO)	Aprotic solvent	Sigma-Aldrich, UK
Forskolin	Direct stimulator of adenylate cyclase activity	Tocris, UK

Table 2.5. Compounds utilised in this study, their description and supplier.

Reagent	Description	Supplier
Apyrase	Enzyme catalysing the hydrolysis of ATP, yielding AMP and organic phosphate	Sigma-Aldrich, UK
Penicillin	Antibiotic for the prevention of bacterial contamination	Gibco
Streptomycin	Antibiotic for the prevention of bacterial contamination	Gibco
Indomethacin	Non-selective cyclooxygenase inhibitor	Sigma-Aldrich, UK
Lipofectamine™ 2000	Transfection reagent	ThermoFischer Scientific, USA
Coelenterazine 400a	Luciferin; substrate for Renilla reniformis (RLuc)	InSight Biotechnology, UK
Trypsin-EDTA	Cell-dissociation reagent	Gibco
Acid citrate dextrose (ACD)	Blood anti-coagulant	BioSight Ltd, Israel
Ethanol	Solvent	Honeywell, UK
Dulbecco's modified eagle medium (DMEM)	Synthetic cell culture medium for the maintenance and proliferation of cells	Sigma-Aldrich, UK
Tyrode's HEPES buffer	Isotonic buffer solution; pH 7.3	Technical staff; University of Bristol, UK
Phosphate-buffered saline (PBS) (1X)	Isotonic buffer solution; pH 7.4	Sigma-Aldrich, UK
Opti-MEM reduced serum media	Cell culture medium for cationic lipid transfections	Sigma-Aldrich, UK

Table 2.6. Reagents used in this study, their description and supplier.

2.2. Methodology

2.2.1. Human platelet isolation

Human blood was donated by healthy, consenting volunteers in accordance with the University of Bristol's Ethics of Research Policy and Procedure, adhering to and aligning with the WMA Declaration of Helsinki.

Donation of human blood was performed via venipuncture, with the use of a butterfly needle affixed to a 50 mL BD Plastipak ™ syringe that was pre-filled with 10% sodium citrate. The collected blood was dispensed equally into LP4 tubes (Appleton Woods, UK), sealed and centrifuged at 161 x g for 17 minutes (Heraeus Megafuge, ThermoFisher Scientific), consequently isolating platelet-rich plasma (PRP). Isolated PRP was then collected and dispensed into a 15 mL Falcon tube (Corning, Germany), where the addition of 0.02 U/mL apyrase and 10 µM indomethacin was included. Following this, the determination of platelet density was calculated utilising the Z1 Coulter particle counter (Beckman Coulter, UK), and platelet concentration was adjusted to $4x10^8$/ml. The PRP-containing falcon tube was incubated via water bath at 30°C for 30 minutes prior to the commencement of light transmission aggregometry (LTA) experiments (Figure 2.1. 1-4).

Remaining blood within the LP4 tubes were centrifuged once more at 465 x g for 10 minutes to separate the platelet-poor plasma (PPP) from the remaining blood constituents. PPP was then collected and transferred to a 1.5 mL Eppendorf tube and further centrifuged at 161 x g for 5 minutes, and the supernatant collected. Whilst collecting the centrifuged PPP supernatant, care was taken not to aspirate any pelleted blood constituents that may have formed following the centrifugation. 240 µL of PPP was dispensed into a 450µL P/N 312 cuvette (Chrono-log corporation) and subsequently diluted with 60 µL of HEPES Tyrode's buffer to make a total volume of 300 µL. This resulting cuvette of diluted PPP was then used as the optical density reference value with respect to unstimulated PRP, due to the lack of aggregatory response resulting from the absence of platelets in PPP following centrifugation.

2.2.2. Light transmission aggregometry (LTA)

To investigate the inhibitory effect of ticagrelor on the functional response of platelet aggregation following stimulation with ADP, light transmission aggregometry experiments were performed utilising an optical lumi-aggregometer (Chrono-log model 700, Chrono-log Corporation). Light transmission aggregometry is a widely utilised diagnostic tool to assess platelet function *ex-vivo* and facilitates the evaluation of anti-platelet therapy efficacy (Hvas and Favaloro 2017).

PRP was dispensed into consecutive P/N 312 cuvettes (Chrono-log corporation) (Fig 2.1. 5-6) where reactions were performed within a total final volume of 300 µL. The inclusion of a stirring bar within each PRP-containing cuvette was mandatory; with an angular speed of 161 x g, indicative of high shear stress conditions resulting from laminar flow within vasculature. 30 µL of 100 µM inhibitor/antagonist (10 µM) was added to 240 µL of unstimulated PRP and allowed to incubate for 2 minutes within the heated optical reading chamber, at 37°C. Once in place, warmed PRP-containing cuvettes within the lumi-aggregometer were baselined with respect to the PPP-containing cuvette. Following the elapsed incubation time of the antagonist, 30 µL of 100 µM ADP (10 µM) was included, stimulating the platelets. Immediately after the addition of the agonist, measurements were started within the Aggrolink8 software, recording aggregation (%) with respect to time (mins) (Figure 2.1. 5-6).

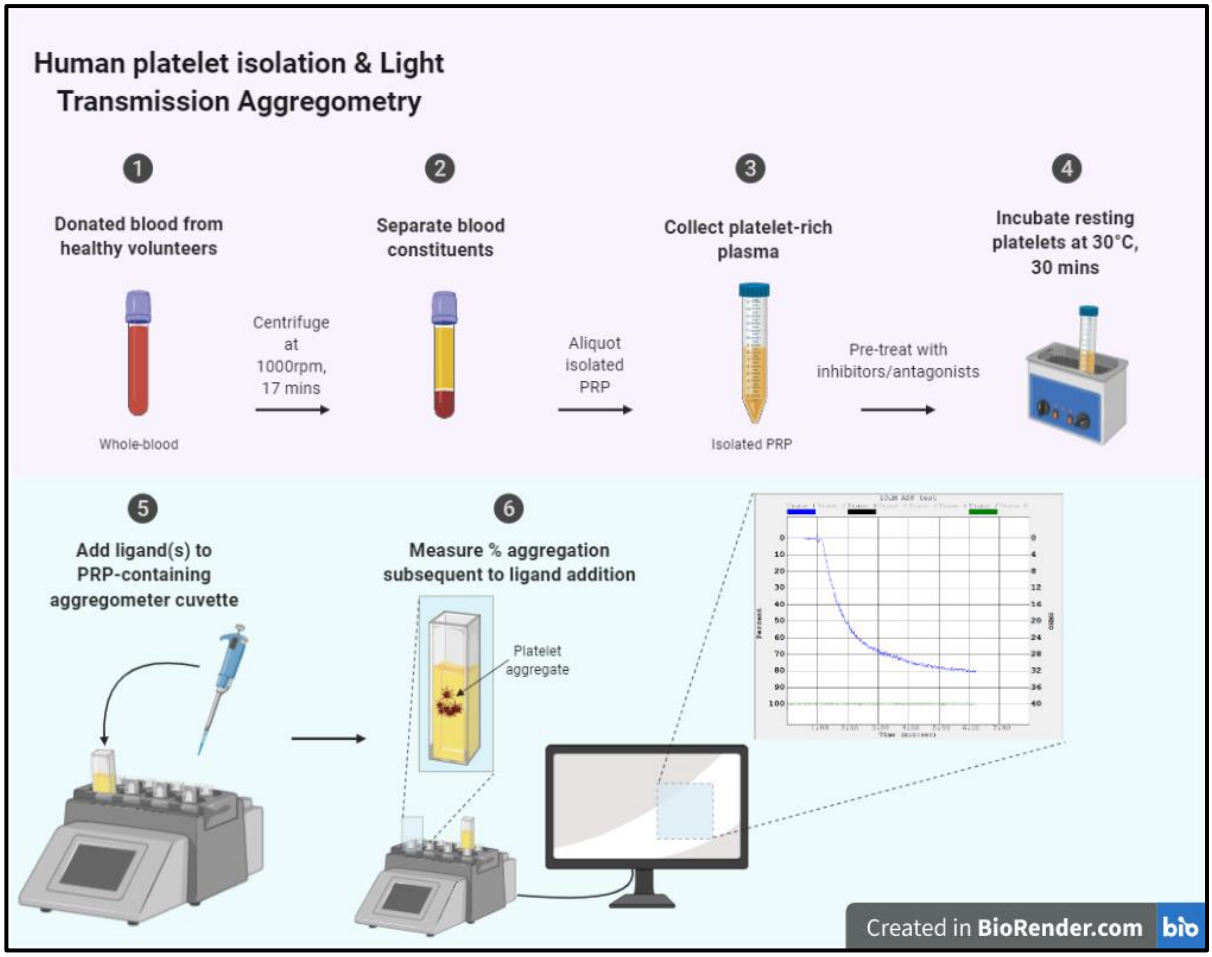

Figure 2.1. Human platelet isolation & light transmission aggregometry. Simplified illustration of platelet isolation (1-4) followed by light transmission aggregometry (5 & 6). Illustration constructed in BioRender.com.

2.2.3. Sterilisation

Where appropriate, lab consumables were sterilised by autoclave at 120°C. Where autoclaving was not deemed appropriate; for buffers and media, sterilisation was performed by filtration with the use of a 250 mL vacuum filter bottle system, 0.22µm pore (Corning, Germany). Mammalian cell culture methods were performed under strict aseptic technique, within a fume hood that was sterilised with 70% ethanol before and after use.

2.2.4. Mammalian cell culture

HEK293T cells were maintained in a humidified incubator, supplemented with 95% O_2 and 5% CO_2 at 37°C. The proliferation of cells was done so in 100 mm x 20 mm dishes (Corning, Germany) with Dulbecco's Modified Eagle medium (DMEM); supplemented with 10% foetal bovine serum (FBS), 2 mM glutamine, 100 µg/mL streptomycin and 100 U/mL penicillin.

Cell confluency was assessed via tabletop microscope (Nikon, UK), where approximately 90% coverage was determined to be ready for cell passage. Spent media was aspirated and removed from the 100 mm x 20 mm dishes and 3 mL of PBS was subsequently dispensed to the inside wall, with the intention to wash the cells whilst minimising their disruption. Following the washing of cells, spent PBS was subsequently aspirated and discarded. 1 mL of pre-warmed trypsin-EDTA was introduced directly to the cells, and the 100 mm x 20 mm dish subsequently incubated in humidified conditions at 37°C for 2 minutes, facilitating the dissociation of cells. Following the elapsed 2-minute incubation, care was taken to ensure that the cells were sufficiently detached from the dish in which they were contained. After this determination of successful detachment of cells, 3 mL of pre-warmed DMEM was introduced, inactivating any aberrant trypsin activity. Detached cells were then homogenised within the introduced DMEM, creating a cell suspension that was subsequently transferred to a 10 mL vial and centrifuged at 161 x g for 3 minutes.

Care was taken to ensure that the cell pellet that formed upon centrifugation was left undisturbed whilst aspirating and discarding the supernatant. Following this, 1 mL of additional pre-warmed DMEM was introduced and the cell pellet subsequently re-suspended. Appropriate volumes of this cell suspension were then used to determine the extent of time taken to reach 100% confluency of the next passage. Fresh 100 mm x 20 mm dishes were prepared and 9 mL fresh DMEM dispensed into each, respectively. The re-suspended cells were then dispensed into to the new DMEM-containing dishes, according to the volume deemed appropriate. For example, 500 - 600 µL of the cell suspension added to a new 100 mm x 20 mm dish; containing 9 mL fresh complete media (DMEM), was determined to be 1:2 in respect to the original 1000 µL cell suspension. The new dish was subsequently incubated in humidified conditions at 37°C, supplemented with 95% O_2 and 5% CO_2. The maintenance and passage of HEK293T cells was performed regularly, generating a constant supply of cells suitable for efficient transient transfection with our receptor of interest, $P2Y_{12}$ and associated G-proteins. 100 mm x 20 mm dishes that were seeded 1:2 was deemed ready for transient transfection the following day.

2.2.5. Transient cell transfection

Transient cell transfection is a widely utilised technique in mammalian cell culture, facilitating the integration of foreign genetic material into the target cell; in this study, the HEK293T. This method of transient gene expression enables the rapid generation of recombinant proteins of interest

suitable for pharmacological and preclinical studies; FLAG-P2Y$_{12}$R, Gα, Gβ and Gγ (Table2.2.) (de Los Milagros Bassani Molinas, Beer et al. 2014).

Cell confluency was observed under tabletop microscope (Nikon, UK) whereby approximately 70-90% confluency was determined to be optimal for transient cell transfection.

Following the determination of optimal cell confluency, 2 x 1.5 mL Eppendorf tubes were set aside for each respective 100 mm x 20 mm dish to be transfected. 500 µL of pre-warmed Opti-MEM® I Reduced-Serum media was subsequently dispensed into each Eppendorf tube. Plasmid constructs were dispensed into one of the Eppendorf tubes at volumes and concentrations as indicated by Table 2.2. Within the remaining Opti-MEM containing Eppendorf tube, Lipofectamine™ 2000 transfection reagent was included at a ratio of 2:1, in respect to Lipofectamine: DNA, and incubated for 5 minutes at room temperature. For example, FLAG-P2Y12 and G-protein constructs included were 5 µg, therefore Lipofectamine was added (10 µL) giving 2:1. Subsequent to the elapsed 5-minutes at room temperature, the contents of the lipofectamine containing Eppendorf tube were combined with the DNA construct-containing Eppendorf tube, and incubated at room temperature for a further 20 minutes.

Following the 20 minutes at room temperature, 100 mm x 20 mm cell dishes determined to be optimal for transfection were aspirated of spent media and cells were subsequently washed with 3 mL of sterilised (PBS) (GIBCO), taking care to minimise disruption to the cell monolayer. Following washing, spent PBS was aspirated and 5 mL of warmed Opti-MEM® I Reduced-Serum media was added to each dish, respectively. The lipofectamine & DNA construct-containing Eppendorf was dispensed into the respective dish, in a drop-wise fashion; taking care to ensure sufficient coverage, and subsequently incubated at 37 °C in humidified conditions (95% O_2 & 5% CO_2) for 5-6 hours to allow lipofectamine/DNA complexes to form. Subsequently, spent Opti-MEM® was aspirated and 8 mL of DMEM complete media; supplemented with FBS and pen/strep, was dispensed into each respective 100 mm x 20 mm dish. Cell dishes were then labelled either pcDNA or FLAG-P2Y$_{12}$, corresponding to the respective transfection, in addition to the cell's passage number. Dishes were then allowed to incubate at 37°C in a humidified atmosphere (95% O_2 & 5% CO_2) for approximately 48 hours. Following this, the bioluminescence resonance energy transfer (BRET^2) assay was ready to be performed.

2.2.6. Bioluminescence Resonance Energy Transfer ($BRET^2$)

Bioluminescence Resonance Energy Transfer ($BRET^2$) is a widely utilised *in-vitro* technique within the field of molecular biology. It facilitates the monitoring of real time protein-protein interactions via the resonance energy transfer between a bioluminescent donor protein; *Renilla* luciferase (RLucII), and a fluorescent acceptor protein; green fluorescent protein (GFP) (Figure 2.2.) (Xie, Soutto et al. 2011).

In this study, the transient transfection of $P2Y_{12}$ and complementary G-proteins enabled their successful synthesis and expression at the HEK293T cell membrane. Moreover, RLucII was fused to the Gα subunit, and GFP fused to Gγ. Following their successful expression and recombination, the G-proteins exist as a heterodimer. Therefore, the distance between the protein subunits gives a valid indication of receptor activation following agonist treatment, or conversely inactivation following antagonist administration. A distance greater than 10 nm between the donor protein and acceptor fluorophore corresponds to receptor activation, indicating a protein-protein interaction that consequently emits green light. Conversely, a distance <10 nm corresponds to receptor inactivation, indicating an absence of interaction, emitting blue light (Figure 2.2.). Thus, the $BRET^2$ assay facilitates the pharmacodynamic assessment of antiplatelet therapeutics in respect to $P2Y_{12}$, at the receptor level. Ultimately, stimulating $P2Y_{12}$ causes a decrease in the BRET signal, indicating the dissociation of the G-protein subunits.

All $BRET_2$ experiments were performed approximately 48 hours following the transient cell transfection as previously described in 2.2.5.

Spent DMEM media was aspirated from the 100 mm x 20 mm dishes containing the transiently transfected HEK293T cells, and 2-3 ml of sterilised PBS was subsequently dispensed into each plate with the intention of washing the cells. 1 mL of pre-warmed 0.05% trypsin-EDTA was dispensed directly to the cells and incubated for 2-3 minutes to dissociate and detach them from their respective dishes. After this incubation time elapsed, 3 mL of phenol-free DMEM supplemented with 10% FBS and 2mM glutamine was dispensed into the cell dish, inactivating the trypsin. Cells were then homogenised into suspension and transferred to a 10 mL centrifugation vial. Centrifugation of the cells followed at 161 x g for 3 minutes at room temperature. Subsequently, the supernatant was aspirated, and care was taken to leave the cell pellet that formed, undisturbed. An additional 3 mL of phenol-free complete media was introduced. The cell pellet was then subsequently homogenised

to suspend the cells in the media. Centrifugation was of the homogenised cells was performed again, at 161 x g for 3 minutes at room temperature, and the supernatant discarded.

The cell pellet was resuspended in 1 ml phenol-free DMEM, and a further 9 ml was dispensed into the vial to give a final volume of cell suspension of 10 ml. Cells were subsequently counted under microscope via haemocytometer (Reichert, USA) and their concentration in suspension was adjusted such that 80 µl of the suspension, seeded into each well of a 96-well white flat bottom microplate (Grenier Bio-One, Austria), yielded approximately $1x10^5$ cells/well. The 96-well plate was then placed into an incubator at 37°C in a humidified atmosphere (95% O_2 & 5% CO_2) and allowed to rest whilst the preparation of drugs was completed.

Drug dilutions were done so within 0.5 ml Eppendorf tubes, and serial dilutions carried out where appropriate in respect to the aims of the experiment performed. Once dilutions were prepared, appropriate volumes of each drug concentration and vehicle (>50 µL) were seeded into a 96-well transparent flat bottom plate (Grenier Bio-One, Austria), and labelled accordingly. Following this, the drug-containing transparent 96-well plate was covered and stored within a refrigerator at 4°C, to minimise any degradation whilst the RLucII substrate was prepared.

The substrate: coelenterazine 400a, is light-sensitive and thus care was taken to ensure the aliquots in which it was prepared and stored in, was covered with aluminium foil to mitigate degradation. Coelenterazine 400a aliquots, stored at -20°C, had a stock concentration of 500 mM in a volume of 150 µl. Thus, 1.35 ml of phenol-free DMEM medium was introduced into the coelenterazine-containing Eppendorf, generating a working concentration of the substrate of 50 mM. The $BRET^2$ assay was then ready to be performed.

The 96-well cell-seeded plate was placed into the tray of the FLUOstar® Omega plate reader (BMG Labtech, UK), its heating block set to a temperature of 37°C and the injection system thoroughly cleaned with 70% ethanol, followed by rinsing with ddH_2O. Once cleaned, the prepared coelenterazine 400a substrate was subsequently primed within the injector system, and delta-BRET measurements were ready to be recorded. The appropriate treatment and incubation of an agonist/antagonist to the desired wells of the 96-well cell-containing plate was performed prior to the measurement of the luminescence and fluorescence signal emitted, according to the aims of the respective experiment. Further, the final concentration of substrate in each cell-well was 5 mM.

The spectrofluorometer instrument of the plate reader was prepared such that the bioluminescence emission was collected with a dedicated filter at a wavelength of 410-480 nm for RLucII, and the fluorescence emission concurrently collected utilising a filter set to 515-530 nm for GFP.

Consequently, the data collected was calculated to give a BRET ratio as indicated by the equation below:

$$\textbf{BRET ratio} = \frac{\text{GFP channel signal of untreated cells}}{\text{Luminescence (RlucII) channel signal of untreated cells}} = \textbf{A}$$

The equation above calculates the ratio of the GFP channel signal and the RLucII channel signal of cells that were untreated, giving a basal signal. This BRET ratio is then utilised in the equation below to determine the change in the basal BRET signal when the same cells were independently treated with agonist/antagonist (ΔBRET):

$$\textbf{ΔBRET} = \textbf{A} - \frac{\text{GFP channel signal of vehicle-only treated cells}}{\text{RLucII channel signal of vehicle-only treated cells}}$$

The equation above is an example of how the ΔBRET values were calculated for vehicle-control treated cells (DMSO 0.1%, or PBS). This process of calculating ΔBRET values was repeated with cells that were treated with agonist/antagonist, producing changes in the basal BRET signal in respect to the BRET ratio measured from untreated cells. Therefore, ΔBRET is the difference in the BRET signal measured between cells treated with agonist/antagonist, subtracted from the BRET signal measured from cells treated with the respective vehicle.

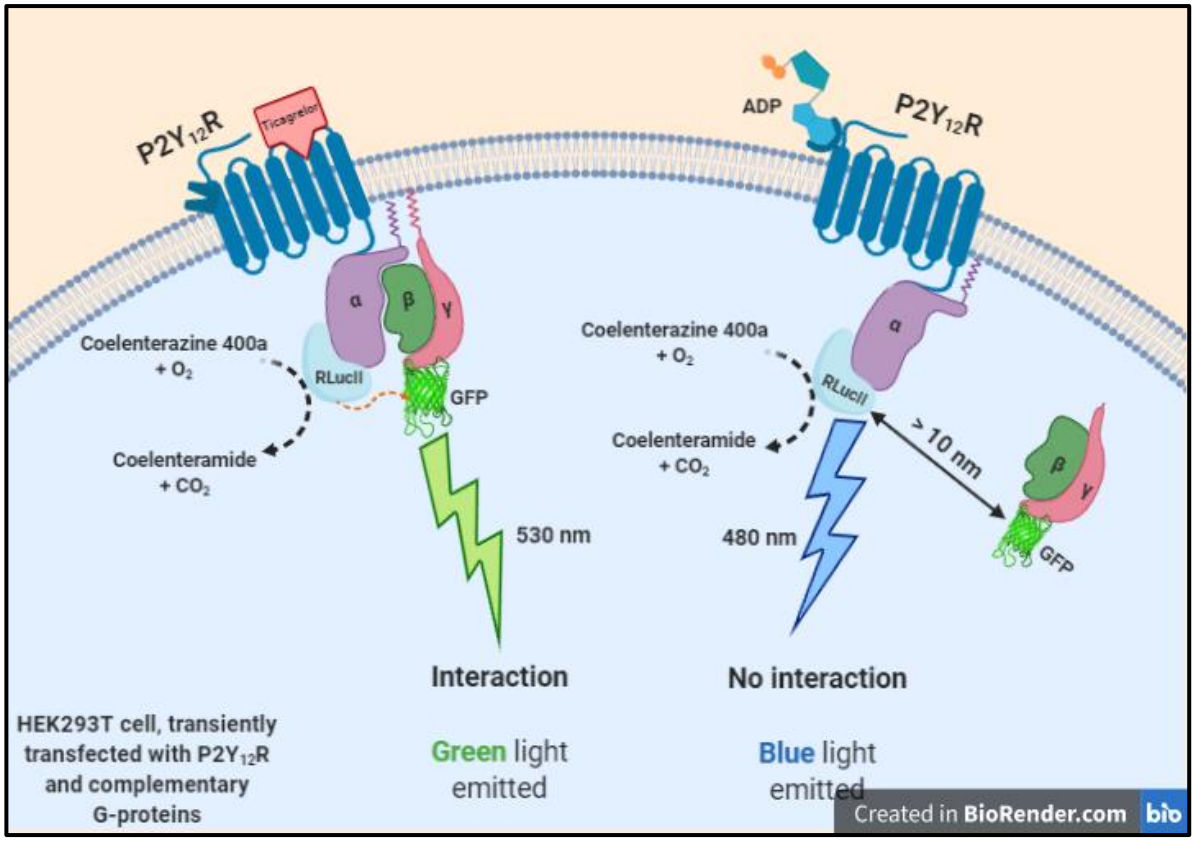

Figure 2.2. BRET^2 assay. Simplified illustration depicting the molecular basis of protein-protein interactions governed by the BRET^2 assay at the receptor level. RLucII catalyses the breakdown of coelenterazine 400a to coelenteramide in the presence of oxygen, emitting green light and indicating receptor inactivation/stabilisation. In situations of receptor activation, whereby RLucII and GFP are separated by a distance >10 nm, resonance energy transfer between donor and acceptor proteins is not facilitated, thus blue light is emitted. The BRET signal is measured as this ratio of green to blue light emission. Illustration constructed in BioRender.com.

2.2.7. Statistics

All statistical analyses were performed utilising GraphPad Prism version 8.0.0 for Windows, GraphPad software, San Diego, California USA, www.graphpad.com. Where applicable, data represent the mean ± SEM of at least 3 independent experiments, unless otherwise indicated by text. Concentration-response curves were fitted with non-linear regression and a non-variable slope to generate EC_{50} values for the agonists, indicating the concentration required to produce 50% of the maximal response. Significant differences in the mean delta-BRET signal obtained upon agonist or antagonist treatment were analysed using a one- or two-way ANOVA, with Bonferroni, Tukey's or Sidak's multiple comparisons *post-hoc* tests applied where appropriate, as indicated by text. ANOVA was employed to establish statistical differences between the means of three or more independent groups. In this study, ANOVA was determined to be appropriate and *post-hoc* tests employed to control the experimental-wise error rate when making pairwise comparisons. In all instances, P values < 0.05 were considered significant. * = P < 0.05, ** = P < 0.01, *** = P < 0.001, **** = P < 0.0001, ns = P > 0.05.

Chapter 3: Results

Ticagrelor has been shown to be clinically superior to many previously described antiplatelet agents. Importantly it is classified as the only orally active and reversibly binding $P2Y_{12}R$ antagonist (Husted and van Giezen 2009, Wise 2016). A possible reason for the markedly increased efficacy of ticagrelor in respect to the previously described antiplatelet agents may be attributed to novel mechanisms of action. This novel mode of action emanates from the discovery of the basal constitutive activity of the $P2Y_{12}R$ receptor and that ticagrelor may act as an inverse agonist at this receptor (Aungraheeta, Conibear et al. 2016). The main aim of this study is to further characterise the pharmacodynamics of ticagrelor in both cell lines and human platelets. To address these aims, two main techniques are employed as described in 1.17. The first, in cell lines utilises bioluminescence resonance energy transfer ($BRET^2$) to assess agonist and antagonist-dependent effects on $P2Y_{12}R$ activity at the receptor-G-protein level. The second, in human platelets, uses light transmission aggregometry (LTA) to assess the efficacy of ticagrelor administration on the functional response of platelet activation, aggregation.

3.1. Characterisation of the pharmacodynamics of ticagrelor antiplatelet therapy at the human $P2Y_{12}R$ utilising $BRET^2$ technology.

$BRET^2$ is a pharmacological technique that facilitates the real-time assessment of protein-protein interactions within cell-based systems (Xie, Soutto et al. 2011). Following the transient transfection of protein constructs as described in 2.2.5., successful recombination of $P2Y_{12}$ and associated G-proteins at the cell surface allows the monitoring of the coupling of the G-protein subunits to the receptor upon agonist/antagonist administration. In the resting state of the receptor, the G-protein subunits; Gαi and Gβγ are associated in proximity. As described in 2.2.6., the energy donor molecule; RLucII is fused to the Gαi subunit (GNAi1-RLucII) and the acceptor molecule; GFP10 is fused to the Gγ subunit of the Gβγ heterodimer (GNG2-GFP10). Upon receptor activation, GNAi1-RLucII and GNG2-GFP10 dissociate. The movement of these subunits to a distance greater than 10 nm apart causes RLucII to emit blue light with a wavelength of 410-480 nm, indicating no protein-protein interaction (Figure 2.2.). Conversely, upon receptor inactivation, GNAi1-RLucII and GNG2-GFP10 associate to facilitate transfer of resonance energy from RLucII to GFP10, with GFP10 emitting green light at a wavelength of 515-530 nm, indicating protein-protein interaction (Figure 2.2.).

Therefore, an increase in the BRET signal correlates to G-protein association and is hence interpreted as receptor inactivation/stabilisation. Conversely, a decrease in the BRET signal correlates to G-protein dissociation and thus, interpreted as receptor activation.

3.1.1. Concentration-dependence of agonist-induced $P2Y_{12}R$ activity.

Incubation of transiently transfected HEK293T cells, as outlined above, with varying concentrations of ADP was performed to assess the concentration-dependence of agonist-induced $P2Y_{12}R$ activity. 5-minute incubations of varying concentration of ADP caused significant decreases in corresponding delta-BRET values respectively (Figure 3.1.B). To determine an appropriate concentration of agonist to utilise in further $BRET^2$ experiments, the EC_{50} value for ADP was calculated and a suitable sub-maximal concentration of ADP chosen (10 µM). To assess if the agonist induced $P2Y_{12}$ activity changed with respect to time, $BRET^2$ time course assays were designed and employed (Figure 3.1.A). Figure 3.1.A indicates that 10 µM ADP caused a decrease in BRET signal that occurred rapidly, indicating a sub-maximal response achieved between 5-10 minutes that was sustained until the 60-minute mark. This incubation time of ADP (10 µM; 5 mins) was deemed sufficient to evoke a submaximal response of P2Y12R activation and was thus employed in subsequent $BRET^2$ assays.

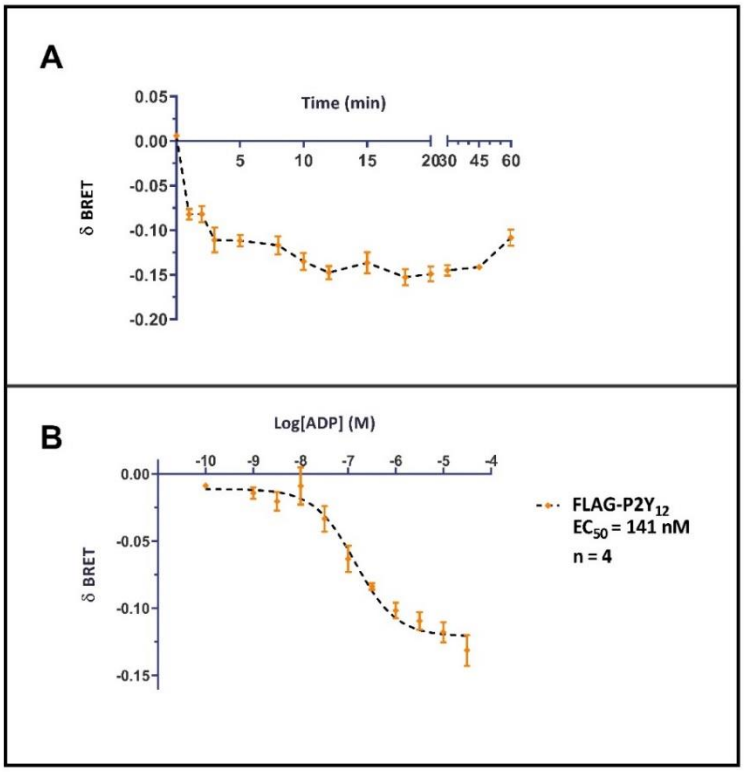

Figure 3.1. Time-course and concentration-dependence of $P2Y_{12}R$ activation with ADP. (A) HEK293T cells, transiently transfected with $P2Y_{12}R$ and associated G-proteins, were incubated with ADP (10 µM, 60 minutes) and delta-BRET measurements were taken immediately after each respective elapsed time point, generating a time course of ADP administration. (B) Transfected cells were incubated with varying concentrations of ADP (0.1 nM - 10 µM) for 5 minutes. Immediately after this elapsed incubation time, delta-BRET measurements were taken for each corresponding concentration, thus generating a dose-response curve for ADP. Data plotted represents the change in BRET ratio upon agonist addition and is displayed as mean ± SEM. EC_{50} value = 141 nM, n = 4.

3.1.2. Inhibition of ADP-induced $P2Y_{12}R$ activity by a range of antiplatelet agents.

As seen in Figure 3.1., ADP administration causes a concentration-dependent decrease in the BRET-signal that is indicative of receptor activation. To assess the efficacy of ticagrelor and previously described antiplatelet agents on the modulation of receptor stabilisation/inactivation, transfected HEK293T cells were incubated with antagonist (10 µM) for 7 minutes, followed by stimulation with ADP (10 µM) for a further 3 minutes (Figure 3.2B). Stimulation of ticagrelor treated cells with 10 µM ADP caused a significant decrease and reversal of the BRET-signal obtained by ticagrelor administration alone (10 µM). Similarly, stimulation of cangrelor-treated cells with ADP (10 µM) caused a decrease in the BRET-signal with respect to cangrelor administration alone. Further, AR-C66096 and R-138727 both similarly ablate the ADP-response with their respective concomitant administration with the agonist. Taken together, these data indicate the relative efficacies of each antiplatelet agent in respect to their antagonism of receptor activation. In summary, the data displayed in figure 3.2. confirms the utility of the antagonists to ablate ADP-induced $P2Y_{12}R$ activity.

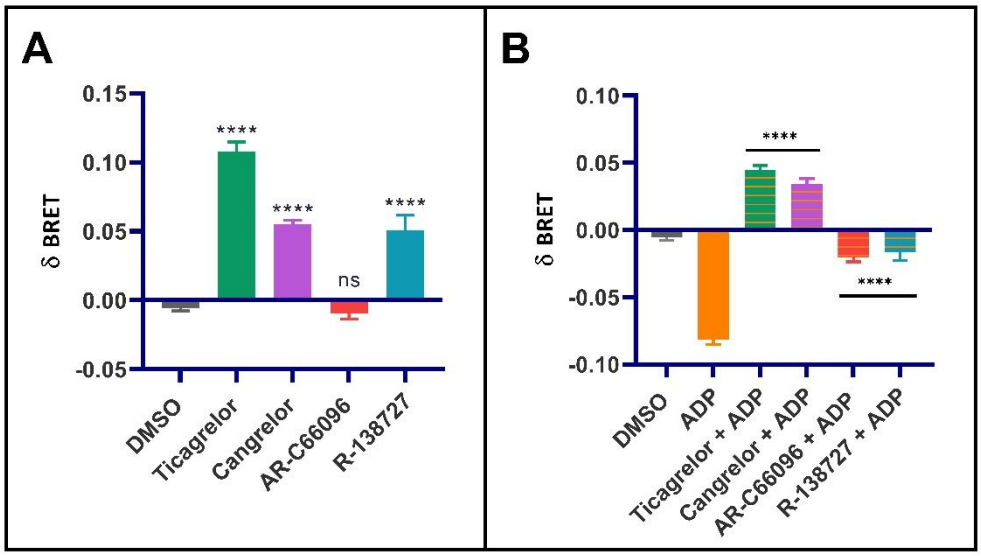

Figure 3.2. Antagonism of ADP-stimulated $P2Y_{12}R$ activity by pre-treatment with a range of $P2Y_{12}R$ inhibitors. HEK293T cells were transiently transfected with $P2Y_{12}R$ and associated G-proteins as indicated in 2.2.5. (A) Cells were treated with antagonists (10 µM) for 10 minutes and measurements were taken immediately after the elapsed time, generating mean delta-BRET values for each respective $P2Y_{12}R$ inhibitor. (B) Cells were pre-treated with antagonist (10 µM) for 7 minutes, followed by treatment with ADP (10 µM) for a further 3 mins and delta-BRET measurements taken immediately following a total elapsed time of 10 minutes. Significant differences between mean delta-BRET values were analysed via one-way ANOVA with Sidak's multiple comparisons *post-hoc* test. Data plotted represent the mean ± SEM, n = 3. ns = $P > 0.05$, **** = $P < 0.0001$. (A) Pairwise comparisons are in respect to DMSO. (B) Pairwise comparisons are in respect to ADP.

3.1.3. Assessment of the onset and duration of inverse agonist activity at the $P2Y_{12}R$.

Previous research emanating from the Mundell laboratory has shown ticagrelor to exhibit inverse agonist activity at the $P2Y_{12}R$ (Aungraheeta, Conibear et al. 2016). As shown previously in figure 3.2., ticagrelor and cangrelor effectively ablate ADP-mediated $P2Y_{12}R$ activation.

To assess whether the inverse agonist action of $P2Y_{12}R$ activity with ticagrelor and cangrelor was time-dependent, time course assays were subsequently employed as shown in Figure 3.3. Transiently transfected HEK293T cells were incubated with ticagrelor (10 µM) or cangrelor (10 µM), and delta-BRET measurements taken immediately following the elapsed incubation times (Figure 3.3.). Ticagrelor administration caused a marked increase in the BRET-signal that was sustained for the duration of the assay (60 mins). Cangrelor administration similarly caused an increase in the BRET-signal that was sustained until the 25-minute mark. In summary, this data facilitated the determination of optimal incubation times of both inhibitors for subsequent experiments, and to additionally provide insight into the speed of onset of action of both antiplatelet therapies.

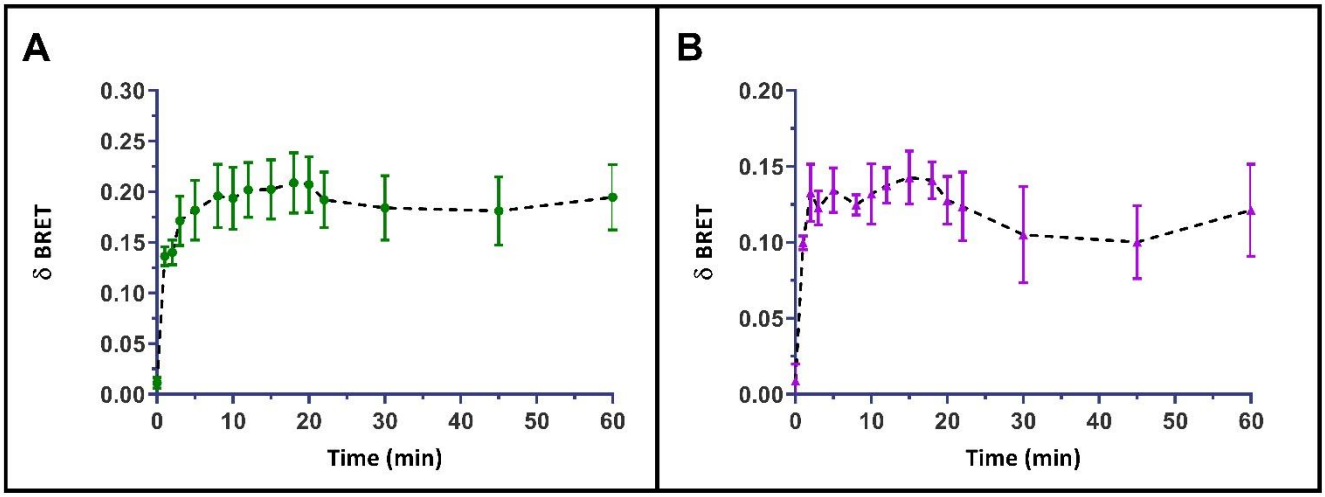

Figure 3.3. Time-course assays of ticagrelor and cangrelor. HEK293T cells, transiently transfected with $P2Y_{12}R$ and associated G-proteins, were incubated with either ticagrelor (10 µM) (A) or cangrelor (10 µM) (B) for a total of 60 minutes. Delta-BRET measurements were taken immediately upon reaching respective elapsed time points, generating time courses of ticagrelor (A) and cangrelor (B) administration. Data plots represent the mean ± SEM. n = 3.

3.1.4. Concentration-dependence of ticagrelor and cangrelor inverse agonist activity at the $P2Y_{12}R$.

To assess whether the inhibition elicited by ticagrelor and cangrelor displayed concentration-dependence, dose-response relationships were subsequently constructed (figure 3.4). Incubation of transiently transfected HEK293T cells with varying concentrations of ADP produced an agonist-mediated response of receptor activation, consequently generating an EC_{50} value of 141 nM. Ticagrelor and cangrelor administration caused a concentration-dependent inhibition of basal receptor activity. With EC_{50} values of 208 nM and 62 nM, respectively. The data shown in figure 3.4. demonstrate ticagrelor and cangrelor to both behave as inverse agonists at the $P2Y_{12}R$. Intriguingly, cangrelor appears to behave as a partial inverse agonist with a reduced Emax, whereas ticagrelor a full inverse agonist (Berg and Clarke 2018). Cangrelor exhibits higher potency than that of ticagrelor, aligning with data from previous studies (Garcia, Maurel-Ribes et al. 2018).

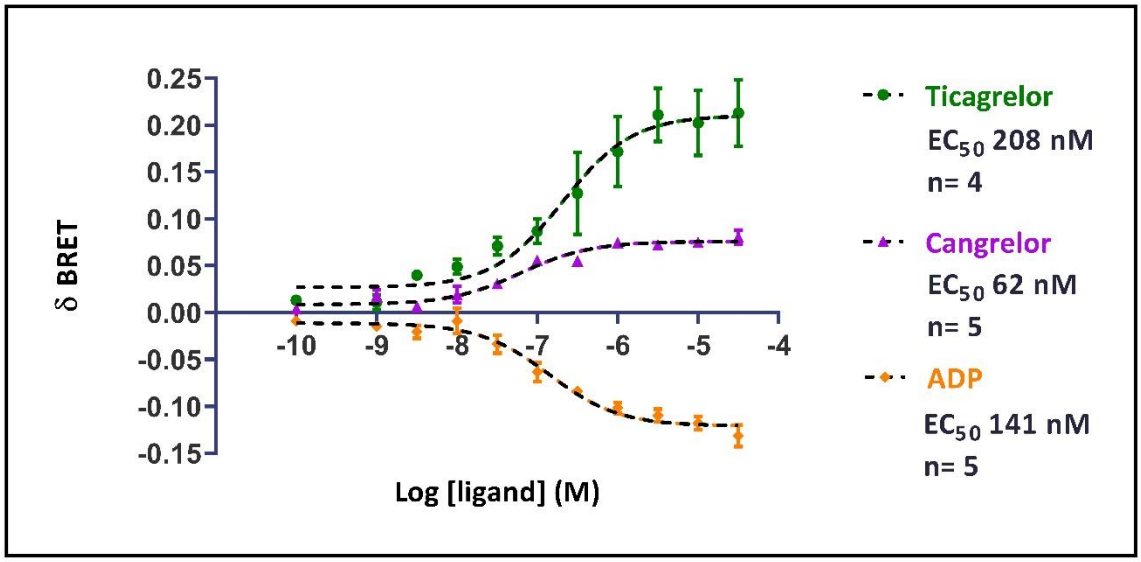

Figure 3.4. Concentration-dependence of Ticagrelor, Cangrelor and ADP. HEK293T cells, transiently transfected with $P2Y_{12}R$ and associated G-proteins, were incubated with varying concentrations of either ticagrelor, cangrelor or ADP for 5 minutes. Delta-BRET measurements were taken immediately after the elapsed incubation time. Data plotted represent the change in BRET ratio upon agonist or antagonist treatment, displayed as mean ± SEM of at least 4 independent experiments. Ticagrelor EC_{50} value = 208 nM (70 – 587 nM, n = 4). Cangrelor EC_{50} value = 62 nM (33 – 117 nM, n = 5). ADP EC_{50} value = 141 nM (80 – 253 nM, n = 5).

3.1.5. Mode of action of ticagrelor.

The mechanism of action of ticagrelor has previously been suggested to be distinct from that of previously described antiplatelet agents (VAN Giezen, Nilsson et al. 2009, Dobesh and Oestreich 2014). Ticagrelor has been shown to inhibit the adenosine transporter ENT1; resulting in the accumulation of extracellular adenosine (Aungraheeta, Conibear et al. 2016). Additionally, off target effects of dyspnoea with ticagrelor use have been reported in a concentration-dependent manner (Cannon, Husted et al. 2007), potentially related to this increase in plasma adenosine levels.

Experiments were designed to further characterise of the mode of action of ticagrelor (Figure 3.5.). We first tested if the accumulation of extracellular nucleotides, including ADP, in our cell line system may affect the basal constitutive activity of $P2Y_{12}R$ and therefore ticagrelor action. Transiently transfected HEK293T cells were incubated with apyrase (0.2 U/mL; 30 minutes) in Figure 3.5.A. No significant differences were observed in the BRET-signal achieved by ticagrelor in the absence or presence of apyrase (ns = P = 0.8671, n = 3). Any accumulation of extracellular nucleotides did not affect the level of inhibition elicited by ticagrelor at the $P2Y_{12}R$.

As previously described in 1.12., potential breakdown of extracellular nucleotides via CD39 results in the generation of extracellular adenosine. Potentially through the inhibition of ENT1 transporters, ticagrelor could lead to accumulation of extracellular adenosine that in turn could activate A2B adenosine, Gαs-coupled receptor signalling (Mundell, Loudon et al. 1999). Transiently transfected HEK293T cells were therefore pre-treated with xanthine amine congener (XAC); a non-specific adenosine receptor antagonist (10 µM; 30 minutes) (Figure 3.5.B). No significant differences were observed in the BRET-signal achieved by ticagrelor in the presence and absence of XAC (ns = P = 0.4893, n = 3). Therefore, adenosine receptor blockade had no effect on ticagrelor activity in this cell line.

Previous studies have indicated that intracellular cAMP levels increase in cells following ticagrelor treatment in part through the increased extracellular adenosine levels described above. To further characterise if increased levels of cAMP could modulate ticagrelor activity, cells were incubated with forskolin (10 µM; 30 minutes) to directly stimulate adenylyl cyclase activity (Figure 3.5.C). No significant differences were observed in the BRET-signal achieved by ticagrelor administration alone and the concomitant administration of ticagrelor + forskolin (ns = P = 0.3289, n = 3). Therefore, increased intracellular cAMP levels did not affect ticagrelor activity.

Another important control experiment was undertaken in HEK293T cells, transiently transfected with μ-opioid receptor (MOR) and associated G-proteins. The MOR is like $P2Y_{12}R$; Gαi-coupled. Transfected cells were incubated with the MOR agonist DAMGO (10 μM), ticagrelor (10 μM) or both (Figure 3.5.D). The MOR is similarly Gαi-coupled in respect to $P2Y_{12}R$, however concomitant ticagrelor + DAMGO administration in these transfected cells does not produce a significant difference in delta-BRET value as seen with DAMGO incubation alone (ns = $P > 0.9999$, n = 3). Therefore, the inhibitory effect of ticagrelor upon G protein-dissociation is dependent upon the expression of the $P2Y_{12}R$ and associated G-proteins.

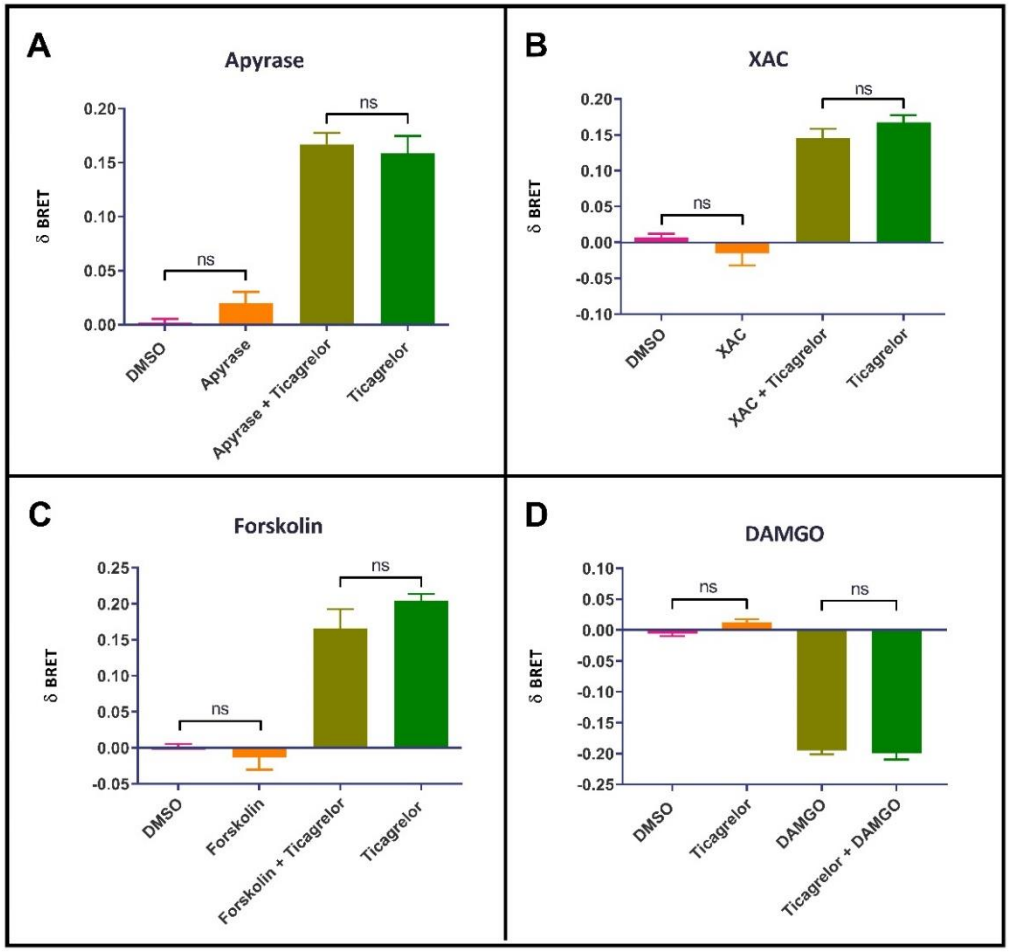

Figure 3.5. Probing the mechanism of action of ticagrelor. HEK293T cells, transiently transfected with P2Y12 and associated G-proteins were incubated with apyrase (0.2 U/ml) (A), XAC (10 μM) (B) or forskolin (10 μM) (C) for 30 minutes, followed by ticagrelor (10 μM) for 5 minutes. HEK293T cells, transiently transfected with the μ-opioid receptor and associated G-proteins were incubated with DAMGO (10 μM) (D) for 15 minutes, followed by ticagrelor (10 μM) for 5 minutes. Upon reaching the elapsed incubation times, delta-BRET measurements were taken immediately, and data plotted represent the mean ± SEM, n = 3. Significant differences between conditions were analysed via one-way ANOVA with Bonferroni's multiple comparisons post-hoc test. ns = $P > 0.05$. The transient

transfection of HEK293T cells with the μ-opioid receptor and associated G-proteins (Fig 3.5.D) was kindly performed by Yahia Alghazwani, Henderson & Kelly Laboratory.

Taken together, the above experiments provide confidence that the inverse agonist utility of ticagrelor is indeed observed at the human $P2Y_{12}R$. Additional experiments were subsequently performed to assess the binding modality of ticagrelor in respect to $P2Y_{12}$.

3.1.6. Evaluation of ticagrelor's binding modality

The binding modality of ticagrelor is currently still under debate (VAN Giezen, Nilsson et al. 2009, Hoffmann, Lutz et al. 2014, Garcia, Maurel-Ribes et al. 2018). Previous mutagenesis studies have suggested the cysteine residue at position 194 (C194) of the receptor protein to be important for the recognition of ticagrelor's antagonist activity (Hoffmann, Lutz et al. 2014). Therefore, we employed mutagenesis experiments to assess these conclusions (Figure 3.6. & Figure 3.7.). HEK293T cells expressing wild-type or mutant $P2Y_{12}R$ (C194A) were treated with a range of previously described antiplatelet agents or ADP to assess the affect, if any, of the mutated receptor on the function of the respective agents.

As seen below in Figure 3.6.A., the C194A mutation produced a statistically significant reduction in mean delta-BRET values elicited by ticagrelor administration alone [orange and blue bars (**** = $P < 0.0001$, n = 3)]. Additionally, the mutation produced a statistically significant reduction in the ability of ticagrelor to inhibit ADP-stimulated $P2Y_{12}R$ activity [brown and purple bars (**** = $P < 0.0001$, n = 3)]. Notably, ADP-stimulated activity was unaffected by the C194A mutation. Further, the mutation had no effect on cangrelor inverse-agonist activity or cangrelor-dependent inhibition of ADP-stimulated $P2Y_{12}R$ activity (Figure 3.6.B). Similarly, the C194A mutation had no effect on AR-C66096-dependent antagonism of ADP-stimulated P2Y12R activity (Figure 3.6.C) (ns = $P > 0.05$, n = 3). Therefore, we agree with the findings of previous studies that demonstrate the significance of the cysteine residue at position 194 of the receptor, in the recognition of ticagrelor antiplatelet activity.

The binding site for ticagrelor has been previously reported to be distinct from that of the orthosteric agonist binding site for ADP, indicating a binding modality of ticagrelor demonstrating a mode of non-competitive action (JJ, Nilsson et al. 2009). The P2Y12R super agonist; 2MeSADP meanwhile is reported to act in a competitive manner with ticagrelor. We therefore investigated if this was affected in respect to the mutant receptor (C194A; Figure 3.7.A). Notably, unlike ADP, 2MeSADP was able to significantly reverse ticagrelor inverse agonist activity. Here we demonstrate significant differences in the level of inhibition elicited by ticagrelor alone between wild-type and mutant cells (**** = $P < 0.0001$, n = 3). Additionally, we report significant differences in delta-BRET values achieved with 2MeSADP alone between wild-type and mutant cells (**** = $P < 0.0001$, n = 3). Therefore, suggesting the cysteine residue located at position 194 of the receptor to be crucial in respect to the binding site of ticagrelor, as well as indicating overlap between the binding sites of the antagonist and super agonist, 2MeSADP.

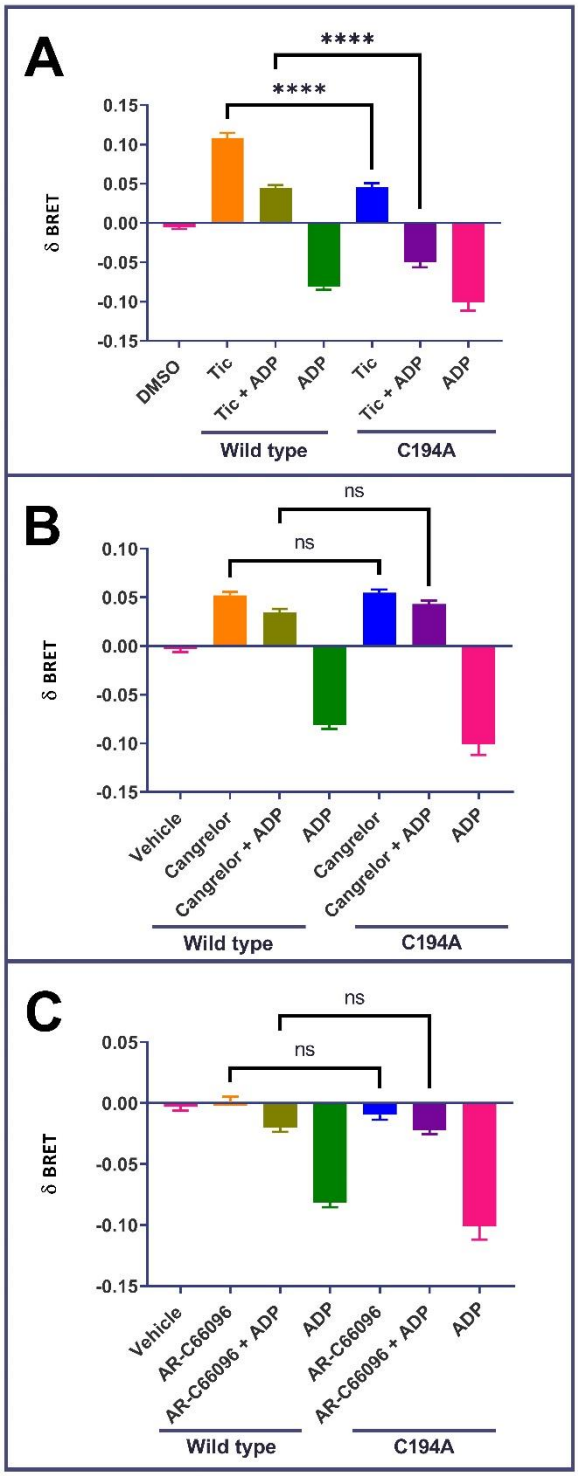

Figure 3.6. Importance of C194A mutation on ticagrelor binding site. HEK293T cells were transiently transfected with either wild-type P2Y12R, or mutant P2Y12R (C194A) and associated G-proteins. Wild-type and mutant cells were both treated with either ticagrelor (10 µM) (A), cangrelor (10 µM) (B) or AR-C66096 (10 µM) (C) for 10 minutes and delta-BRET measurements taken immediately after this elapsed incubation time. Significant differences in mean delta-BRET values were analysed via one-way ANOVA with Bonferroni's multiple comparisons post-hoc test. Data plotted represent the mean + SEM, n = 3. ns = $P > 0.05$, **** = $P < 0.001$.

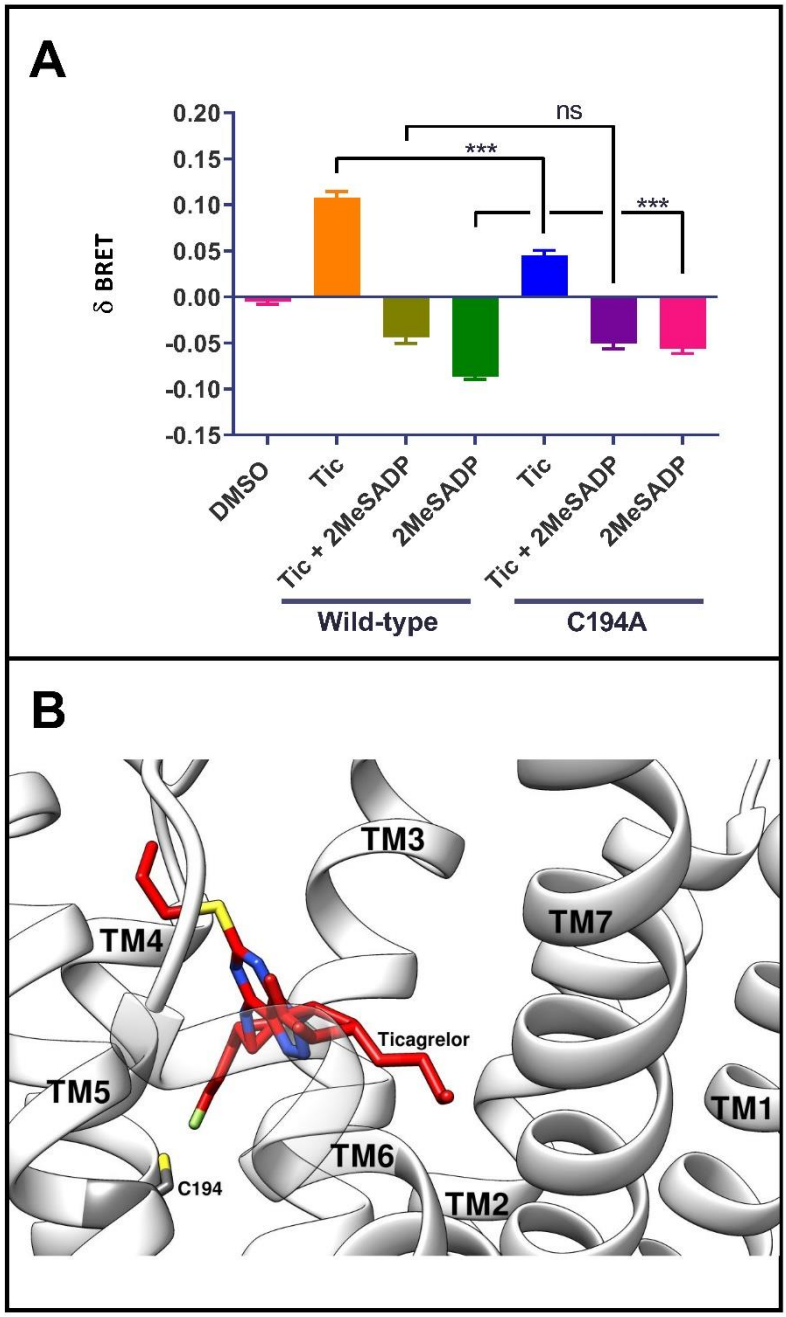

Figure 3.7. C194A mutation importance for agonist and antagonist activity. A) HEK293T cells were transiently transfected with either wild-type $P2Y_{12}R$, or mutant $P2Y_{12}R$ (C194A) and associated G-proteins. Wild-type and mutant cells were preincubated with ticagrelor (10 µM) for a total time of 10 minutes. 2MeSADP was added at minute-7 and allowed to incubate for 3 further minutes. Following this total elapsed time of 10 minutes, delta-BRET measurements were taken accordingly. B) Molecular dynamics simulations were performed and crystal structure images of $P2Y_{12}R$, with ticagrelor bound, were kindly generated by Sukhvinder Bancroft, Mundell laboratory. Significant differences in mean delta-BRET values between conditions were analysed via one-way ANOVA with Bonferroni's multiple comparisons *post-hoc* test. Data plotted represent the mean $\pm$ SEM, n = 3. ns = $P > 0.05$, *** = $P < 0.001$.

3.1.7. Reversibility of ticagrelor and other $P2Y_{12}R$ antagonists.

Ticagrelor has been hailed as the first orally bioactive and reversible $P2Y_{12}R$ antagonist, providing a higher degree of efficacy than the previously described antiplatelet agents (Husted and van Giezen 2009). However, clinically relevant adverse side effects with ticagrelor; as well as the other antiplatelet therapeutics, exist in the form of increased bleeding profiles. Therefore, when evaluating the pharmacodynamics of antiplatelet therapies, the mode of action, onset and reversibility of each agent becomes fundamental in the subsequent assessment of relative efficacy. This in turn influences their use within a clinical setting. Therefore, we designed reversibility experiments as shown in Figure 3.8., to assess the "off-set" of ticagrelor activity.

HEK293T cells, transiently transfected with $P2Y_{12}R$ and associated G-proteins, were incubated with antagonist (10 µM; 10 minutes). Following which, cells were then centrifuged and either resuspended in the existing supernatant (unwashed). Alternatively, the centrifuged cells had their supernatant aspirated and fresh phenol-free media introduced, followed by resuspension of the cell pellet. This was subsequently repeated, centrifuging the cells again and resuspending the cell pellet once more in phenol-free media (washed). Importantly, there were no statistical differences in the delta-BRET values achieved with ticagrelor incubation alone in unwashed cells compared to that of cells that underwent washing steps (Figure 3.8.A.) (ns = $P > 0.9999$, n = 3). Additionally, there were no significant differences in mean delta-BRET values observed in cells treated with the concomitant administration of ticagrelor + ADP, between unwashed and washed cells (ns = $P = 0.6807$, n = 3).

Conversely, washing steps produced a statistically significant decrease in mean delta-BRET measurements, versus unwashed cangrelor-treated cells (* = $P = 0.0479$, n = 3) (Figure 3.8.B). Additionally, a reversal of the BRET-signal was observed in cells that underwent washing steps that were then subsequently treated with cangrelor + ADP (**** = $P < 0.0001$, n = 3).

The reversibility of the active metabolite of prasugrel (R-138727), an established irreversible antagonist at the $P2Y_{12}R$ was next assessed (Figure 3.8.C). Unsurprisingly, washing produced no significant differences in the BRET-signal achieved by R-138727 alone or the effects of this antagonist upon ADP-stimulated P2Y12R activity, between unwashed cells and cells that underwent washing steps. An assessment of AR-C66096 reversibility was also performed (Figure 3.8.D). Like cangrelor, washing reversed AR-C66096-dependent inhibition of ADP-stimulated $P2Y_{12}R$ activity [green and blue bars (*** = $P = 0.0005$, n = 3)].

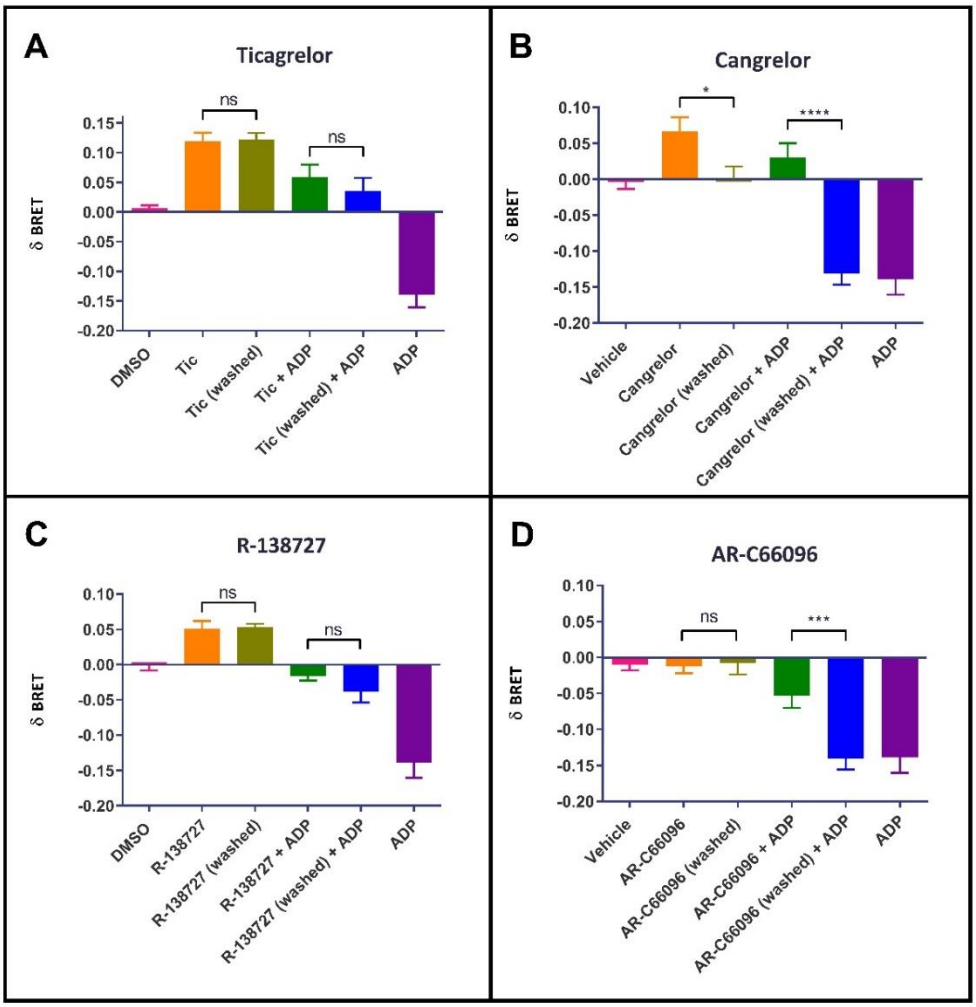

Figure 3.8. Anti-platelet agent reversibility. Transiently transfected HEK293T cells, with $P2Y_{12}R$ and associated G-proteins, were pre-incubated with either ticagrelor (10 µM) (A), cangrelor (10 µM) (B), R-138727 (10 µM) (C) or AR-C66096 (10 µM) (D) for 10 minutes, immediately followed by centrifugation. Cells were then either resuspended in the existing supernatant (unwashed) or alternatively, the supernatant aspirated and fresh untreated media introduced to resuspend the cell pellet. Subsequently, cells were centrifuged and resuspended in fresh media once more (washed). δBRET measurements were taken immediately after the elapsed incubation time of the antagonist (10 minutes). Concurrently, cells were pre-treated with each antagonist (10 µM) for 7 minutes. At which time, ADP (10 µM) was added for 3 minutes, such that the total time of inhibitor incubation was 10 minutes. δBRET measurements were taken immediately following the elapsed incubation time of the inhibitor. Significant differences in mean δBRET values were analysed via one-way ANOVA with Tukey's multiple comparisons post-hoc test. Data plotted represent the mean ± SEM, n = 3. ns = $P > 0.05$, * = $P < 0.05$, *** = $P < 0.001$.

In summary, the data above demonstrates that the active metabolite of prasugrel (R-138727), an established $P2Y_{12}R$ antagonist, unsurprisingly appears irreversible. Interestingly, the inverse agonist

activity of ticagrelor also appears irreversible. Conversely, cangrelor and AR-C66096; established reversible $P2Y_{12}R$ antagonists, appear reversible after washing steps.

3.1.8. Clinical implications of antiplatelet therapy switching guidelines.

It is not uncommon for antiplatelet therapies to be switched within the clinical setting. However, guidelines indicating their appropriate use; particularly in scenarios whereby emergency percutaneous coronary intervention is indicated, until recently were not clearly defined (Angiolillo, Rollini et al. 2017). Consequently, switching is broadly characterised as:

i) escalation; switching from a less intensive to more intensive agent (clopidogrel to ticagrelor or prasugrel
ii) de-escalation; from a more intensive to less intensive agent (ticagrelor or prasugrel to clopidogrel), or
iii) change; switching between similarly efficacious agents (ticagrelor to prasugrel or vice versa).

Therefore, we employed preincubation experiments as shown below in Figures 3.9. and 3.10., to assess if there were any significant differences in the level of inhibition achieved with the coadministration of the $P2Y_{12}R$ antagonists.

HEK293T cells transiently transfected with $P2Y_{12}R$ and associated G-proteins were pre-incubated with either cangrelor or ARC-66096 (10 µM) for 30 minutes, followed by ticagrelor administration (10 µM) for 5 minutes. Following which, delta-BRET measurements were immediately taken (Figure 3.9.). There was no significant difference in the BRET-signal observed between AR-C66096 alone, and coadministration of AR-C66096 + ticagrelor (Figure 3.9.A) (ns = $P > 0.9999$, $n = 3$). Similarly, no significant differences were observed in the BRET-signal achieved between cangrelor alone, and the concomitant administration of cangrelor + ticagrelor (Figure 3.9.B) (ns = $P > 0.9999$, $n = 3$). Intriguingly, a significant difference in the BRET-signal achieved between R-138727 alone and the coadministration of R-138727 + ticagrelor was observed (Figure 3.9.C) (** = $P = 0.0025$, $n = 3$). Indicating potential synergism between ticagrelor and the thienopyridine active metabolite, confirming similar suggestions in previous studies (Franchi, Rollini et al. 2018).

The assessment of the clinical switching modality of de-escalation was subsequently performed, as shown below in Figure 3.10. The preincubation of ticagrelor (10 μM) for 30 minutes was performed before the subsequent addition of an additional $P2Y_{12}R$ antagonist (10 μM) for 5 minutes. Immediately following the elapsed incubation time of the additional antagonist, delta-BRET measurements were taken. No significant differences in the BRET-signal achieved with ticagrelor alone, and the coadministration of ticagrelor + cangrelor were observed (Figure 3.10.A) (ns = P = 0.3577, n = 3). Additionally, there were no significant differences observed in the BRET-signal elicited by ticagrelor alone in respect to the concomitant administration of ticagrelor + R-138727 (Figure 3.10.B) (ns = P > 0.9999, n = 3).

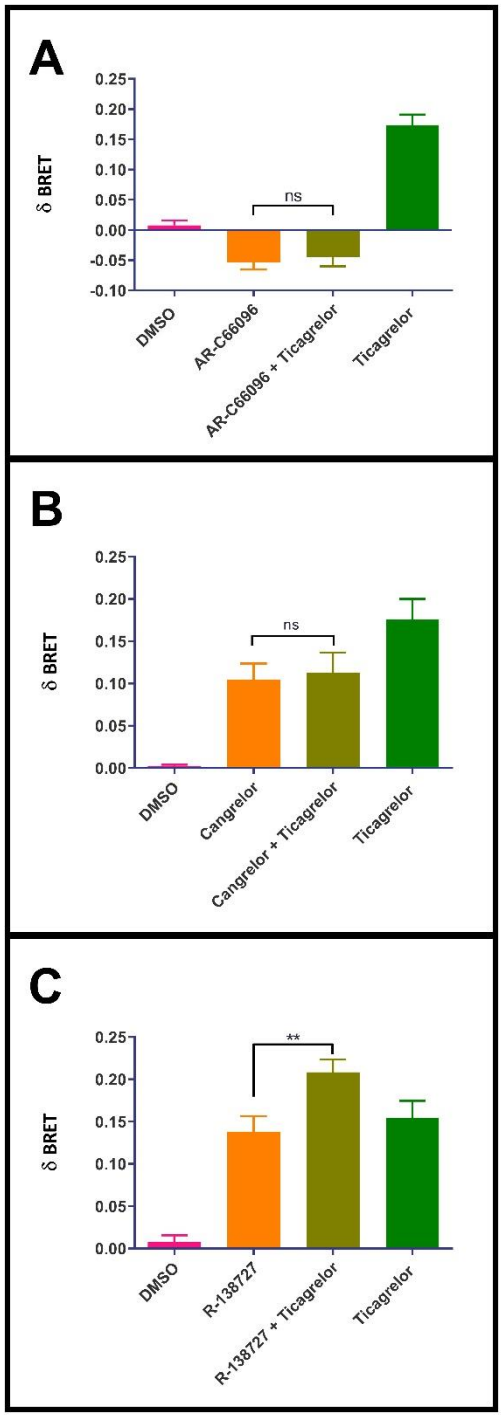

Figure 3.9. Pre-incubation of antagonists before ticagrelor (Escalation). Transiently transfected HEK293T cells were pre-incubated with AR-C66096 (10 µM) (A), cangrelor (10 µM) (B) or R-138727 (10 µM) (C) for 30 minutes, followed by incubation with ticagrelor (10 µM) for 5 minutes. Following the elapsed incubation time of both inhibitors, delta-BRET measurements were taken, whereby the data plotted represents the mean ± SEM, n = 3. Statistically significant differences between conditions were analysed via one-way ANOVA with Bonferroni's multiple comparisons *post-hoc* test. ** = $P < 0.01$. ns = $P > 0.05$.

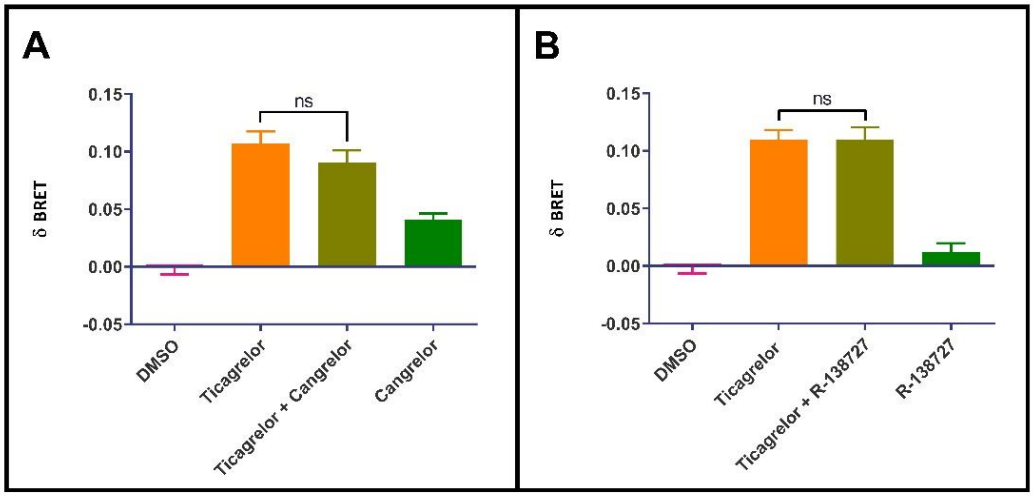

Figure 3.10. Pre-incubation of ticagrelor before antagonists (De-escalation). Transiently transfected HEK293T cells were pre-incubated with ticagrelor (10 µM) for 30 minutes, followed by incubation with either cangrelor (10 µM) (A) or R-138727 (10 µM) (B) for 5 minutes. Following the elapsed incubation time of both inhibitors, delta-BRET measurements were taken, whereby the data plotted represents the mean ± SEM, n = 3. Statistically significant differences between conditions were analysed via one-way ANOVA with Bonferroni's multiple comparisons *post-hoc* test. ns = P > 0.05.

3.2. Ticagrelor-dependent inhibition of ADP-mediated aggregation in human platelet-rich plasma.

All studies above were in a cell-based system. To further characterise some of the pharmacodynamic qualities of ticagrelor (onset and offset) in a more physiologically and clinically relevant system, we used human platelets.

Light transmission aggregometry (LTA) is a widely used diagnostic tool, utilised in the assessment of platelet function and additionally in the evaluation of patients with suspected bleeding disorders, *ex vivo.* The core principles of LTA have barely changed since its initial description over 50 years ago (O'Brien 1961). As described in 2.2.2., the technique involves the isolation of human platelet-rich plasma (PRP) from whole blood that is included within a cuvette, placed between a light source and photocell. The isolated PRP appears cloudy, due to the suspension of platelets within the plasma. Therefore, light is impeded within the sample. Under conditions whereby the platelets are stimulated with an agonist such as ADP, the platelets consequently aggregate, thus permitting light transmission through the sample which is detected by the photocell and measured as a function of time.

3.2.1. Inhibition of agonist-induced aggregation by ticagrelor in human platelets.

The results previously described (Figures 3.1-3.10) led to questions regarding whether we can replicate this within a system where the $P2Y_{12}R$ is not forcefully expressed (as seen in transiently transfected HEK293T cells). Therefore, experiments regarding the inhibitory effect of ticagrelor within a platelet-based system were required in respect to providing confidence in our previous results. Consequently, concentration-dependence LTA experiments were employed within a system whereby platelet aggregation is the functional readout (Figure 3.11.).

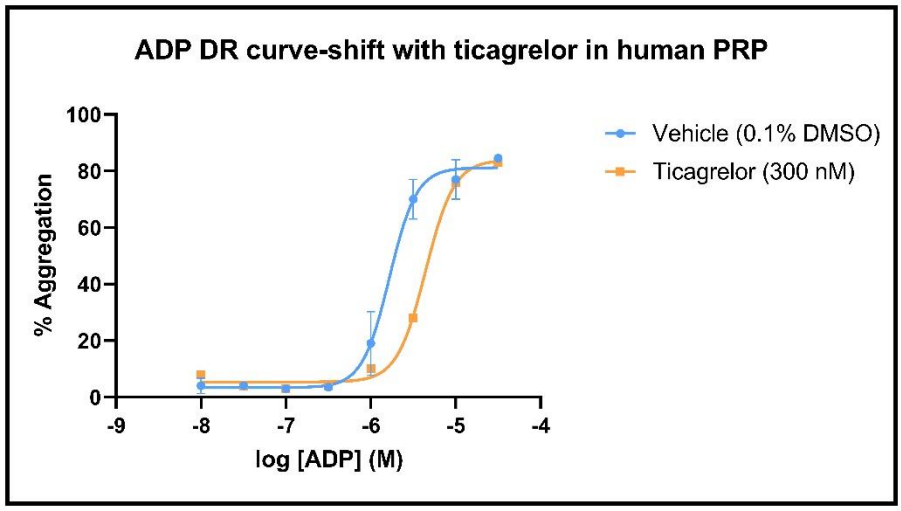

Figure 3.11. ADP concentration-response curve in human isolated platelets. Human platelet rich plasma was stimulated with increasing concentrations of ADP, in the presence and absence of incubated ticagrelor (300 nM, 10 mins). % aggregation measurements began immediately following agonist addition and continued for an elapsed time of 2 mins. Data plotted represents % aggregation achieved upon [agonist] (M) addition, displayed as mean + SEM. EC50 value (ADP) (with 95% CI) = 1.67 µM (1.326 - 2.052, n=3). EC_{50} value (ADP + ticagrelor 300 nM) = 4.47 µM.

3.2.2. Assessment of the onset of action of ticagrelor in human platelets.

Following the confirmation of the concentration-dependence of agonist activity in human PRP (Figure 3.11.), coupled with the results of experiments regarding the initial determination of the onset of action of ticagrelor in transiently transfected HEK293T cells (Figure 3.3.A.), we designed and employed a time course assay of ticagrelor administration utilising LTA in human platelet-rich plasma, shown below (Figure 3.12.). The aim of this experiment was to assess the onset of action of ticagrelor administration in respect to time (mins), measuring the functional readout following platelet activation; aggregation (%). Here, we demonstrate there to be no significant differences in the % aggregation achieved between PRP treated with ticagrelor (300 nM), in respect to vehicle (0.1% DMSO) at all time points (ns = P > 0.05, n = 4). Significant differences in % aggregation was observed at all time points for ticagrelor (1 µM), in respect to vehicle (** = P = 0.0040, N = 4). Interestingly, we observe a significant decrease in the max % aggregation elicited in PRP subsequently treated with ticagrelor (10 µM), at all corresponding time points in respect to vehicle (0.1% DMSO) (**** = P < 0.0001).

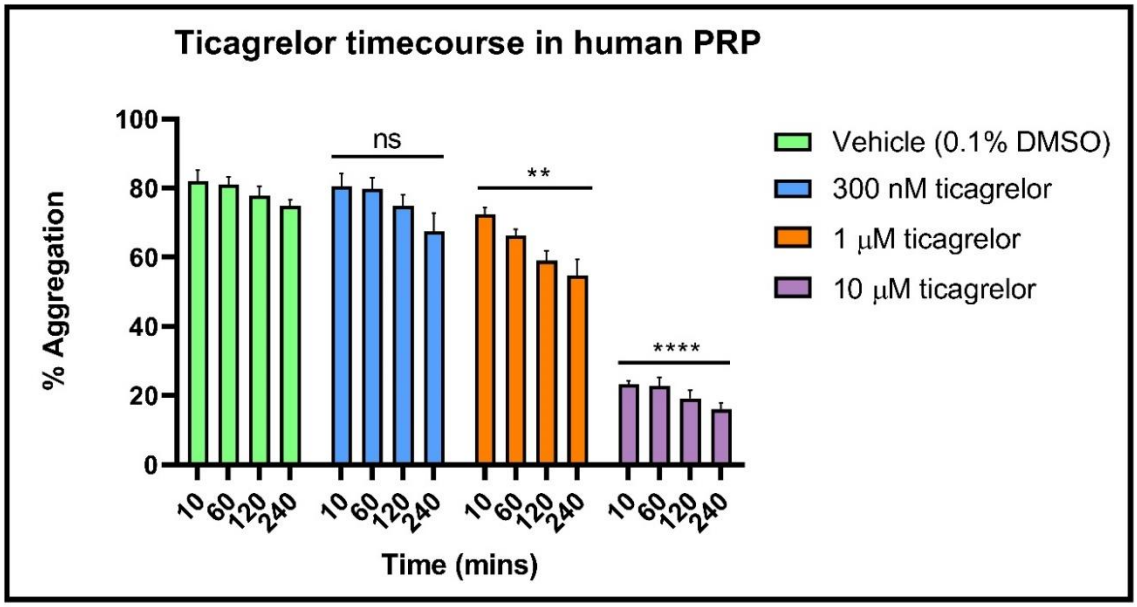

Figure 3.12. Time course assay of ticagrelor administration in human PRP. Human platelet rich plasma was incubated with varying concentrations of ticagrelor; vehicle (0.1% DMSO), 300 nM, 1 μM or 10 μM for either; 10, 60, 120 or 240 minutes. Immediately following the elapsed incubation time for each respective ticagrelor-treated aliquot of PRP, platelets were stimulated with ADP (10 μM) and % aggregation measurements were recorded. Data plotted represent the maximum % aggregation elicited following stimulation with ADP (10 μM) for each treatment [ticagrelor] (M) and time point (mins), respectively. Data is displayed as the mean ± SEM, n = 4. Significant differences in % aggregation between conditions was assessed via one-way ANOVA with Dunnett's multiple comparisons *post-hoc* test. Pairwise comparisons are made in respect to Vehicle control (0.1% DMSO) for each respective time point. Vehicle vs. ticagrelor; **** = $P < 0.0001$. ** = $P < 0.01$. ns = $P > 0.05$.

3.2.3. Ticagrelor reversibility in human platelet-rich plasma.

Following the results from Figure 3.8., we sought to determine whether the reversibility of ticagrelor can be achieved within a platelet-based system. The reversibility of drug administration is fundamental when considering determinations about the offset of action of the respective antiplatelet agent. Therefore, we employed subsequent reversibility experiments regarding ticagrelor administration in human PRP (Figure 3.13.). Analysis of the data gathered below (Figure 3.13.) indicates there were no significant differences in the % aggregation measurements achieved in PRP treated with ticagrelor (1 μM vs. 10 μM) before washout, after washout 1 and after washout 2 (ns = P = 0.294, 0.9219 & 0.1357, respectively).

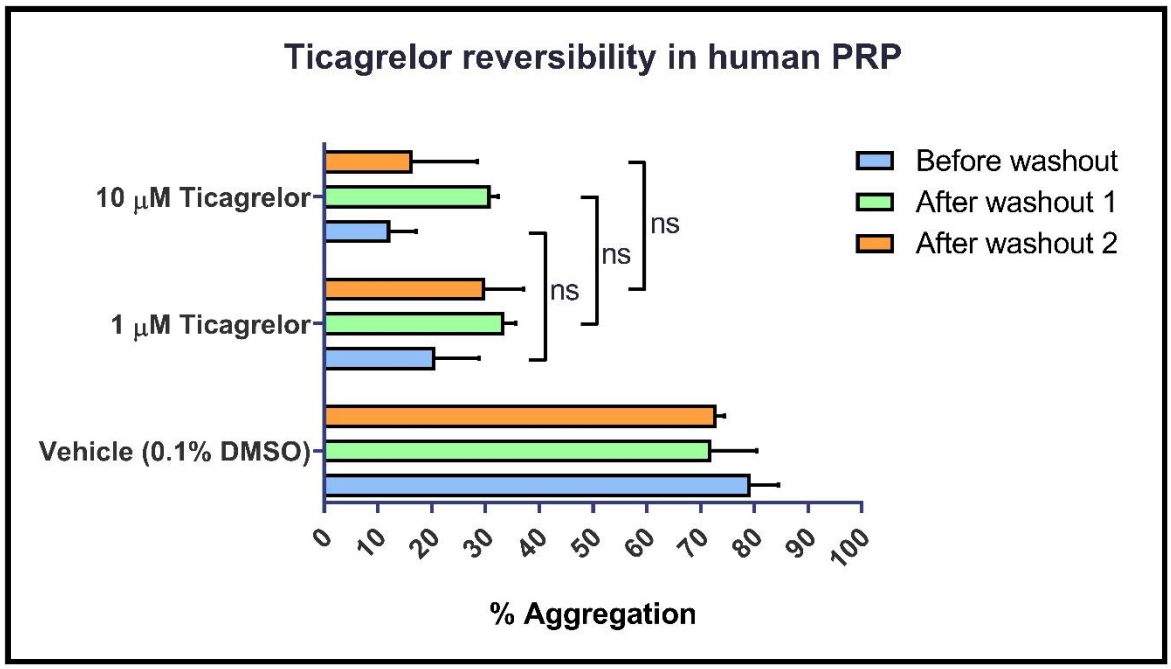

Figure 3.13. Ticagrelor reversibility in human PRP. Human platelet rich plasma was isolated as indicated in 2.2.1. The isolated PRP was divided into 3 aliquots. The first aliquot was treated with either ticagrelor (10 µM or 1 µM) or vehicle (0.1% DMSO) for 10 minutes. Following the elapsed incubation time for aliquot 1, the treated PRP was stimulated with ADP (10 µM) and LTA measurements taken immediately following this, as indicated in 2.2.2. Consequently, generating % aggregation values corresponding to the respective treatment before subsequent washout steps as indicated above (Before washout). Concurrently, the second aliquot was similarly treated with ticagrelor (10 µM) or vehicle (0.1% DMSO) for 10 minutes. Following this, treated PRP in aliquot 2 was centrifuged to remove the supernatant (PPP), forming a pellet of platelets. The pelleted platelets were then resuspended in fresh, untreated PPP and subsequently stimulated with ADP (10 µM), generating aggregation values for each treatment (veh, 1uM or 10uM tic) that was indicated as 'after washout 1'. The same procedure of treatment, centrifugation and resuspending was applied to the third aliquot of PRP, such that stimulation occurred following a second successive washout (After washout 2). Data plotted represent the maximum % aggregation elicited following stimulation with ADP (10 µM) for each treatment [ticagrelor] (M) and respective washout step. Data presented as the mean ± SEM. Significant differences in % aggregation between groups was analysed via 2-way ANOVA with Dunnett's multiple comparisons *post-hoc* test. [veh vs. 1 µM ticagrelor = ****, $p < 0.0001$ (37.30-56.14)], [veh vs. 10 µM ticagrelor = ****, $p < 0.0001$ (45.31-64.25)], [1 µM ticagrelor vs. 10 µM ticagrelor = ns, $p = 0.0948$ (-1.310-17.53)].

In summary, the above data (Figures 3.11-3.13) demonstrates that the utility of $P2Y_{12}R$ inhibition via ticagrelor administration can be replicated *ex-vivo*, in a platelet-based system. Thus, additionally providing confidence that the results obtained in previous BRET experiments align with that seen in platelets.

Chapter 4: Discussion

4.1. Antiplatelet therapies for the treatment of acute coronary syndromes.

Patients with acute coronary syndromes often require emergency intervention strategies to mitigate epicardial damage that results from coronary vessel occlusion. The functional responses elicited by platelets at sites of vessel injury is known to be a major player in the pathogenesis of the disease. Notably, resulting from the auto- and paracrine release of inflammatory mediators such as ADP that promotes the formation of pro-thrombotic platelet aggregates via $P2Y_{12}R$ activation and resultant signal transduction. As such, antiplatelet therapies utilise a combination of drugs that target multiple pro-thrombotic signalling pathways including the $P2Y_{12}R$. Antagonism of that have cemented themselves as cornerstones of vascular medicine.

Following an ACS, the aim for clinicians is to prevent any further vessel occlusion that results from inappropriate platelet aggregation via pro-thrombotic platelet activation. The clinician may prescribe one of several different $P2Y_{12}R$ inhibitors, in combination with aspirin (Figure 1.7), for the prophylactic treatment of the disease. Drawbacks in the therapeutic efficacy of the older generation of $P2Y_{12}R$ inhibitors, termed thienopyridines (ticlopidine & clopidogrel; see figure 1.8 & 1.9), became evident with various caveats in treatment resulting with their use. Notably, these include patients who are non-responsive or resistant to treatment especially to clopidogrel. In patients not responsive to clopidogrel therapy, prasugrel (figure 1.10) has offered some respite, addressing the inconsistencies in the formation of the active metabolite within patients who are identified as non-responders/resistant. Conversely, there are some patients who are prone to bleeding upon antiplatelet therapy, potentially due to the irreversible blockade of $P2Y_{12}R$ for the lifespan of the platelets by the thienopyridines clopidogrel and prasugrel.

Newer generations of $P2Y_{12}R$ inhibitors have been ushered into clinical practice to fill these shortfalls in therapeutic efficacy. The newest iteration are the cyclopentyl-triazolo-pyrimidines, ticagrelor and cangrelor (see figure 1.11). Ticagrelor has been shown to be clinically superior to that of the previously prescribed $P2Y_{12}R$ inhibitors, both in clinical trials and laboratory studies. Possible reasons for the observed clinical superiority seen with ticagrelor may be, in part, due to novel mechanisms of action that arise from the unique pharmacodynamic characteristics attributed to the drug.

The central aim of this thesis was to further elucidate the pharmacodynamics of ticagrelor antiplatelet therapy that may contribute to its reported superiority in the clinical setting. As such, two distinct but interrelated areas were investigated:

1) The utility of ticagrelor to act as an inverse agonist at the human $P2Y_{12}R$, attenuating basal constitutive activity.
2) To determine whether ticagrelor is reversible versus the endogenous $P2Y_{12}R$ agonist, ADP.

4.2. The inverse agonist utility of ticagrelor.

According to the classical two-state model of receptor function, receptors can exist in an equilibrium between an active (R*) and inactive state (R) (Figure 4.1). A ligand has two properties that determines its biological activity within a receptor population: affinity and intrinsic efficacy. Affinity refers to the ability of any ligand to bind to a given receptor and intrinsic efficacy describes the effect the drug has on the receptor that causes a change in receptor activity. Agonists bind with higher affinity to the active state of the receptor (R*) and enriches a larger proportion of the receptor population to adopt a signalling conformation (R*), demonstrating positive intrinsic efficacy and is a function of conformational selection. The ability of agonists to produce varying maximal responses via the same receptor allows for varying degrees of positive intrinsic efficacy and therefore an agonist can be described as partial, giving a submaximal response, or full, giving the maximal response.

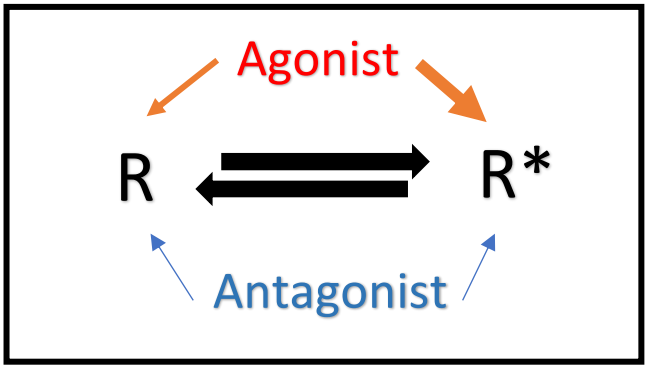

Figure 4.1. Simplified schematic illustration of the two-state model of receptor function. A receptor is said to exist between two states under equilibrium. Agonists preferentially bind to the active state of the receptor (R*), keeping the receptor in a signalling conformation (R*) (conformational selection). Antagonists bind to the active (R*) or inactive (R) state of the receptor and block the intracellular signalling elicited by an agonist.

Conversely, antagonists bind with equal affinity to both R and R*, but they do not elicit a biological response via the receptor and demonstrate zero (neutral) intrinsic efficacy. Antagonists therefore

decrease the probability of an agonist to bind to a receptor by binding to an orthosteric (competitive) or allosteric (non-competitive) site. This traditional iteration of drug-receptor theory is predicated on the assumption that receptors in a given population exist in an inactive, non-signalling conformation unless acted upon by a ligand that has agonist activity (both affinity & intrinsic efficacy at the receptor). However, the two-state model was initially designed to only describe ligand-gated ion channels. As such, with the discovery of receptor populations that can signal in the absence of an agonist, termed constitutive activity, the three-state model is now the 'simplest' currently accepted multiple active state model of GPCR function (Figure 4.2A).

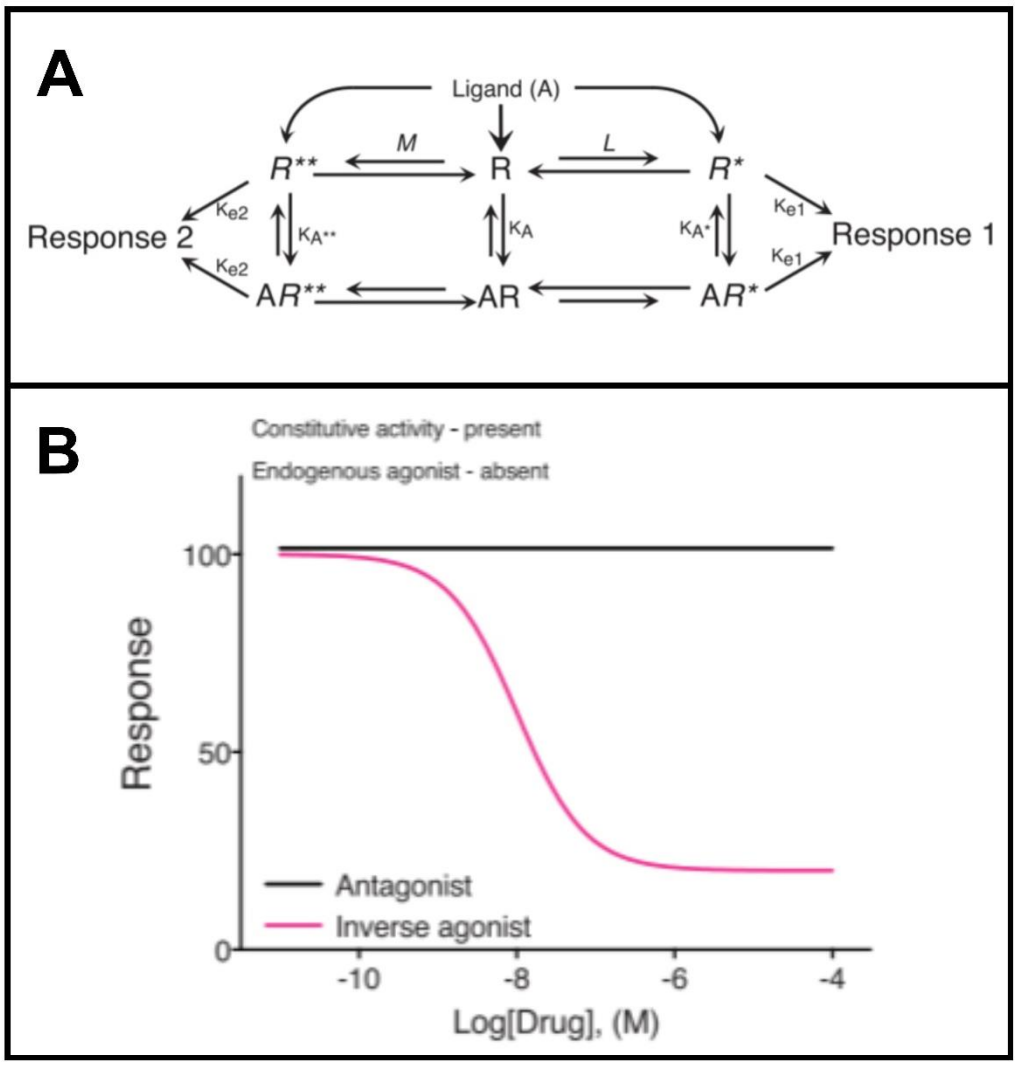

Figure 4.2. The three-state model of receptor function. A) illustrative diagram of the currently accepted, three-state model of receptor function. B) Illustrative graph demonstrating the utility of inverse agonists within a receptor population that exhibits constitutive activity. (Berg and Clarke 2018).

The demonstration of constitutive activity was first reported in reconstituted beta-2 adrenergic receptors from the guinea pig lung which showed increased GTPase activity in the absence of a ligand

following addition of Gαs G-protein isolated from human erythrocytes (Cerione, Codina et al. 1984). Soon after, studies demonstrated that endogenously expressed delta-opioid receptors (WT) (NG108-15 cells) exhibit constitutive activity via intrinsic Gαi-coupling in the absence of a ligand (Costa and Herz 1989). Together, these studies help to facilitate the expansion of the previously accepted framework of drug-receptor theory and consequently added a new dimension to the toolbox of pharmacology, inverse agonism. Unlike agonists, ligands that increase receptor activity, inverse agonists are ligands that reduce basal receptor activity (Berg and Clarke 2018).

The human purinoceptor $P2Y_{12}$ was first demonstrated to exhibit basal constitutive activity following the stable expression of a $P2Y_{1\&12}R$ chimera in cell lines (Ding, Kim et al. 2006). The constitutive activity displayed by $P2Y_{12}$ is suggested to be a normal feature of the receptor (Garcia, Maurel-Ribes et al. 2018), and additionally thought to be a contributor to the occurrence of platelet hyperactivity seen in patients with diabetes mellitus (type II) (Hu, Chang et al. 2017). *Ding et al* additionally revealed potent inverse agonist activity of the $P2Y_{12}R$ antagonist, AR-C78511. More recently, work from the Mundell laboratory confirmed the observation of inverse agonism at the receptor, both in cell lines and human platelets (Aungraheeta, Conibear et al. 2016). The inverse agonism observed was elicited by ticagrelor, which increased platelet cAMP and vasodilator-stimulated phosphoprotein phosphorylation (pVASP) in an agonist-independent manner. In addition, ticagrelor was demonstrated to inhibit the platelet ENT1 transporter. This thesis further characterises the mode of action of ticagrelor at the receptor-G-protein which may influence its perceived clinical superiority over the previously described antiplatelet therapies.

Employing $BRET^2$ assays in HEK293T cells transfected with $P2Y_{12}R$ and associated G-proteins, we sought to assess the pharmacodynamic effects of ticagrelor on receptor activation at the G-protein level. As described in 3.1 (see figure 2.2), a change in the BRET ratio correlates to either receptor activation or inactivation. For example, a decrease in the BRET signal correlates to G-protein dissociation and is hence interpreted as receptor activation. Initial studies validated this assay system with the endogenous agonist ADP stimulating a time- and concentration-dependent increase in $P2Y_{12}R$ activity. The data from these experiments gave confidence that the $BRET^2$ assay was viable following the transient transfection of $P2Y_{12}R$ and associated G-proteins.

The inhibitory effect of ticagrelor alongside a range of $P2Y_{12}R$ antagonists (all at 10 μM) was subsequently assessed via further $BRET^2$ experiments (figure 3.2A & B). Notably, ticagrelor incubation

increased the delta BRET signal, indicating receptor inactivation. Importantly, incubation with the $P2Y_{12}R$ antagonist AR-C66096 produced no change in the BRET signal, indicative that it is a neutral antagonist (see figure 4.2). This demonstrates that not all the antiplatelet drugs utilised within our $BRET^2$ assay caused a change in the BRET signal. Additionally, this result is further evidence that ticagrelor does not appear to behave as a traditional antagonist but rather as an inverse agonist. Furthermore, the lack of change in the BRET signal in response to treatment of ticagrelor to mu-opioid receptor transfected cells (figure 3.5D) serves as a negative control experiment, and evidence that the inhibition resulting from ticagrelor is specific to the $P2Y_{12}R$. Interestingly, cangrelor incubation resulted in a similar reversal of the ADP-mediated response to that seen with ticagrelor. However, the max BRET signal achieved by cangrelor incubation alone was roughly half of that observed with ticagrelor. This would suggest that cangrelor also has inverse agonist activity at the $P2Y_{12}R$. This aligns with similar findings from previous studies utilising BRET technology in $P2Y_{12}R$-transfected HEK293 cells (Garcia, Maurel-Ribes et al. 2018).

Further detailed study of both the concentration- and time-dependence of ticagrelor and cangrelor was performed. Both produced a sustained reduction in receptor activity for the duration of the assay (60 mins) although that of cangrelor was lower than ticagrelor. The concentration-dependence of ticagrelor-alone and cangrelor-alone administration revealed EC50s of 208 nM (70 – 587 nM, n = 4) and 62 nM (33 – 117 nM, n = 5), respectively. This assessment of relative potency is comparable with that reported from previous studies (Cattaneo 2010). Our data suggests cangrelor to be more potent than ticagrelor but with a markedly reduced Emax. Therefore, in respect to ticagrelor, cangrelor potentially behaves as a partial inverse agonist whereas ticagrelor behaves as a full inverse agonist. The distinction between full and partial agonism is understood to refer to the relative intrinsic efficacy that can be achieved by different drugs at the same receptor. A possible reason for the noted difference in intrinsic efficacy found between cangrelor and ticagrelor has been suggested to be as a result of biased inverse agonism attributed to cangrelor (Garcia, Maurel-Ribes et al. 2018). Functional selectivity gives rise to the phenomenon of biased agonism and refers to the ligand-dependent preferential activation of selective intracellular signalling pathways at the same receptor (Urban, Clarke et al. 2007). Importantly, ticagrelor's superiority in $P2Y_{12}R$ inhibition has been attributed and suggested to be due to the inactive conformation of the receptor adopted with ticagrelor treatment rather than a result of biased inverse agonism involving preferential downstream pathway activation.

4.3. Ticagrelor antagonism of ADP-stimulated platelet aggregation.

Further evidence of ticagrelor activity at the $P2Y_{12}R$ in a physiologically relevant context was exemplified in platelets via LTA (see figures 3.11 & 3.12). As outlined previously in 3.2, LTA is a widely utilised diagnostic tool that facilitates the assessment of the inhibitory effect of antiplatelet therapeutics on the pro-thrombotic response of platelet aggregation. In agreement with previous studies (Jarvis, Humphries et al. 2000) and as shown in figure 3.11, ADP increased platelet aggregation in a concentration-dependent manner. Preincubation of platelets with ticagrelor (300 nM) caused a visible rightward shift of the dose-response curve for ADP-stimulated platelet aggregation. This is indicative of effective $P2Y_{12}R$ inhibition by ticagrelor. Furthermore, this selected concentration of 300 nM ticagrelor is comparable with that found under physiological conditions in patients, with reported plasma concentration ranging from 0.4 – 1.5 µM (Storey, Husted et al. 2007). Subsequent time course experiments of ticagrelor action in human PRP were performed (figure 3.12) to assess the speed of onset and duration of ticagrelor antiplatelet therapy. Ticagrelor at 1 µM & 10 µM effectively inhibited ADP-induced (10 µM) platelet aggregation across a range of time points in a concentration-dependent manner. The onset of ticagrelor action was rapid, complementing our results observed in previous $BRET^2$ experiments (see figure 3.3). Interestingly, ticagrelor action did not display any reversal in platelet inhibition at the 240-minute time point at all concentrations, indicating the stability of ticagrelor in this assay platform and potentially the reversibility of ticagrelor, which is discussed in detail later.

4.4. Ticagrelor-dependent inhibition of the ENT1 transporter.

Previous work from the Mundell laboratory has suggested there to be a second novel mechanism of action of ticagrelor aside from the inverse agonist activity at the $P2Y_{12}R$, as a result of inhibition of platelet-expressed ENT1 (Aungraheeta, Conibear et al. 2016). Inhibition of ENT1 was shown to lead to an accumulation of extracellular adenosine, capable of activating Gαs-coupled A_2A receptors. Mundell and colleagues suggest this may in part contribute to the adenosine-related side effects reported with ticagrelor use, dyspnoea. We sought to assess if this additional novel mode of action contributed to the effect, if any, on the mode of action of ticagrelor at the $P2Y_{12}R$ in our $BRET^2$ cell-based system (figure 3.5A-D). These studies revealed that the preincubation of either apyrase, XAC or forskolin had no effect on the BRET signal achieved by ticagrelor when compared to ticagrelor-alone treated cells. Additionally, cells that were transfected with the MOR and G-proteins showed

no change in the BRET signal when treated with ticagrelor-alone. As outlined in 3.1.5, the data from these experiments serve as further controls and give confidence that the inverse agonist utility seen at the $P2Y_{12}R$ is indeed specific to the mode of action of ticagrelor.

The therapeutic usefulness of inverse agonists rests on the assumption that the enhanced constitutive activity present within a given receptor population contributes to the disease pathology. It has now been identified that platelets from patients with diabetes mellitus type II express constitutively activated $P2Y_{12}Rs$ (Hu, Chang et al. 2017), increasing the risk of prothrombotic complications in this subset of patients. Therefore, ticagrelor's superiority within the clinical setting may be explained in part by its inverse agonist activity. To further define the pharmacodynamics of ticagrelor antiplatelet therapy, we sought to assess the reversibility of the drug both in cell lines and in human platelets.

4.5. Importance of C194 on the $P2Y_{12}R$ for ticagrelor activity

The binding site of ticagrelor at the $P2Y_{12}R$ has been under debate for some time (VAN Giezen, Nilsson et al. 2009, von Kügelgen, Lutz et al. 2014, Parker and Storey 2016). It has now been established that the active metabolites for the thienopyridines, clopidogrel and prasugrel, exert their antagonist effect via their interaction with the cysteine residue at position 97 of the $P2Y_{12}R$ (Hoffmann, Lutz et al. 2014). *Hoffmann* and colleagues utilised further mutagenesis experiments and identified C194 as a cysteine residue within the $P2Y_{12}R$, to be crucial for the recognition of ticagrelor's antagonist activity.

As shown in figure 3.6, C194A mutation in the $P2Y_{12}R$ resulted in a significant reduction of both ticagrelor's inverse agonist activity and ability to antagonise ADP. ADP-stimulated $P2Y_{12}R$ activity was unaffected by the C194A mutation. This difference between ADP and ticagrelor activity is further evidence supporting the non-competitive mode of action of ticagrelor. This is comparable to the findings from *Mundell* and colleagues (Aungraheeta, Conibear et al. 2016), previous mutagenesis studies(Garcia, Maurel-Ribes et al. 2018) and studies from others (VAN Giezen, Nilsson et al. 2009). Notably, the C194A mutation had no effect on the antagonist activity of the inverse agonist, cangrelor, as well as the neutral antagonist AR-C66096. The data shown in figure 3.6 therefore gives confidence that the cysteine residue at position 194, within TM5 of the receptor protein is crucial in the recognition and interaction specific to ticagrelor antagonist activity at the $P2Y_{12}R$.

Further study using the synthetic agonist 2MeSADP further confirmed that C194 residue is important for the recognition of ticagrelor (*** = P < 0.001, n = 3). Ticagrelor was previously shown to act as a competitive antagonist at the P2Y12R versus 2MeSADP. Notably, we show that 2MeSADP agonist activity is significantly reduced by the C194A mutation. This indicates that this cysteine residue is also important for 2MeSADP agonist activity and that the binding site for ticagrelor and 2MeSADP potentially overlap. This data was additionally exemplified via molecular dynamic simulations (see figure 3.7B) and further evidence that ADP binds to the $P2Y_{12}R$ independently from ticagrelor and indicating C194 seems important for 2MeSADP activity. Overall, this data help to define the unique binding modality of ticagrelor that may influence both its reversibility at the $P2Y_{12}R$, and its perceived superiority over the previously described antiplatelet agents.

4.6. Is ticagrelor reversible?

The reversibility of a drug correlates to the ratio of the rate constant of dissociation of the ligand from the receptor (K_{off}) and the rate constant of association of the ligand to the receptor (K_{on}). This ratio of K_{off}/K_{on} is known as the dissociation constant (K_d), the inverse of the ligand's affinity for the receptor protein (Tonge 2018). This, in turn, is influenced by the intramolecular forces between the functional groups of the ligand, interacting with that of the substituent amino acid residues within the receptor's binding pocket. This pharmacodynamic parameter of drug reversibility is crucially important to consider when assessing the safety and efficacy of pharmacological therapeutics in the context of drug discovery and pharmacovigilance (Strelow 2017).

The reported clinical superiority in efficacy of ticagrelor over other previously described antiplatelet agents is clear, as outlined above (see 1.15.5). However, the untenable side effect profile of spontaneous major bleeding and bleeding during invasive procedures exists and remains with ticagrelor, as with all antiplatelet agents. In respect to the thienopyridines, clopidogrel and prasugrel, the cause for this unwanted bleeding is thought in part to be due to their mode of action and irreversible blockade of the $P2Y_{12}R$. These drugs effectively attenuate platelet function for the duration of their lifespan.

The need for reversible $P2Y_{12}R$ antagonists especially in the context of antiplatelet drug switching in patients undergoing emergency invasive procedures such as PCI and CABG is clear. Ticagrelor has been licensed as the first perorally active and reversible $P2Y_{12}R$ antagonist (Hoffmann, Lutz et al.

2014). However, clinical and laboratory evidence has emerged contesting ticagrelor's reversibility at the $P2Y_{12}R$. The results from the PLATO study demonstrated ticagrelor to be more advantageous than clopidogrel in platelet inhibition, however both displayed similar bleeding profiles during invasive procedures (James, Akerblom et al. 2009). In this study, ticagrelor was withheld for 24-72 hours and clopidogrel for 5 days. The reported half-life of ticagrelor is approximately 7 hours, so it is perhaps surprising the degree of bleeding found in patients. More recently, in-vitro studies have emerged suggesting platelet supplementation via transfusion may not rescue platelet inhibition resulting from ticagrelor action (Martin, Berndt et al. 2016). Furthermore, ticagrelor-targeted monoclonal antibody fragments have been engineered, appearing efficacious in the rapid reversal of the drug (Bhatt, Pollack et al. 2019) (Zhang, Xu et al. 2019). The data from these studies ultimately underscores the inconsistencies in the reported reversibility of ticagrelor.

Initially, we used our cell-based BRET assay to assess ticagrelor reversibility. Notably, the inverse agonist activity of ticagrelor was not reduced following multiple washing steps. In addition, ticagrelor antagonist of ADP-stimulated $P2Y_{12}R$ activity persisted following washing. Notably, both cangrelor's inverse agonist activity and antagonism of ADP-stimulated $P2Y_{12}R$ was reversed following washing steps (figure 3.8B). As expected, ADP-stimulated activity could not be restored following washing in cells treated with R-138727, an irreversible antagonist, whilst AR-C66096 antagonism could be reversed by washing. The data with both cangrelor and AR-C66096 shows that cell washing could effectively remove ligand.

Ultimately, ticagrelor shows minimal reversibility and is more akin to R-138727. Moreover, when compared with that of the reversible inverse agonist cangrelor, ticagrelor appears to bind to the $P2Y_{12}R$ irreversibly.

To complement our cell line studies we performed similar experiments in human platelets (figure 3.13). As in our cell line studies, ticagrelor-dependent inhibition of ADP-stimulated platelet aggregation failed to reverse following platelet washing. This is further evidence of the suggested irreversibility of ticagrelor at the $P2Y_{12}R$ and ultimately gives confidence in the accuracy of the results obtained from previous $BRET^2$ reversibility experiments (figure 3.8). It appears that ticagrelor, in our hands, behaves as an irreversible inverse agonist at the human $P2Y_{12}R$.

4.7. Implications of switching guidelines on $P2Y_{12}R$ stabilisation.

As outlined in 3.1.8, a clinical concern regarding the use of all antiplatelet agents is the risk of DDIs when switching pharmacotherapies. Switching is common, especially in patients who are to undergo emergency invasive procedures. Consequently, expert consensus guidance for switching antiplatelet therapies has emerged (Angiolillo, Rollini et al. 2017). *Angiolillo* and others characterise switching as escalation, de-escalation or change. Escalation refers to the switching from a less-intensive to a more-intensive antiplatelet agent. De-escalation refers to the switching from a more-intensive to a less-intensive agent. Change refers to the switching between similarly efficacious agents. The pharmacodynamics of antiplatelet agents, and particularly their reversibility profile is therefore a crucial parameter to consider in the context of influencing antiplatelet agent use in clinical practice. This thesis describes data regarding the effect of concomitant antiplatelet agent treatment on the level of inhibition achieved at the G-protein/receptor level of the $P2Y_{12}R$.

We firstly sought to determine if ticagrelor was able to act on the $P2Y_{12}R$ if the receptor was preincubated with a range of $P2Y_{12}R$ antagonists. Cell line studies revealed that preincubation with either the neutral antagonist AR-C66096 or partial inverse agonist cangrelor blocked ticagrelor action at the $P2Y_{12}R$. This may indicate that a large proportion of the receptor population once occupied by either of these ligands blocks subsequent ticagrelor binding to the receptor. Notably, R-138727 preincubation followed by ticagrelor treatment resulted in a significant increase in the level of $P2Y_{12}R$ G-protein association that surpassed that achieved by both R-138727-alone and ticagrelor-alone treated cells (** = $P < 0.01$, $n = 3$). This result suggests that the concomitant administration of a thienopyridine alongside ticagrelor may result in a greater degree of inverse agonist activity, and hence greater inhibition of $P2Y_{12}R$ agonist-mediated signal transduction. This data confirms suggestions from previous clinical studies indicating the potential for DDIs when switching from prasugrel to ticagrelor (Rollini, Franchi et al. 2016). This result may indicate that R-138727 perhaps changes the conformation of the $P2Y_{12}R$ and its ligand binding pocket such that subsequent ticagrelor binding may enable the receptor to adopt a more inactive conformation.

We secondly sought to establish whether ticagrelor effects could be reversed by adding other $P2Y_{12}R$ antagonists. None of the ligands (AR-C66096, R-138727 or cangrelor) were able to reduce ticagrelor activity. Ultimately the data from the experiments in figure 3.10 suggest that the switching modality of de-escalation, switching from a more intensive agent to a less intensive one, may not induce any potential DDI. This is interesting, considering the data exemplified in figure 3.9C regarding the

observed potentiation in G-protein association resulting from preincubation of R-138727, followed by treatment with ticagrelor (escalation). The explanation of this phenomenon is unclear, however certainly warrants further extensive investigation in platelets and in a clinical setting. Ongoing molecular modelling should hopefully provide at least a greater mechanistic understanding of this phenomenon.

4.8. Experimental limitations & future direction.

This thesis describes data characterising the molecular mechanisms of ticagrelor action at the human $P2Y_{12}R$, both in cell lines and in human platelets. As such, experimental limitations exist in this study and must be considered.

1) The $BRET^2$ technology employed in experiments in this thesis may contain intrinsic limitations that could influence observed results. The $BRET^2$ technique requires the successful transient transfection of the $P2Y_{12}R$ and associated G-proteins. Following the successful recombination of the $P2Y_{12}R$ at the cell membrane, $BRET^2$ technology facilitates a highly sensitive assessment of intracellular G-protein dissociation ($P2Y_{12}R$ activation) and association ($P2Y_{12}R$ stabilisation) via the mechanism previously outlined in 3.1 (see figure 2.2). It must be noted that the fused constituents (RlucII & GFP10) to the G protein-subunits may cause steric hindrance, and perhaps may not accurately reflect observations seen in wild type interactions. To assess the level of receptor activation more accurately in the context of ticagrelor action, stable cell lines expressing the receptor could perhaps be utilised and GTPase assays employed.

2) Receptor/G-protein over-expression in cell lines may induce constitutive activity. Increased G-protein could lead to more coupling in the absence of agonist and therefore this may produce false negatives. Additionally, increased receptor expression achieved by transient transfection may further enhance the signal detected by the BRET system. The results in this thesis therefore may not accurately represent what takes place with the $P2Y_{12}R$ in platelets. In this study, DNA expression via transfection was controlled at constant levels (1 µg), however we did not quantify $P2Y_{12}R$ surface expression. To address this, Immunofluorescence (IF) IHC techniques utilising fluorophore-tagged antibodies against the $P2Y_{12}R$ should perhaps

be performed, providing a quantifiable comparison of $P2Y_{12}R$ expression levels between our HEK293T cell line and platelets. In addition, further studies characterising how changes in receptor expression could impact upon basal receptor activity should be performed. Ideally, these studies would be undertaken with both the $P2Y_{12}R$ and another Gi-coupled GPCR (i.e. μ-opioid receptor). This would allow us to determine if simply overexpression of any receptor increases basal receptor reactivity, or if it is a fundamental property of the $P2Y_{12}R$.

3) The $BRET^2$ data in this thesis came from studies performed solely in HEK293T cells. In the future, additional cell lines could be utilised to account for any cell-line specific caveats.

4) When designing and employing the LTA experiments exemplified in figures 3.11-3.13, a limitation to consider was the potential incidence of interindividual variability in platelet responses observed between healthy blood donors. Additionally, the process of platelet isolation requires centrifugation and increased sample manipulation. Therefore, the incidence of unwanted platelet activation may have influenced these results. To address these caveats, experiments in platelets assessing changes in intracellular cAMP following treatment with ticagrelor should be undertaken.

5) In this study, all experiments were carried out on independent days and at least in triplicate (n=3), following standard lab procedure. Many scientific peer-reviewed journals now require a minimum of n=5 for successful submission. It must be noted that some key experiments in this study did not meet the n=5 criteria that is now required. However, the data collected by each independent experiment was an average of quadruplicate measurements for each treatment. Additionally, among replicates between experiments, the data was very consistent. Therefore, although some key experiments not meeting the current criteria for submission to a peer reviewed journal, we ultimately have confidence in the reproducibility of our results.

It is important to consider the future direction of the work within this thesis, especially in the context of confirming the results presented in this study. Although we provide evidence that further

elucidates the pharmacodynamics of ticagrelor antiplatelet therapy at the human $P2Y_{12}R$, a more comprehensive understanding of the molecular interactions underpinning its perceived clinical superiority are still needed. For example, a more detailed exploration of competitive/non-competitive interactions of ticagrelor with that of the $P2Y_{12}R$ could be employed. How ticagrelor activity is affected by a range of $P2Y_{12}R$ ligands could be explored using detailed pharmacological analysis (i.e. Schild plot analysis). This data would be even more powerful if it were backed by In-Silico docking techniques and molecular modelling/dynamics. The combination of these approaches may provide a more mechanistic insight into the interactions of ticagrelor with that of the receptor. Further molecular dynamics could be used to assess specific amino acid residues that may confer both ticagrelor activity and irreversibility. Site directed mutagenesis of potential $P2Y_{12}R$/ticagrelor interacting residues could further help define ticagrelor's mode of action.

4.9. Final conclusions.

The data in this thesis has further defined the parameters that contribute to the pharmacodynamics of ticagrelor antiplatelet therapy at the human $P2Y_{12}R$. It appears increasingly likely that the reported superiority of ticagrelor in clinical settings may be the result of both the inverse agonist activity of ticagrelor and the suggested irreversible molecular interaction of ticagrelor with the receptor. This irreversibility may also contribute in part to the increased bleeding risk seen in patients and the tangible clinical concerns evidenced by the recent development of ticagrelor reversal agents (Bhatt, Pollack et al. 2019). Moreover, the data presented may help to further inform the newly described guidelines for antiplatelet switching, of which the accurate characterisation of the pharmacodynamics of each drug is imperative. In the context of ticagrelor, the interesting pharmacology exhibited at the $P2Y_{12}R$ is a demonstration of the therapeutic usefulness of inverse agonism, allowing clinicians greater control of receptor function and thus expected to translate to a better treatment of vascular disease.

Considering the wide-spread use of DAPT in the treatment of ACS and the increased efficacy of ticagrelor over the previously described antiplatelet agents, coupled with that from projected increases in the incidence of the disease globally, it appears that ticagrelor may be prescribed more in the future, potentially as a monotherapy. Therefore, the accurate characterisation of the pharmacodynamics of ticagrelor; its mode of action, onset and reversibility is even more critical. For the older generation of thienopyridines, clopidogrel, it took 10 years after its initial discovery that its

mechanism of action was fully elucidated (Maffrand 2012). Ticagrelor was first approved for use in the EU, December 3rd, 2010 and July 20th, 2011 by the US FDA. Therefore, it is entirely possible that the characterisation of ticagrelor action at the $P2Y_{12}R$ will continue to evolve.

Most recently, a novel coronavirus outbreak (COVID-19) has circulated the world, resulting in a global pandemic. The disease state caused by severe acute respiratory syndrome coronavirus 2 (SARS-CoV-2) has been reported to affect multiple organ systems. Notably, patients with diabetes mellitus, obesity and/or hypertension are at markedly increased risk of mortality (Dariya and Nagaraju 2020). Further evidence has emerged suggesting cardiac troponin I levels are elevated in patients with severe infection (Imazio, Klingel et al. 2020), indicative of cardiac injury. Additionally, platelet-rich microthrombi are reported to be present in the vasculature of the lungs, heart, kidneys and liver of patients infected with the virus (Rapkiewicz, Mai et al. 2020). Moreover, megakaryocytes were identified to be localised in the microvasculature of the heart, glomeruli and the lungs as well as increased numbers in the bone marrow. This may indicate a heightened prothrombotic response of platelets in COVID-19.

Therefore, antiplatelet therapies may become increasingly indicated in the future and thus may result in the increased clinical use of ticagrelor. The results from this thesis further defines the pharmacodynamics of ticagrelor antiplatelet therapy and gives insight into its molecular pharmacology contributing to its perceived clinical superiority, which may in turn help to inform the debate regarding the complex switching guidelines for antiplatelet agents.

Chapter 5: References

- (2001). "Effects of Clopidogrel in Addition to Aspirin in Patients with Acute Coronary Syndromes without ST-Segment Elevation." New England Journal of Medicine **345**(7): 494-502.
- Alexander, S. P. H., A. Christopoulos, A. P. Davenport, E. Kelly, A. Mathie, J. A. Peters, E. L. Veale, J. F. Armstrong, E. Faccenda, S. D. Harding, A. J. Pawson, J. L. Sharman, C. Southan, J. A. Davies and C. Collaborators (2019). "THE CONCISE GUIDE TO PHARMACOLOGY 2019/20: G protein-coupled receptors." Br J Pharmacol **176 Suppl 1**: S21-S141.
- Angiolillo, D. J., F. Rollini, R. F. Storey, D. L. Bhatt, S. James, D. J. Schneider, D. Sibbing, D. Y. F. So, D. Trenk, D. Alexopoulos, P. A. Gurbel, W. Hochhoizer, L. De luca, L. Bonello, D. Aradi, T. Cuisset, U. S. Tantry, T. Y. Wang, M. Valgimigli, R. Waksman, R. Mehran, G. Montalescot, F. Franchi and M. J. Price (2017). "International Expert Consensus on Switching Platelet P2Y12 Receptor-Inhibiting Therapies." Circulation **136**(20): 1955-1975.
- Angiolillo, D. J., F. Rollini, R. F. Storey, D. L. Bhatt, S. James, D. J. Schneider, D. Sibbing, D. Y. F. So, D. Trenk, D. Alexopoulos, P. A. Gurbel, W. Hochholzer, L. De Luca, L. Bonello, D. Aradi, T. Cuisset, U. S. Tantry, T. Y. Wang, M. Valgimigli, R. Waksman, R. Mehran, G. Montalescot, F. Franchi and M. J. Price (2017). "International Expert Consensus on Switching Platelet P2Y(12) Receptor-Inhibiting Therapies." Circulation **136**(20): 1955-1975.
- Angiolillo, D. J., D. J. Schneider, D. L. Bhatt, W. J. French, M. J. Price, J. F. Saucedo, T. Shaburishvili, K. Huber, J. Prats, T. Liu, R. A. Harrington and R. C. Becker (2012). "Pharmacodynamic effects of cangrelor and clopidogrel: the platelet function substudy from the cangrelor versus standard therapy to achieve optimal management of platelet inhibition (CHAMPION) trials." J Thromb Thrombolysis **34**(1): 44-55.
- Aungraheeta, R., A. Conibear, M. Butler, E. Kelly, S. Nylander, A. Mumford and S. J. Mundell (2016). "Inverse agonism at the P2Y12 receptor and ENT1 transporter blockade contribute to platelet inhibition by ticagrelor." Blood **128**(23): 2717-2728.
- Bahadoran, Z., P. Mirmiran and F. Azizi (2015). "Fast Food Pattern and Cardiometabolic Disorders: A Review of Current Studies." Health Promot Perspect **5**(4): 231-240.
- Baker, D. E. and K. T. Ingram (2015). "Cangrelor." Hospital pharmacy **50**(10): 922-929.
- Benjamin, E. J., P. Muntner, A. Alonso, M. S. Bittencourt, C. W. Callaway, A. P. Carson, A. M. Chamberlain, A. R. Chang, S. Cheng, S. R. Das, F. N. Delling, L. Djousse, M. S. V. Elkind, J. F. Ferguson, M. Fornage, L. C. Jordan, S. S. Khan, B. M. Kissela, K. L. Knutson, T. W. Kwan, D. T. Lackland, T. T. Lewis, J. H. Lichtman, C. T. Longenecker, M. S. Loop, P. L. Lutsey, S. S. Martin, K. Matsushita, A. E. Moran, M. E. Mussolino, M. O'Flaherty, A. Pandey, A. M. Perak, W. D. Rosamond, G. A. Roth, U. K. A. Sampson, G. M. Satou, E. B. Schroeder, S. H. Shah, N. L. Spartano, A. Stokes, D. L. Tirschwell, C. W. Tsao, M. P. Turakhia, L. B. VanWagner, J. T. Wilkins, S. S. Wong, S. S. Virani, E. American Heart Association Council on, C. Prevention Statistics and S. Stroke Statistics (2019). "Heart Disease and Stroke Statistics-2019 Update: A Report From the American Heart Association." Circulation **139**(10): e56-e528.
- Berg, K. A. and W. P. Clarke (2018). "Making Sense of Pharmacology: Inverse Agonism and Functional Selectivity." International Journal of Neuropsychopharmacology **21**(10): 962-977.
- Best, L. C., T. J. Martin, R. G. Russell and F. E. Preston (1977). "Prostacyclin increases cyclic AMP levels and adenylate cyclase activity in platelets." Nature **267**(5614): 850-852.

- Bhatt, D. L., C. V. Pollack, J. I. Weitz, L. K. Jennings, S. Xu, S. E. Arnold, B. R. Umstead, M. C. Mays and J. S. Lee (2019). "Antibody-Based Ticagrelor Reversal Agent in Healthy Volunteers." N Engl J Med **380**(19): 1825-1833.
- Bhatt, D. L., G. W. Stone, K. W. Mahaffey, C. M. Gibson, P. G. Steg, C. W. Hamm, M. J. Price, S. Leonardi, D. Gallup, E. Bramucci, P. W. Radke, P. Widimský, F. Tousek, J. Tauth, D. Spriggs, B. T. McLaurin, D. J. Angiolillo, P. Généreux, T. Liu, J. Prats, M. Todd, S. Skerjanec, H. D. White and R. A. Harrington (2013). "Effect of platelet inhibition with cangrelor during PCI on ischemic events." N Engl J Med **368**(14): 1303-1313.
- Brandt, J. T., S. L. Close, S. J. Iturria, C. D. Payne, N. A. Farid, C. S. Ernest, 2nd, D. R. Lachno, D. Salazar and K. J. Winters (2007). "Common polymorphisms of CYP2C19 and CYP2C9 affect the pharmacokinetic and pharmacodynamic response to clopidogrel but not prasugrel." J Thromb Haemost **5**(12): 2429-2436.
- Cannon, C. P., S. Husted, R. A. Harrington, B. M. Scirica, H. Emanuelsson, G. Peters, R. F. Storey and D.-. Investigators (2007). "Safety, tolerability, and initial efficacy of AZD6140, the first reversible oral adenosine diphosphate receptor antagonist, compared with clopidogrel, in patients with non-ST-segment elevation acute coronary syndrome: primary results of the DISPERSE-2 trial." J Am Coll Cardiol **50**(19): 1844-1851.
- Carlsson, A. C., N. Bandstein, A. Roos, O. Hammarsten and M. J. Holzmann (2017). "High-sensitivity cardiac troponin T levels in the emergency department in patients with chest pain but no myocardial infarction." Int J Cardiol **228**: 253-259.
- Cattaneo, M. (2004). "Aspirin and Clopidogrel." Arteriosclerosis, Thrombosis, and Vascular Biology **24**(11): 1980-1987.
- Cattaneo, M. (2006). "ADP receptors: inhibitory strategies for antiplatelet therapy." Timely Top Med Cardiovasc Dis **10**: E22.
- Cattaneo, M. (2006). "P2Y12 receptor antagonists: a rapidly expanding group of antiplatelet agents." Eur Heart J **27**(9): 1010-1012.
- Cattaneo, M. (2010). "New P2Y(12) inhibitors." Circulation **121**(1): 171-179.
- Cattaneo, M. (2015). "P2Y12 receptors: structure and function." Journal of Thrombosis and Haemostasis **13**(S1): S10-S16.
- Cattaneo, M., A. Lecchi, A. M. Randi, J. L. McGregor and P. M. Mannucci (1992). "Identification of a new congenital defect of platelet function characterized by severe impairment of platelet responses to adenosine diphosphate." Blood **80**(11): 2787-2796.
- Cerione, R. A., J. Codina, J. L. Benovic, R. J. Lefkowitz, L. Birnbaumer and M. G. Caron (1984). "The mammalian beta 2-adrenergic receptor: reconstitution of functional interactions between pure receptor and pure stimulatory nucleotide binding protein of the adenylate cyclase system." Biochemistry **23**(20): 4519-4525.
- Chaloupka FJ, Yurekli A and F. GT. (2012). "Tobacco taxes as a tobacco control strategy. ." Tobacco Control **21**(21): 172-180.
- Chen, D., P. P. Lemons, T. Schraw and S. W. Whiteheart (2000). "Molecular mechanisms of platelet exocytosis: role of SNAP-23 and syntaxin 2 and 4 in lysosome release." Blood **96**(5): 1782-1788.
- Chrzanowska-Wodnicka, M., S. S. Smyth, S. M. Schoenwaelder, T. H. Fischer and G. C. White, 2nd (2005). "Rap1b is required for normal platelet function and hemostasis in mice." J Clin Invest **115**(3): 680-687.
- Costa, T. and A. Herz (1989). "Antagonists with negative intrinsic activity at delta opioid receptors coupled to GTP-binding proteins." Proc Natl Acad Sci U S A **86**(19): 7321-7325.

- Danaei, G., E. L. Ding, D. Mozaffarian, B. Taylor, J. Rehm, C. J. Murray and M. Ezzati (2009). "The preventable causes of death in the United States: comparative risk assessment of dietary, lifestyle, and metabolic risk factors." PLoS Med **6**(4): e1000058.
- Dariya, B. and G. P. Nagaraju (2020). "Understanding novel COVID-19: Its impact on organ failure and risk assessment for diabetic and cancer patients." Cytokine Growth Factor Rev **53**: 43-52.
- Dawkins, K. D., T. Gershlick, M. de Belder, A. Chauhan, G. Venn, P. Schofield, D. Smith, J. Watkins and H. H. Gray (2005). "Percutaneous coronary intervention: recommendations for good practice and training." Heart **91 Suppl 6**(Suppl 6): vi1-27.
- de Los Milagros Bassani Molinas, M., C. Beer, F. Hesse, M. Wirth and R. Wagner (2014). "Optimizing the transient transfection process of HEK-293 suspension cells for protein production by nucleotide ratio monitoring." Cytotechnology **66**(3): 493-514.
- DeVol, R., A. Bedroussian and A. Charuworn (2007). An Unhealthy America: The economic burden of chronic disease The Milken Institute.
- Ding, Z., S. Kim and S. P. Kunapuli (2006). "Identification of a Potent Inverse Agonist at a Constitutively Active Mutant of Human P2Y₁₂ Receptor." Molecular Pharmacology **69**(1): 338-345.
- Dobesh, P. P. and J. H. Oestreich (2014). "Ticagrelor: pharmacokinetics, pharmacodynamics, clinical efficacy, and safety." Pharmacotherapy **34**(10): 1077-1090.
- Durrant, T. N., M. T. van den Bosch and I. Hers (2017). "Integrin $\alpha_2b\beta_3$ outside-in signalling." Blood **130**(14): 1607-1619.
- Eckly, A., C. Strassel, M. Freund, J. P. Cazenave, F. Lanza, C. Gachet and C. Leon (2009). "Abnormal megakaryocyte morphology and proplatelet formation in mice with megakaryocyte-restricted MYH9 inactivation." Blood **113**(14): 3182-3189.
- Elder, R. W., B. Lawrence, A. Ferguson, T. S. Naimi, R. D. Brewer, S. K. Chattopadhyay, T. L. Toomey, J. E. Fielding and S. Task Force on Community Preventive (2010). "The effectiveness of tax policy interventions for reducing excessive alcohol consumption and related harms." Am J Prev Med **38**(2): 217-229.
- Farid, N. A., C. D. Payne, D. S. Small, K. J. Winters, C. S. Ernest, 2nd, J. T. Brandt, C. Darstein, J. A. Jakubowski and D. E. Salazar (2007). "Cytochrome P450 3A inhibition by ketoconazole affects prasugrel and clopidogrel pharmacokinetics and pharmacodynamics differently." Clin Pharmacol Ther **81**(5): 735-741.
- Feletou, M., R. A. Cohen, P. M. Vanhoutte and T. J. Verbeuren (2010). "TP receptors and oxidative stress hand in hand from endothelial dysfunction to atherosclerosis." Adv Pharmacol **60**: 85-106.
- Fitch-Tewfik, J. L. and R. Flaumenhaft (2013). "Platelet granule exocytosis: a comparison with chromaffin cells." Front Endocrinol (Lausanne) **4**: 77.
- Franchi, F., F. Rollini, J. R. Rios, A. Rivas, M. Agarwal, M. Kureti, D. Nagaraju, M. Wali, Z. Shaikh, M. Briceno, A. Nawaz, J. Y. Moon, L. Been, S. Suryadevara, D. Soffer, M. M. Zenni, T. A. Bass and D. J. Angiolillo (2018). "Pharmacodynamic Effects of Switching From Ticagrelor to Clopidogrel in Patients With Coronary Artery Disease." Circulation **137**(23): 2450-2462.
- Fuentes, E., M. Fuentes, J. Caballero, I. Palomo, S. Hinz, A. El-Tayeb and C. E. Muller (2018). "Adenosine A2A receptor agonists with potent antiplatelet activity." Platelets **29**(3): 292-300.

- Gaarder, A., J. Jonsen, S. Laland, A. Hellem and P. A. Owren (1961). "Adenosine Diphosphate in Red Cells as a Factor in the Adhesiveness of Human Blood Platelets." Nature **192**(4802): 531-532.
- Garcia, C., A. Maurel-Ribes, M. Nauze, D. N'Guyen, L. O. Martinez, B. Payrastre, J. M. Sénard, C. Galés and V. Pons (2018). "Deciphering biased inverse agonism of cangrelor and ticagrelor at P2Y." Cell Mol Life Sci.
- Geddis, A. E. and K. Kaushansky (2006). "Endomitotic megakaryocytes form a midzone in anaphase but have a deficiency in cleavage furrow formation." Cell Cycle **5**(5): 538-545.
- Gerrard, J. M., J. G. White and D. A. Peterson (1978). "The platelet dense tubular system: its relationship to prostaglandin synthesis and calcium flux." Thromb Haemost **40**(2): 224-231.
- Golebiewska, E. M. and A. W. Poole (2015). "Platelet secretion: From haemostasis to wound healing and beyond." Blood Rev **29**(3): 153-162.
- Greenbaum, A. B., C. L. Grines, J. A. Bittl, R. C. Becker, D. J. Kereiakes, I. C. Gilchrist, J. Clegg, J. E. Stankowski, D. R. Grogan, R. A. Harrington, H. Emanuelsson and W. D. Weaver (2006). "Initial experience with an intravenous P2Y12 platelet receptor antagonist in patients undergoing percutaneous coronary intervention: results from a 2-part, phase II, multicenter, randomized, placebo- and active-controlled trial." Am Heart J **151**(3): 689.e681-689.e610.
- Guidetti, G. F., I. Canobbio and M. Torti (2015). "PI3K/Akt in platelet integrin signaling and implications in thrombosis." Adv Biol Regul **59**: 36-52.
- Guo, T., X. Wang, Y. Qu, Y. Yin, T. Jing and Q. Zhang (2015). "Megakaryopoiesis and platelet production: insight into hematopoietic stem cell proliferation and differentiation." Stem Cell Investig **2**: 3.
- Hechler, B., A. Eckly, P. Ohlmann, J. P. Cazenave and C. Gachet (1998). "The P2Y1 receptor, necessary but not sufficient to support full ADP-induced platelet aggregation, is not the target of the drug clopidogrel." Br J Haematol **103**(3): 858-866.
- Hoffmann, K., D. A. Lutz, J. Straßburger, Y. Baqi, C. E. Müller and I. von Kügelgen (2014). "Competitive mode and site of interaction of ticagrelor at the human platelet P2Y12 - receptor." J Thromb Haemost **12**(11): 1898-1905.
- Hollopeter, G., H. M. Jantzen, D. Vincent, G. Li, L. England, V. Ramakrishnan, R. B. Yang, P. Nurden, A. Nurden, D. Julius and P. B. Conley (2001). "Identification of the platelet ADP receptor targeted by antithrombotic drugs." Nature **409**(6817): 202-207.
- Hu, L., L. Chang, Y. Zhang, L. Zhai, S. Zhang, Z. Qi, H. Yan, Y. Yan, X. Luo, S. Zhang, Y. Wang, S. P. Kunapuli, H. Ye and Z. Ding (2017). "Platelets Express Activated P2Y12 Receptor in Patients With Diabetes Mellitus." Circulation **136**(9): 817-833.
- Husted, S. and J. J. van Giezen (2009). "Ticagrelor: the first reversibly binding oral P2Y12 receptor antagonist." Cardiovasc Ther **27**(4): 259-274.
- Huynh, T., S. Perron, J. O'Loughlin, L. Joseph, M. Labrecque, J. V. Tu and P. Theroux (2009). "Comparison of primary percutaneous coronary intervention and fibrinolytic therapy in ST-segment-elevation myocardial infarction: bayesian hierarchical meta-analyses of randomized controlled trials and observational studies." Circulation **119**(24): 3101-3109.
- Hvas, A. M. and E. J. Favaloro (2017). "Platelet Function Analyzed by Light Transmission Aggregometry." Methods Mol Biol **1646**: 321-331.
- Imazio, M., K. Klingel, I. Kindermann, A. Brucato, F. G. De Rosa, Y. Adler and G. M. De Ferrari (2020). "COVID-19 pandemic and troponin: indirect myocardial injury, myocardial inflammation or myocarditis?" Heart **106**(15): 1127-1131.

- Jackson, S. P. (2011). "Arterial thrombosis--insidious, unpredictable and deadly." Nat Med **17**(11): 1423-1436.
- Jackson, S. P., S. M. Schoenwaelder, I. Goncalves, W. S. Nesbitt, C. L. Yap, C. E. Wright, V. Kenche, K. E. Anderson, S. M. Dopheide, Y. Yuan, S. A. Sturgeon, H. Prabaharan, P. E. Thompson, G. D. Smith, P. R. Shepherd, N. Daniele, S. Kulkarni, B. Abbott, D. Saylik, C. Jones, L. Lu, S. Giuliano, S. C. Hughan, J. A. Angus, A. D. Robertson and H. H. Salem (2005). "PI 3-kinase p110β: a new target for antithrombotic therapy." Nature Medicine **11**(5): 507-514.
- Jackson, S. P., C. L. Yap and K. E. Anderson (2004). "Phosphoinositide 3-kinases and the regulation of platelet function." Biochem Soc Trans **32**(Pt 2): 387-392.
- James, S., A. Akerblom, C. P. Cannon, H. Emanuelsson, S. Husted, H. Katus, A. Skene, P. G. Steg, R. F. Storey, R. Harrington, R. Becker and L. Wallentin (2009). "Comparison of ticagrelor, the first reversible oral P2Y(12) receptor antagonist, with clopidogrel in patients with acute coronary syndromes: Rationale, design, and baseline characteristics of the PLATelet inhibition and patient Outcomes (PLATO) trial." Am Heart J **157**(4): 599-605.
- Jantzen, H. M., D. S. Milstone, L. Gousset, P. B. Conley and R. M. Mortensen (2001). "Impaired activation of murine platelets lacking G alpha(i2)." J Clin Invest **108**(3): 477-483.
- Jarvis, G. E., R. G. Humphries, M. J. Robertson and P. Leff (2000). "ADP can induce aggregation of human platelets via both P2Y(1) and P(2T) receptors." British journal of pharmacology **129**(2): 275-282.
- Jastrzebska, B. (2013). "GPCR: G protein complexes--the fundamental signaling assembly." Amino Acids **45**(6): 1303-1314.
- Jin, J., J. L. Daniel and S. P. Kunapuli (1998). "Molecular basis for ADP-induced platelet activation. II. The P2Y1 receptor mediates ADP-induced intracellular calcium mobilization and shape change in platelets." J Biol Chem **273**(4): 2030-2034.
- JJ, V. A. N. G., L. Nilsson, P. Berntsson, B. M. Wissing, F. Giordanetto, W. Tomlinson and P. J. Greasley (2009). "Ticagrelor binds to human P2Y(12) independently from ADP but antagonizes ADP-induced receptor signaling and platelet aggregation." J Thromb Haemost **7**(9): 1556-1565.
- Jurk, K. and B. E. Kehrel (2005). "Platelets: physiology and biochemistry." Semin Thromb Hemost **31**(4): 381-392.
- Kahner, B. N., H. Shankar, S. Murugappan, G. L. Prasad and S. P. Kunapuli (2006). "Nucleotide receptor signaling in platelets." J Thromb Haemost **4**(11): 2317-2326.
- Kanthi, Y. M., N. R. Sutton and D. J. Pinsky (2014). "CD39: Interface between vascular thrombosis and inflammation." Curr Atheroscler Rep **16**(7): 425.
- Kim, S., J. Jin and S. P. Kunapuli (2004). "Akt activation in platelets depends on Gi signaling pathways." J Biol Chem **279**(6): 4186-4195.
- Konstantinidis, K., R. S. Whelan and R. N. Kitsis (2012). "Mechanisms of cell death in heart disease." Arterioscler Thromb Vasc Biol **32**(7): 1552-1562.
- Leon, C., C. Vial, C. Gachet, P. Ohlmann, B. Hechler, J. P. Cazenave, A. Lecchi and M. Cattaneo (1999). "The P2Y1 receptor is normal in a patient presenting a severe deficiency of ADP-induced platelet aggregation." Thromb Haemost **81**(5): 775-781.
- Levi, F., F. Lucchini, E. Negri and C. La Vecchia (2002). "Trends in mortality from cardiovascular and cerebrovascular diseases in Europe and other areas of the world." Heart **88**(2): 119-124.
- Li, R. and J. Emsley (2013). "The organizing principle of the platelet glycoprotein Ib-IX-V complex." J Thromb Haemost **11**(4): 605-614.

- Lifestyles Team, N. D. (2019). "Statistics on Obesity, Physical Activity and Diet, England, 2019." Retrieved 29/03, 2020, from https://digital.nhs.uk/data-and-information/publications/statistical/statistics-on-obesity-physical-activity-and-diet/statistics-on-obesity-physical-activity-and-diet-england-2019.
- Lippi, G. and G. Cervellin (2016). "Acute coronary syndrome: many doubts, some answers." Ann Transl Med **4**(10): 187.
- Lippi, G., F. Sanchis-Gomar and G. Cervellin (2016). "Chest pain, dyspnea and other symptoms in patients with type 1 and 2 myocardial infarction. A literature review." Int J Cardiol **215**: 20-22.
- Machlus, K. R., J. N. Thon and J. E. Italiano, Jr. (2014). "Interpreting the developmental dance of the megakaryocyte: a review of the cellular and molecular processes mediating platelet formation." Br J Haematol **165**(2): 227-236.
- MacKenzie, R. D. (1977). Chapter 9. Antithrombotic Agents. Annual Reports in Medicinal Chemistry. F. H. Clarke, Academic Press. **12:** 80-90.
- Maffrand, J.-P. (2012). "The story of clopidogrel and its predecessor, ticlopidine: Could these major antiplatelet and antithrombotic drugs be discovered and developed today?" Comptes Rendus Chimie **15**(8): 737-743.
- Martin, A. C., C. Berndt, L. Calmette, I. Philip, B. Decouture, P. Gaussem, I. Gouin-Thibault, C. M. Samama, C. Bachelot-Loza and A. Godier (2016). "The effectiveness of platelet supplementation for the reversal of ticagrelor-induced inhibition of platelet aggregation: An in-vitro study." Eur J Anaesthesiol **33**(5): 361-367.
- Mauri, L., D. J. Kereiakes, R. W. Yeh, P. Driscoll-Shempp, D. E. Cutlip, P. G. Steg, S.-L. T. Normand, E. Braunwald, S. D. Wiviott, D. J. Cohen, D. R. Holmes, M. W. Krucoff, J. Hermiller, H. L. Dauerman, D. I. Simon, D. E. Kandzari, K. N. Garratt, D. P. Lee, T. K. Pow, P. Ver Lee, M. J. Rinaldi and J. M. Massaro (2014). "Twelve or 30 Months of Dual Antiplatelet Therapy after Drug-Eluting Stents." New England Journal of Medicine **371**(23): 2155-2166.
- McCartney, P. J. and C. Berry (2019). "Redefining successful primary PCI." Eur Heart J Cardiovasc Imaging **20**(2): 133-135.
- Mehta, S. R., J. P. Bassand, S. Chrolavicius, R. Diaz, J. W. Eikelboom, K. A. Fox, C. B. Granger, S. Jolly, C. D. Joyner, H. J. Rupprecht, P. Widimsky, R. Afzal, J. Pogue and S. Yusuf (2010). "Dose comparisons of clopidogrel and aspirin in acute coronary syndromes." N Engl J Med **363**(10): 930-942.
- Mehta, S. R., S. Yusuf, R. J. Peters, M. E. Bertrand, B. S. Lewis, M. K. Natarajan, K. Malmberg, H. Rupprecht, F. Zhao, S. Chrolavicius, I. Copland, K. A. Fox and I. Clopidogrel in Unstable angina to prevent Recurrent Events trial (2001). "Effects of pretreatment with clopidogrel and aspirin followed by long-term therapy in patients undergoing percutaneous coronary intervention: the PCI-CURE study." Lancet **358**(9281): 527-533.
- Midgett, C., J. Stitham, K. Martin and J. Hwa (2011). "Prostacyclin receptor regulation--from transcription to trafficking." Curr Mol Med **11**(7): 517-528.
- Moscardo, A., M. T. Santos, M. P. Fuset, M. Ruano and J. Valles (2011). "Residual cyclooxygenase-1 activity and epinephrine reduce the antiplatelet effect of aspirin in patients with acute myocardial infarction." Thromb Haemost **105**(4): 663-669.
- Mundell, S. J., R. P. Loudon and J. L. Benovic (1999). "Characterization of G protein-coupled receptor regulation in antisense mRNA-expressing cells with reduced arrestin levels." Biochemistry **38**(27): 8723-8732.

- Nakamura, F., M. R. Amieva and H. Furthmayr (1995). "Phosphorylation of threonine 558 in the carboxyl-terminal actin-binding domain of moesin by thrombin activation of human platelets." J Biol Chem **270**(52): 31377-31385.
- NCBI. (2004). "Aspirin, CID = 2244." Retrieved May 4th, 2020, from https://pubchem.ncbi.nlm.nih.gov/compound/2244.
- NCBI. (2005). "Ticlopidine, CID = 5472." Retrieved May 3, 2020, 2020, from https://pubchem.ncbi.nlm.nih.gov/compound/Ticlopidine.
- Niblett, P., N. Coyle, E. Little, C. Beaton, J. Burton, S. Chisholm, A. Tedstone, V. Targett, J. Nicholas, S. Montel, B. Knowles, V. Pyne, J. Lynas and J. Fitzpatrick (2019). Sugar reduction: Report on progress between 2015 and 2018, PHE publications**:** 5.
- Nichols, M., N. Townsend, P. Scarborough and M. Rayner (2014). "Cardiovascular disease in Europe 2014: epidemiological update." Eur Heart J **35**(42): 2929.
- Nieswandt, B., I. Pleines and M. Bender (2011). "Platelet adhesion and activation mechanisms in arterial thrombosis and ischaemic stroke." J Thromb Haemost **9 Suppl 1**: 92-104.
- Niitsu, Y., J. A. Jakubowski, A. Sugidachi and F. Asai (2005). "Pharmacology of CS-747 (prasugrel, LY640315), a novel, potent antiplatelet agent with in vivo P2Y12 receptor antagonist activity." Semin Thromb Hemost **31**(2): 184-194.
- Nurden, A. T. and P. Nurden (2003). "Advantages of fast-acting ADP receptor blockade in ischemic heart disease." Arterioscler Thromb Vasc Biol **23**(2): 158-159.
- Nurden, P., P. Savi, E. Heilmann, C. Bihour, J. M. Herbert, J. P. Maffrand and A. Nurden (1995). "An inherited bleeding disorder linked to a defective interaction between ADP and its receptor on platelets. Its influence on glycoprotein IIb-IIIa complex function." The Journal of Clinical Investigation **95**(4): 1612-1622.
- O'Brien, J. R. (1961). "The adhesiveness of native platelets and its prevention." J Clin Pathol **14**(2): 140-149.
- Oestreich, J. H., S. P. Ferraris, S. R. Steinhubl and W. S. Akers (2013). "Pharmacodynamic interplay of the P2Y(1), P2Y(12), and TxA(2) pathways in platelets: the potential of triple antiplatelet therapy with P2Y(1) receptor antagonism." Thromb Res **131**(2): e64-70.
- Offermanns, S., C. F. Toombs, Y. H. Hu and M. I. Simon (1997). "Defective platelet activation in G alpha(q)-deficient mice." Nature **389**(6647): 183-186.
- Okrainec, K., D. K. Banerjee and M. J. Eisenberg (2004). "Coronary artery disease in the developing world." Am Heart J **148**(1): 7-15.
- Paez Espinosa, E. V., J. P. Murad and F. T. Khasawneh (2012). "Aspirin: pharmacology and clinical applications." Thrombosis **2012**: 173124.
- Parker, W. A. E. and R. F. Storey (2016). "Ticagrelor: agonising over its mechanisms of action." Blood **128**(23): 2595-2597.
- Parravicini, C., M. P. Abbracchio, P. Fantucci and G. Ranghino (2010). "Forced unbinding of GPR17 ligands from wild type and R255I mutant receptor models through a computational approach." BMC Structural Biology **10**(1): 8.
- Patel, S. R., J. H. Hartwig and J. E. Italiano (2005). "The biogenesis of platelets from megakaryocyte proplatelets." J Clin Invest **115**(12): 3348-3354.
- Paul, B. Z., J. L. Daniel and S. P. Kunapuli (1999). "Platelet shape change is mediated by both calcium-dependent and -independent signaling pathways. Role of p160 Rho-associated coiled-coil-containing protein kinase in platelet shape change." J Biol Chem **274**(40): 28293-28300.

- Payne, C. D., Y. G. Li, D. S. Small, C. S. Ernest, 2nd, N. A. Farid, J. A. Jakubowski, J. T. Brandt, D. E. Salazar and K. J. Winters (2007). "Increased active metabolite formation explains the greater platelet inhibition with prasugrel compared to high-dose clopidogrel." J Cardiovasc Pharmacol **50**(5): 555-562.
- Pell, D., T. Penney, D. Hammond, L. Vanderlee, M. White and J. Adams (2019). "Support for, and perceived effectiveness of, the UK soft drinks industry levy among UK adults: cross-sectional analysis of the International Food Policy Study." BMJ Open **9**(3): e026698.
- Purves, D., G. Augustine and D. Fitzpatrick (2001). G-Proteins and Their Molecular Targets, Sinauer Associates, Inc.
- Rao, G. H. and J. G. White (1985). "Role of arachidonic acid metabolism in human platelet activation and irreversible aggregation." Am J Hematol **19**(4): 339-347.
- Rapkiewicz, A. V., X. Mai, S. E. Carsons, S. Pittaluga, D. E. Kleiner, J. S. Berger, S. Thomas, N. M. Adler, D. M. Charytan, B. Gasmi, J. S. Hochman and H. R. Reynolds (2020). "Megakaryocytes and platelet-fibrin thrombi characterize multi-organ thrombosis at autopsy in COVID-19: A case series." EClinicalMedicine.
- Reininger, A. J., H. F. Heijnen, H. Schumann, H. M. Specht, W. Schramm and Z. M. Ruggeri (2006). "Mechanism of platelet adhesion to von Willebrand factor and microparticle formation under high shear stress." Blood **107**(9): 3537-3545.
- Rendu, F. and B. Brohard-Bohn (2001). "The platelet release reaction: granules' constituents, secretion and functions." Platelets **12**(5): 261-273.
- ResearchStraits. (2019). Fast Food Market: Information by Type (Burgers, Pizzas, Chinese Food), Distribution Platform (Quick Service Restaurants, Food Delivery Services) and Regional Outlook—Forecast Till 2026, Straits Research**:** 110.
- Rivera, J., M. L. Lozano, L. Navarro-Nunez and V. Vicente (2009). "Platelet receptors and signaling in the dynamics of thrombus formation." Haematologica **94**(5): 700-711.
- Roger, V. L. (2007). "Coronary disease surveillance: a public heath imperative." Eur Heart J **28**(17): 2051-2052.
- Rollini, F., F. Franchi, J. R. Cho, C. DeGroat, M. Bhatti, A. Muniz-Lozano, K. Singh, E. Ferrante, R. E. Wilson, E. C. Dunn, M. M. Zenni, L. A. Guzman, T. A. Bass and D. J. Angiolillo (2016). "A head-to-head pharmacodynamic comparison of prasugrel vs. ticagrelor after switching from clopidogrel in patients with coronary artery disease: results of a prospective randomized study." European Heart Journal **37**(35): 2722-2730.
- Rovati, G. E. and V. Capra (2014). "The DRY motif at work: the P2Y12 receptor case." Journal of Thrombosis and Haemostasis **12**(5): 713-715.
- Rumbaut, R. E. and P. Thiagarajan (2010). Platelet-Vessel Wall Interactions in Hemostasis and Thrombosis. San Rafael (CA).
- Sanchis-Gomar, F., C. Perez-Quilis, R. Leischik and A. Lucia (2016). "Epidemiology of coronary heart disease and acute coronary syndrome." Ann Transl Med **4**(13): 256.
- Sangkuhl, K., A. R. Shuldiner, T. E. Klein and R. B. Altman (2011). "Platelet aggregation pathway." Pharmacogenet Genomics **21**(8): 516-521.
- Scavone, M., E. A. Femia and M. Cattaneo (2017). "P2Y12 receptor gene mutations associated with bleeding." Platelets **28**(4): 421-423.
- Seifert, R. and K. Wenzel-Seifert (2002). "Constitutive activity of G-protein-coupled receptors: cause of disease and common property of wild-type receptors." Naunyn-Schmiedeberg's Archives of Pharmacology **366**(5): 381-416.

- Selvadurai, M. V. and J. R. Hamilton (2018). "Structure and function of the open canalicular system - the platelet's specialized internal membrane network." Platelets **29**(4): 319-325.
- Shankar, H., B. N. Kahner, J. Prabhakar, P. Lakhani, S. Kim and S. P. Kunapuli (2006). "G-protein-gated inwardly rectifying potassium channels regulate ADP-induced cPLA2 activity in platelets through Src family kinases." Blood **108**(9): 3027-3034.
- Stalker, T. J., D. K. Newman, P. Ma, K. M. Wannemacher and L. F. Brass (2012). "Platelet signaling." Handb Exp Pharmacol(210): 59-85.
- Stefanini, L., D. S. Paul, R. F. Robledo, E. R. Chan, T. M. Getz, R. A. Campbell, D. O. Kechele, C. Casari, R. Piatt, K. M. Caron, N. Mackman, A. S. Weyrich, M. C. Parrott, Y. Boulaftali, M. D. Adams, L. L. Peters and W. Bergmeier (2015). "RASA3 is a critical inhibitor of RAP1-dependent platelet activation." The Journal of Clinical Investigation **125**(4): 1419-1432.
- Steg, P. G., D. L. Bhatt, C. W. Hamm, G. W. Stone, C. M. Gibson, K. W. Mahaffey, S. Leonardi, T. Liu, S. Skerjanec, J. R. Day, R. S. Iwaoka, T. D. Stuckey, H. S. Gogia, L. Gruberg, W. J. French, H. D. White and R. A. Harrington (2013). "Effect of cangrelor on periprocedural outcomes in percutaneous coronary interventions: a pooled analysis of patient-level data." Lancet **382**(9909): 1981-1992.
- Storey, R. F., S. Husted, R. A. Harrington, S. Heptinstall, R. G. Wilcox, G. Peters, M. Wickens, H. Emanuelsson, P. Gurbel, P. Grande and C. P. Cannon (2007). "Inhibition of platelet aggregation by AZD6140, a reversible oral P2Y12 receptor antagonist, compared with clopidogrel in patients with acute coronary syndromes." J Am Coll Cardiol **50**(19): 1852-1856.
- Storey, R. F., R. G. Wilcox and S. Heptinstall (2002). "Comparison of the pharmacodynamic effects of the platelet ADP receptor antagonists clopidogrel and AR-C69931MX in patients with ischaemic heart disease." Platelets **13**(7): 407-413.
- Strelow, J. M. (2017). "A Perspective on the Kinetics of Covalent and Irreversible Inhibition." SLAS DISCOVERY: Advancing the Science of Drug Discovery **22**(1): 3-20.
- Thon, J. N. and J. E. Italiano (2012). "Platelets: production, morphology and ultrastructure." Handb Exp Pharmacol(210): 3-22.
- Timmis, A. (2015). "Acute coronary syndromes." BMJ **351**: h5153.
- Tonge, P. J. (2018). "Drug-Target Kinetics in Drug Discovery." ACS Chem Neurosci **9**(1): 29-39.
- Urban, J. D., W. P. Clarke, M. von Zastrow, D. E. Nichols, B. Kobilka, H. Weinstein, J. A. Javitch, B. L. Roth, A. Christopoulos, P. M. Sexton, K. J. Miller, M. Spedding and R. B. Mailman (2007). "Functional selectivity and classical concepts of quantitative pharmacology." J Pharmacol Exp Ther **320**(1): 1-13.
- van Giezen, J. J. and R. G. Humphries (2005). "Preclinical and clinical studies with selective reversible direct P2Y12 antagonists." Semin Thromb Hemost **31**(2): 195-204.
- VAN Giezen, J. J., L. Nilsson, P. Berntsson, B. M. Wissing, F. Giordanetto, W. Tomlinson and P. J. Greasley (2009). "Ticagrelor binds to human P2Y(12) independently from ADP but antagonizes ADP-induced receptor signaling and platelet aggregation." J Thromb Haemost **7**(9): 1556-1565.
- Veliz, C., H. Maslen, M. Essman, L. S. Taillie and J. Savulescu (2019). "Sugar, Taxes, & Choice." Hastings Cent Rep **49**(6): 22-31.
- von Kügelgen, I., D. Lutz, J. Straburger, Y. Baqi, C. Müller and K. Hoffmann (2014). "Mode and site of interaction of the novel antiplatelet drug ticagrelor at the recombinant human P2Y12 receptor." The FASEB Journal **28**: 1057.1011.

- Wardell, M. R., C. C. Reynolds, M. C. Berndt, R. W. Wallace and J. E. Fox (1989). "Platelet glycoprotein Ib beta is phosphorylated on serine 166 by cyclic AMP-dependent protein kinase." J Biol Chem **264**(26): 15656-15661.
- White, J. G. and C. C. Clawson (1980). "The surface-connected canalicular system of blood platelets--a fenestrated membrane system." Am J Pathol **101**(2): 353-364.
- Wilcox, R., K. Iqbal, T. Costigan, J. Lopez-Sendon, Y. Ramos and P. Widimsky (2014). "An analysis of TRITON-TIMI 38, based on the 12 month recommended length of therapy in the European label for prasugrel." Current Medical Research and Opinion **30**(11): 2193-2205.
- Wilkins, E., L. Wilson, K. Wickramasinghe, P. Bhatnagar, M. Rayner and N. Townsend (2017). European Cardiovascular Disease Statistics 2017. Brussels, European Heart Network.
- Wise, J. (2016). "NICE recommends ticagrelor with aspirin for three years post-MI." BMJ **354**: i4438.
- World Health Organisation, W. (2017, 17/05/2017). "Cardiovascular diseases (CVDs)." from https://www.who.int/en/news-room/fact-sheets/detail/cardiovascular-diseases-(cvds).
- Woronowicz, K., J. R. Dilks, N. Rozenvayn, L. Dowal, P. S. Blair, C. G. Peters, L. Woronowicz and R. Flaumenhaft (2010). "The platelet actin cytoskeleton associates with SNAREs and participates in alpha-granule secretion." Biochemistry **49**(21): 4533-4542.
- Woulfe, D. S. (2005). "Platelet G protein-coupled receptors in hemostasis and thrombosis." J Thromb Haemost **3**(10): 2193-2200.
- Woulfe, D. S. (2010). "Akt signaling in platelets and thrombosis." Expert Rev Hematol **3**(1): 81-91.
- Xie, Q., M. Soutto, X. Xu, Y. Zhang and C. H. Johnson (2011). "Bioluminescence resonance energy transfer (BRET) imaging in plant seedlings and mammalian cells." Methods in molecular biology (Clifton, N.J.) **680**: 3-28.
- Yan, R., S. Li and K. Dai (2009). "The critical roles of cyclic AMP/cyclic AMP-dependent protein kinase in platelet physiology." Frontiers of Biology in China **4**(1): 7-14.
- Yano, Y., J. Stamler, D. B. Garside, M. L. Daviglus, S. S. Franklin, M. R. Carnethon, K. Liu, P. Greenland and D. M. Lloyd-Jones (2015). "Isolated systolic hypertension in young and middle-aged adults and 31-year risk for cardiovascular mortality: the Chicago Heart Association Detection Project in Industry study." J Am Coll Cardiol **65**(4): 327-335.
- Zhang, J., K. Zhang, Z. G. Gao, S. Paoletta, D. Zhang, G. W. Han, T. Li, L. Ma, W. Zhang, C. E. Müller, H. Yang, H. Jiang, V. Cherezov, V. Katritch, K. A. Jacobson, R. C. Stevens, B. Wu and Q. Zhao (2014). "Agonist-bound structure of the human P2Y12 receptor." Nature **509**(7498): 119-122.
- Zhang, K., J. Zhang, Z.-G. Gao, D. Zhang, L. Zhu, G. W. Han, S. M. Moss, S. Paoletta, E. Kiselev, W. Lu, G. Fenalti, W. Zhang, C. E. Müller, H. Yang, H. Jiang, V. Cherezov, V. Katritch, K. A. Jacobson, R. C. Stevens, B. Wu and Q. Zhao (2014). "Structure of the human P2Y12 receptor in complex with an antithrombotic drug." Nature **509**(7498): 115-118.
- Zhang, S., K. Xu, L. Mei, H. Zhu, J. Li, F. Wang, L. Yang, J. Zhang, Y. Fan, F. Zou, K. Niles, J. W. Eikelboom and C. Li (2019). "Reversal of the antiplatelet effect of ticagrelor by simulated platelet transfusion." Transfusion **59**(5): 1850-1856.